Memoirs of the Faculty of Engineering, Nagoya University
Vol. 35, No. 2 (1983)

VIBRATIONS OF A ROTATING SHAFT WITH NONLINEAR SPRING CHARACTERISTICS AND UNSYMMETRY

TOSHIO YAMAMOTO, YUKIO ISHIDA and TAKASHI IKEDA

Department of Mechanical Engineering

(Received October 26, 1983)

Abstract

Rotating machines with nonlinear spring characteristics and the unsymmetry of shaft stiffness or rotor inertia have been often used in industries. Since vibrations due to the coexistence of nonlinearity and unsymmetry are complicated in theoretical treatments, there have been few studies on these vibrations.

This paper mainly deals with the nonlinear forced oscillations at the major critical and other subcritical speeds in a rotating shaft system having both nonlinearity and unsymmetry. Such systems have unique vibratory characteristics different from those of a symmetrical system with nonlinearity. For example, at the major critical speed various types of resonance curves are obtained depending on the angular position of rotor unbalance. The unstable vibrations of subharmonic and summed-and-differential harmonic oscillations appear although only stable oscillations occur in the symmetrical system. And, stable and unstable vibrations of super-summed-and-differential harmonic oscillations occur only in the system with both nonlinearity and unsymmetry.

In addition, we investigated the sub-combination tones in a symmetrical system with nonlinearity and the unstable vibrations of an unsymmetrical shaft with linear spring characteristics at the secondary critical speed.

CONTENTS

General Introduction

With the recent rapid developments of industries, the machinery equipped in various plants has kept growing larger and increasing its speed and efficiency. Especially rotating machines, such as turbines, pumps, blowers, generators, motors and compressors which are used in thermoelectric and atomic power plants, large industrial complexes and large transportation facilities often operate at very high speed, far in excess of the first critical speed. Nowadays, in order to realize the high generating power and high-speed running of these rotating machines, the shaft length is increased but its diameter is not enlarged because the diameter is restricted by stresses due to centrifugal force. This makes an elastic shaft still more flexible and vibrations in high-speed operation become a serious problem. Therefore high-performance above the critical speed is required in rotating machines which are regarded as the heart of each industrial plant.

The first problem in the design of these machines is the determination of the natural frequencies. For a long time, Stodola's method[1], Rayleigh's method[2] and an experimental formula of Dunkerlay[2] have been used for the approximate calculation of the whirling natural frequencies of an elastic shaft. Holzer's method and Lewis's method[2, 3] have been used for determination of the tortional natural frequencies. Nowadays, since the calculation method for critical speeds and balancing technics have made rapid progress thanks to the advance and propagation of electronic computers, it becomes possible for rotating machines to operate with small amplitude at the high speed above the major critical speed. But, the following problems remain for vibration proofing. For example, the shaft of a turbogenerator has slots where the winding is set up, and then the unsymmetry of flexural stiffness is generated. Similarly, the two-pole motor and propellar shaft of an aircraft have the unsymmetry of moment of inertia. As the results of these unsymmetries, the shaft stiffness and the moment of inertia vary with double the shaft speed. Then these systems belong to a parametrically excited system. The study of parametric resonance in a linear system has been carried out on the unstable vibration at the major critical speed[4~7], and on the dynamical unstable region at the sub-critical speed[8, 9]. In addition, there exist studies on the secondary critical speed of the unsymmetrical shaft supported horizontally[4~7, 10~13, 20~23]. In the neighborhood of this critical speed, the shaft whirls with double the shaft speed. Most papers on the rotating shaft system having such unsymmetries are confined to studies in linear systems. In general, rotating machines often have such unsymmetries with various degrees. As the rotating speed of machinery increases recently, the necessity of solving various troubles caused by the unsymmetries tends to increase.

The literatures on nonlinear oscillations are confined to rectilinear systems. The research of nonlinear oscillations originated in the work on acoustics by Lord Rayleigh, and the problem of three bodies in celestical mechanics by Poincarè at the end of the 19th century. In 1918, Duffing reported on the equation known as "Duffing's Equation" which expressed the forced oscillation in a mechanical system with nonlinear restoring forces. After Van der Pol, a physicist in the Netherlands,

reported a paper on the theory of a triode's oscillation in 1926, many researchers had interest in the nonlinear problems. Thereafter, the theory of nonlinear oscillations was advanced remarkably, especially in the Soviet Union. Untill now, a large number of papers on this problem have been reported in many countries, and most of these papers are summerized in the book of Nayfeh[24]. But there are few studies on rotating shaft systems with nonlinear spring characteristics. The rotating shaft system has dynamical characteristics different from those of a rectilinear vibratory system. For example, because of the existence of gyro moments, the shaft performs forward and backward precessional movements and the natural frequencies have positive and negative values whose magnitudes vary with the rotating speed of the shaft. The nonlinearities in rotating shaft systems are produced by the characteristics of oil film in journal bearings, the angular clearance in rolling bearings, the hysteresis and the spring characteristics of rubbers for vibration proofing, the construction of bearing pedestals, the fitting condition between a rotor and a shaft, and the structure of a foundation. In rotating machines, plain and rolling bearings are generally used. The former are often used in a large high-speed rotating machine. There exist many studies on oil whip caused by oil films in journal bearings[25, 26]. Subharmonic oscillations of order $1/2$[27] and $1/3$[28] which are caused by the nonlinearity of oil film have also been reported in practical machines. For reasons of economy, maintenance and care, rolling bearings are often used in the general rotating machines. In rotating machines where ball bearings are used, there appear oscillations due to the irregularity of ball diameters or the passing of balls[29~31], and nonlinear oscillations, such as subharmonic oscillations[32~36] and summed-and differential harmonic oscillations[33~37]. Nonlinear characteristics are caused by the angular clearance of a bearing. Recently, a new consideration for nonlinear spring characteristics in a rotating shaft system was reported[38, 39], and then the physical meanings of nonlinear oscillations become clear. In the rectilinear vibratory system, there are some reports on other kinds of nonlinear oscillations — that is, super-harmonic oscillations[40, 41], super-subharmonic oscillations[42], super-summed-and-differential harmonic oscillations[43, 44], combination tones[45~47], sub-combination tones[48~50], and internal resonances[51~55] which occur when there is a proportional relation among the natural frequencies in the multidegree-of-freedom system.

In previous studies on the vibrations of a rotating shaft system, nonlinear spring characteristics and unsymmetries of a rotor and a shaft have been treated independently. But, as for the nonlinear oscillations in a rotating shaft system with both nonlinearity and unsymmetry, only the subharmonic oscillation of an unsymmetrical shaft[56] was recently reported. We have developed studies on an unsymmetrical shaft system and an unsymmetrical rotor system where unsymmetry and nonlinearity coexist, and have clarified the characteristics of various oscillations occuring in such systems[57~60]. Furthermore, we also experimentally and theoretically solved new vibratory phenomena in the system with either nonlinearity or unsymmetry[61, 62].

This paper is composed of seven chapters. Chapter 1 is related to the experimental apparatus and the equations of motion of the rotating shaft system.

Chapter 2 deals with nonlinear forced oscillation at the major critical speed[57]. In this chapter, we have clarified that the unstable vibration appearing in a linear system with an unsymmetrical rotor vanishes in a nonlinear system and the stationary resonance curves of hard or soft spring type are obtained. It is also

clarified that jump phenomena appear once or twice during the deceleration process of the shaft speed and which type of phenomenon appears depends on the angular position of a rotor unbalance.

In Chapters 3, 4 and 5, we discuss other kinds of nonlinear forced oscillations in the system where a disc is mounted on an unsymmetrical shaft (called an unsymmetrical shaft system) and the system where an unsymmetrical rotor is mounted on a round shaft (called an unsymmetrical rotor system). In Chapter 3, we analyze the summed-and-differential harmonic oscillation[58] in the unsymmetrical shaft system with nonlinear spring characteristics, and find that owing to the coexistence of nonlinearity and unsymmetry an unstable vibration appears in a certain type of summed-and-differential harmonic oscillation. In this type of oscillation, four typical kinds of resonance curves were obtained by changing the assembly condition. Also, it is clarified that no unstable vibration appears in the other types of summed-and-differential harmonic oscillations. The characteristics of summed-and-differential harmonic oscillations are qualitatively the same as those of corresponding subharmonic oscillations[56]. These analytical results were verified by experiments. Chapter 4 deals with the subharmonic and the summed-and-differential harmonic oscillations in an unsymmerical rotor system with nonlinear spring characteristics[59]. Such a characteristic as unstable vibrations appears due to the coexistence of the nonlinearity and the unsymmetry of a rotor is qualitatively the same as that in the unsymmetrical shaft system[56, 58].

In Chapter 5, we discuss the super-summed-and-differential harmonic oscillations in the unsymmetrical shaft system and the unsymmetrical rotor system[60]. Comparing with the symmetrical system where a disc is mounted on a round shaft, we clarify the points that the unsymmetry of a shaft or a rotor makes the oscillation apt to occur, and that an unstable vibration sometimes appears.

In Chapter 6, we show that sub-combination tones[61] appear with the frequency of 3/2 times the precessional speed of the steel ball owing to the irregularity of balls in the bearing. Also we present the theoretical and the experimental results relevant to the cause of appearance, mechanism, and the vibratory characteristics of this type of oscillation.

In Chapter 7, we treat the linear phenomenon of the secondary critical speed[62] in the system where an unsymmetrical shaft is vertically supported by single-row deep groove ball bearings. It is clarified that the cause of this unstable vibration is the coexistence of the shaft unsymmetry and the non-uniform elastic support. In experiments, we observed the unstable vibration of double the frequency of the shaft speed which appeared in a comparatively wide region near the secondary critical speed. Furthermore, we have clarified theoretically and experimentally that this kind of unstable vibration does not appear at all in an unsymmetrical rotor system, and then that this vibration is a peculiar phenomenon to an unsymmetrical shaft system.

1. Experimental Apparatus and Equations of Motion

1. 1. Introduction

Practical machines often have the unsymmetry of a shaft stiffness due to a key way and a slot installed on a shaft, or the unsymmetry of a moment of inertia of a rotor such as a bipolar generator or a propeller. As simple models of the

above systems, we manufactured the vertical rotating shaft systems, such as an unsymmetrical shaft system where a disc was mounted on an unsymmetrical shaft and an unsymmetrical rotor system where an unsymmetrical rotor was mounted on an elastic shaft with circular cross section.

The experimental apparatus is a four-degree-of-freedom system where the deflection r and the inclination θ of a rotor couple each other. When these two quantities do not couple, the inclination oscillation is independent of the deflection oscillation. As given in the following chapters, the qualitative characteristics of the coupled four-degree-of-freedom system are the same as those of this two-degree-of-freedom system expressing the inclination oscillation. In this chapter, we give outlines of the experimental apparatus and the method of experiments. In addition, we present the equations of motion of r and θ in the four-degree-of-freedom system and those of θ in the two-degree-of-freedom system used in Chapters 2~5. The nonlinear terms in those equations are represented by the rectangular coordinates and the polar coordinates, respectively[38,39]. Also, we give the frequency equation for each system.

1. 2. Experimental apparatus and method of experiments

Figures 1.1 and 1.2 show the experimental apparatuses of an unsymmetrical rotor system where an unsymmetrical rotor was mounted on a round shaft and an

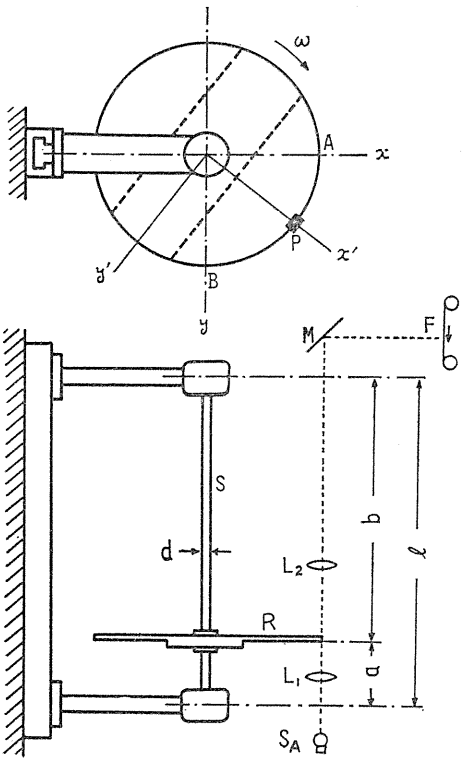

Fig. 1. 1. Experimental apparatus (an unsymmetrical rotor system).

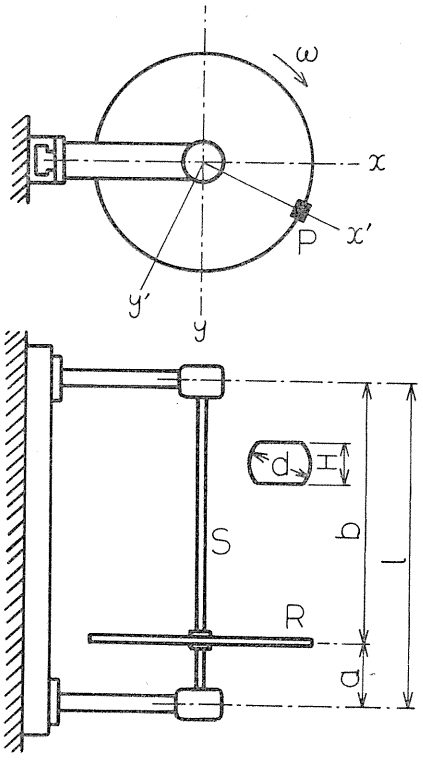

Fig. 1. 2. Experimental apparatus (an unsymmetrical shaft system).

unsymmetrical shaft system where a disc was mounted on an unsymmetrical shaft, respectively. The system in Fig. 1.1 was used in Chapters 2, 4, 5 and 7, and the system in Fig. 1.2 was used in Chapters 3, 5 and 7. In addition to these systems, a symmetrical system where a disc was mounted on a round shaft was used in Chapter 6. In Figs. 1.1 and 1.2, the shaft is 700mm in length, and the rotor is mounted at the position of $a : b = 1 : 4$. The boundary condition is a simple support at the upper shaft end where a self-aligning double-row ball bearing (#1200) is used. The dimensions of a rotor, a shaft and a single-row deep groove ball bearing at the lower end are different in each chapter. Tables 1.1 and 1.2 show the dimensions of the rotors $R_1 \sim R_4$, the shafts $S_1 \sim S_5$ and the lower bearings which were used in each chapter. In Table 1.1, the mass of a rotor is denoted by m, the moments of inertia of an unsymmetrical rotor about the x'- and y'-axes shown

Table 1. 1. Dimensions of rotors.

Unsymmetrical rotor	m (kg)	I_p(kg·m²)	I_1(kg·m²)	I_2(kg·m²)	Relating chapters
R_1	9.746	0.2342	0.1558	0.0799	2
R_2	8.791	0.2039	0.1593	0.0479	4, 5, 7

Disc	m (kg)	D(mm)	h (mm)	I_p(kg·m²)	I(kg·m²)	Relating chapters
R_3	7.87	481.3	5.55	0.2279	0.1140	3, 5, 6, 7
R_4	6.655	364.8	8.24	0.1131	0.0566	3

Table 1. 2. Dimensions of shafts and bearings at the lower end.

Round shaft	d (mm)	l (mm)	Bearing No.	Relating chapters
S_1	12	700	#6204	2, 6
S_2	12	700	#6200	4, 5, 7

Unsymmetrical shaft	d (mm)	l (mm)	H (mm)	Bearing No.	Relating chapters
S_3	12	700	8	#6200	3
S_4	16	700	11.5	#6200	5
S_5	16	700	11	#6200	7

in Fig. 1.1 by I_1 and I_2 $(I_1 > I_2)$ respectively, the polar moment of inertia of a rotor by I_p, the diameter of a disc by D, the thickness by h, and the diametral moment of inertia of a disc by I. In Table 1.2, the diameter of a round shaft is denoted by d, and the thickness of an unsymmetrical shaft, which was made by cutting both sides of a round shaft of the diameter d, by H (see Fig. 1.2). In Chapters 2~5, the shaft had nonlinear spring characteristics owing to the angular clearance in the lower bearing, and various types of nonlinearities appeared depend-

ing on the degree of discrepancy between the center lines of the upper and the lower bearings.

The shaft was driven in the direction of an arrow (see Figs. 1.1 and 1.2) through a V-pulley and a spring coupling by a 5 HP DC motor. The rotating speed of a shaft varied from 0 to 6000rpm.

In experiments, the shaft deflections were measured optically in x- and y-directions by recording the movement of a rotor edge as shown in Fig. 1.1. A light source S_A with a band-shaped filament was set under the rotor and a real image was produced at the rotor edge (the point A). This image was partly obscured by the rotor before passing through the lens L_2, then it was reflected away by the mirror M and focused again on the film F. The deflection in the y-direction was also measured at the point B in the same way. The rotating marks were recorded on the film F at each revolution of the shaft by a piece of paper P mounted at the rotor edge. The rotating speed of the shaft could be directly read by a digital counter, or it could be found by counting the rotating marks and the time marks with the interval of 0.01 seconds recorded on the film F.

1. 3. Equations of motion

In order to present the equations of motion which express the movement of a shaft in the systems shown in Figs. 1.1 and 1.2, we show the coordinate systems of experimental apparatuses in Figs. 1.3 (an unsymmetrical rotor system) and 1.4 (an unsymmetrical shaft system), respectively. The system where a rotor is mounted on a light elastic shaft generally has six degrees of freedom. But, if the deflection and the inclination of the rotor is small, this system can be approximately treated as a four-degree-of-freedom system. This is because the deflection in the longitudinal direction of the shaft is negligible and the angle of rotation is determined approximately by the rotating speed of the motor.

In Fig. 1.3, O-xyz represents the stationary rectangular coordinate system, M-XYZ the rectangular coordinate system which has its origin at the geometrical center M of the system O-xyz, and M-$X_2Y_2Z_1$ the rotating rectangular coordinate system whose axes coincide with the principle axes of the moments of inertia of

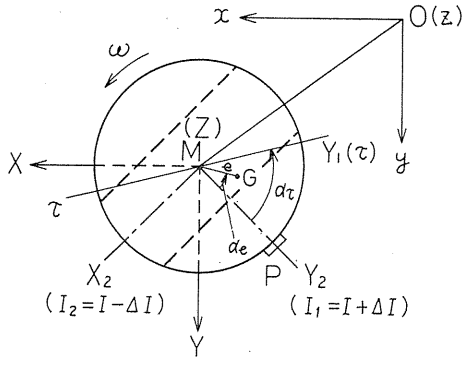

Fig. 1. 3. Coordinate system (an unsymmetrical rotor system).

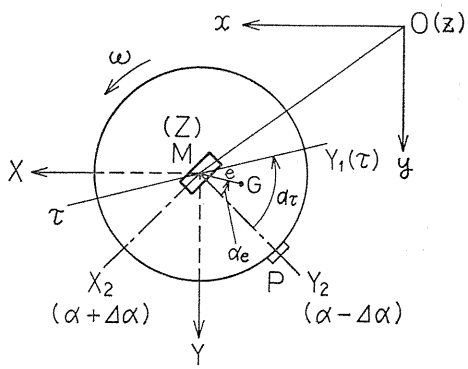

Fig. 1. 4. Coordinate system (an unsymmetrical shaft system).

the rotor. When the shaft is at rest, the point M coincides with the original point O. Though M moves in the longitudinal direction of the shaft as the shaft deflects, M is considered to move in the xy-plane because of the small shaft deflection. The distance between the gravitational center G and the geometrical center M of the rotor represents the eccentricity e (i. e., the static unbalance), and the deviation angle between the direction of the polar moment of inertia of the rotor (Z_1-axis) and the tangential direction of the shaft is denoted by τ (i. e., the dynamic unbalance). We suppose that the unbalances e and τ exist at the angular positions α_e and α_τ measured from the MY_2-axis in the direction of the shaft rotation. Let the rotating speed of the shaft be ω, the mass of the rotor be m, the polar moment of inertia of the unsymmetrical rotor I_p, the other principal moments of inertia I_1 and I_2 ($I_1>I_2$), the mean and the difference of these diametral moments of inertia $I=(I_1+I_2)/2$ and $\Delta I=(I_1-I_2)/2$, the spring constants of the shaft α, γ and δ, and the damping coefficients c_{11}, c_{12}, c_{21} ($=c_{12}$) and c_{22}. We denote the coordinates of the geometrical center M by x and y, the projectional angles of inclination of the shaft θ to the xz- and yz- planes by θ_x and θ_y, and the nonlinear restoring forces in x, y, θ_x and θ_y by N_x, N_y, $N_{\theta x}$ and $N_{\theta y}$, respectively. The time when the principal axis MY_2 passes the XMZ plane is taken as $t=0$.

Here, for simplicity, we difine the following dimensionless quantities by using the quality $e_0=mg/\alpha$:

$$\left.\begin{aligned}
&x'=x/e_0,\ y'=y/e_0,\ \theta'_x=\theta_x/(e_0\sqrt{m/I}),\ \theta'_y=\theta_y/(e_0\sqrt{m/I}),\\
&i_p=I_p/I,\ \Delta_i=\Delta I/I,\ t'=t\sqrt{\alpha/m},\ \omega'=\omega\sqrt{m/\alpha},\ \gamma'=\gamma/(\alpha\sqrt{I/m}),\\
&\delta'=m\delta/(\alpha I),\ c'_{11}=c_{11}/\sqrt{m\alpha},\ c'_{12}=c'_{21}=c_{12}/\sqrt{\alpha I},\ c'_{22}=c_{22}/(I\sqrt{\alpha/m}),\\
&e'=e/e_0,\ \tau'=\tau/(e_0\sqrt{m/I}),\ N'_x=N_x/(\alpha e_0),\ N'_y=N_y/(\alpha e_0),\\
&N'_{\theta x}=N_{\theta x}/(\alpha e_0\sqrt{I/m}),\ N'_{\theta y}=N_{\theta y}/(\alpha e_0\sqrt{I/m})
\end{aligned}\right\}\quad(1.1)$$

Then, we obtain the following equations of motion[16] for the unsymmetrical rotor system having four degrees of freedom provided we omit the primes from the symbols:

$$\left.\begin{aligned}
&\ddot{x}+c_{11}\dot{x}+c_{12}\dot{\theta}_x+x+\gamma\theta_x+N_x=e\omega^2\cos(\omega t+\alpha_e)\\
&\ddot{y}+c_{11}\dot{y}+c_{12}\dot{\theta}_y+y+\gamma\theta_y+N_y=e\omega^2\sin(\omega t+\alpha_e)\\
&\ddot{\theta}_x+i_p\omega\dot{\theta}_y+c_{21}\dot{x}+c_{22}\dot{\theta}_x+\gamma x+\delta\theta_x-\Delta_i\frac{d}{dt}(\dot{\theta}_x\cos 2\omega t+\dot{\theta}_y\sin 2\omega t)\\
&\qquad+N_{\theta x}=\tau\omega^2\{(i_p-1)\cos(\omega t+\alpha_\tau)-\Delta_i\cos(\omega t-\alpha_\tau)\}\\
&\ddot{\theta}_y-i_p\omega\dot{\theta}_x+c_{21}\dot{y}+c_{22}\dot{\theta}_y+\gamma y+\delta\theta_y-\Delta_i\frac{d}{dt}(\dot{\theta}_x\sin 2\omega t-\dot{\theta}_y\cos 2\omega t)\\
&\qquad+N_{\theta y}=\tau\omega^2\{(i_p-1)\sin(\omega t+\alpha_\tau)-\Delta_i\sin(\omega t-\alpha_\tau)\}
\end{aligned}\right\}\quad(1.2)$$

We select the quantity $\tau_0=e_0\sqrt{m/I}$ and exchange some of Eq. (1.1) for the

following dimensionless quantities:

$$\left.\begin{aligned} &t'=t\sqrt{\delta/I},\ \omega'=\omega\sqrt{I/\delta},\ c'=c/\sqrt{\delta I},\ \tau'=\tau/\tau_0,\\ &N'_{\theta x}=N_{\theta x}/(\delta\tau_0),\ N'_{\theta y}=N_{\theta y}/(\delta\tau_0)\end{aligned}\right\} \tag{1.3}$$

Then, from Eq. (1.2), we get the equations of motion for the inclination oscillation in the two-degree-of-freedom system as follows:

$$\left.\begin{aligned} &\ddot{\theta}_x+i_p\omega\dot{\theta}_y+c\dot{\theta}_x+\theta_x-\Delta_i\frac{d}{dt}(\dot{\theta}_x\cos 2\omega t+\dot{\theta}_y\sin 2\omega t)+N_{\theta x}\\ &\qquad=\tau\omega^2\{(1-i_p)\cos(\omega t+\alpha_i)+\Delta_i\cos(\omega t-\alpha_i)\}\\ &\ddot{\theta}_y-i_p\omega\dot{\theta}_x+c\dot{\theta}_y+\theta_y-\Delta_i\frac{d}{dt}(\dot{\theta}_x\sin 2\omega t-\dot{\theta}_y\cos 2\omega t)+N_{\theta y}\\ &\qquad=\tau\omega^2\{(1-i_p)\sin(\omega t+\alpha_i)+\Delta_i\sin(\omega t-\alpha_i)\}\end{aligned}\right\} \tag{1.4}$$

where we denote the damping coefficient by c, and transform α_τ to α_i $(=\alpha_\tau+\pi)$ in order to make the amplitude of excitation positive because we consider the cylindrical rotor such as $i_p<1$ in Eq. (1.4).

Next, we consider the unsymmetrical shaft system. As the coordinates of this system shown in Fig. 1.4 is nearly the same as that in Fig. 1.3, we state only the different points. The system M-$X_2Y_2Z_1$ is the rotating rectangular coordinate system which composes of the principal axes of the second moments of area of the unsymmetrical shaft. We denote the polar and the diametral moments of inertia by I_p and I, the spring constants in the direction of the MX_2-axis of the unsymmetrical shaft by $\alpha+\Delta\alpha$, $\gamma+\Delta\gamma$ and $\delta+\Delta\delta$, and those in the direction of the MY_2-axis by $\alpha-\Delta\alpha$, $\gamma-\Delta\gamma$ and $\delta-\Delta\delta$. Here, we designate the second moments of area about the MX_2- and MY_2-axes as I_y' and I_x' $(I_y'<I_x')$, respectively. If the shape of the cross section of the unsymmetrical shaft is uniform all over the shaft, the following relation holds[16]:

$$\frac{\Delta\alpha}{\alpha}=\frac{\Delta\gamma}{\gamma}=\frac{\Delta\delta}{\delta}=\frac{I_x'-I_y'}{I_x'+I_y'} \tag{1.5}$$

For simplicity, using Eq. (1.1) and the symbols $\Delta_{11}=\Delta\alpha/\alpha$, $\Delta_{12}=\gamma'$ $(\Delta\gamma/\gamma)$, and $\Delta_{22}=\delta'(\Delta\delta/\delta)$, we obtain the dimensionless equations of motion for the unsymmetrical shaft system having four degrees of freedom as follows[16]:

$$\left.\begin{aligned} &\ddot{x}+c_{11}\dot{x}+c_{12}\dot{\theta}_x+x+\gamma\theta_x-\Delta_{11}(x\cos 2\omega t+y\sin 2\omega t)\\ &\qquad-\Delta_{12}(\theta_x\cos 2\omega t+\theta_y\sin 2\omega t)+N_x=e\omega^2\cos(\omega t+\alpha_e)\\ &\ddot{y}+c_{11}\dot{y}+c_{12}\dot{\theta}_y+y+\gamma\theta_y-\Delta_{11}(x\sin 2\omega t-y\cos 2\omega t)\\ &\qquad-\Delta_{12}(\theta_x\sin 2\omega t-\theta_y\cos 2\omega t)+N_y=e\omega^2\sin(\omega t+\alpha_e)\\ &\ddot{\theta}_x+i_p\omega\dot{\theta}_y+c_{21}\dot{x}+c_{22}\dot{\theta}_x+\gamma x+\delta\theta_x-\Delta_{12}(x\cos 2\omega t+y\sin 2\omega t)\\ &\qquad-\Delta_{22}(\theta_x\cos 2\omega t+\theta_y\sin 2\omega t)+N_{\theta x}=(i_p-1)\tau\omega^2\cos(\omega t+\alpha_\tau)\end{aligned}\right\} \tag{1.6}$$

$$\left.\begin{aligned}&\ddot{\theta}_y-i_p\omega\dot{\theta}_x+c_{21}\dot{y}+c_{22}\dot{\theta}_y+\gamma y+\delta\theta_y-\Delta_{12}(x\sin 2\omega t-y\cos 2\omega t)\\&\quad-\Delta_{22}(\theta_x\sin 2\omega t-\theta_y\cos 2\omega t)+N_{\theta y}=(i_p-1)\tau\omega^2\sin(\omega t+\alpha_\tau)\end{aligned}\right\}$$

where the primes of the dimensionless quantities are omitted. Putting $\gamma=0$ and $c_{12}=c_{21}=0$ in Eq. (1.6), we get the equations of motion for the inclination oscillation in the two-degree-of-freedom system as follows:

$$\left.\begin{aligned}&\ddot{\theta}_x+i_p\omega\dot{\theta}_y+c\dot{\theta}_x+\theta_x-\Delta_s(\theta_x\cos 2\omega t+\theta_y\sin 2\omega t)+N_{\theta x}\\&\qquad=(1-i_p)\tau\omega^2\cos(\omega t+\alpha_s)\\&\ddot{\theta}_y-i_p\omega\dot{\theta}_x+c\dot{\theta}_y+\theta_y-\Delta_s(\theta_x\sin 2\omega t-\theta_y\cos 2\omega t)+N_{\theta y}\\&\qquad=(1-i_p)\tau\omega^2\sin(\omega t+\alpha_s)\end{aligned}\right\}\qquad(1.7)$$

where the dimensionless quantities in Eq. (1.3), $c(=c_{22})$ and Δ_s $(=\Delta_{22})$ are used. We transform α_τ to α_i $(=\alpha_\tau+\pi)$.

Supposing that the nonlinear terms in the above equations of motion compose of the second power terms of coordinates (the unsymmetrical nonlinear terms) and the third power terms (the symmetrical nonlinear terms), we obtain the dimensionless potential energy V in the two-degree-of-freedom system as follows [38, 39]:

$$V=V_0+\sum_{\substack{i,j=0\\(i+j=3)}}^{3}\varepsilon_{ij}\theta_x^i\theta_y^j+\sum_{\substack{i,j=0\\(i+j=4)}}^{4}\beta_{ij}\theta_x^i\theta_y^j\qquad(1.8)$$

where V_0 is the potential energy due to linear restoring forces, and ε_{ij} $(i+j=3)$ and β_{ij} $(i+j=4)$ are the coefficients of the unsymmetrical and the symmetrical nonlinear terms, respectively. Partially differentiating Eq. (1.8) with respect to θ_x and θ_y, we get the nonlinear terms $N_{\theta x}$ and $N_{\theta y}$ as follows:

$$\left.\begin{aligned}N_{\theta x}&=(3\varepsilon_{30}\theta_x^2+2\varepsilon_{21}\theta_x\theta_y+\varepsilon_{12}\theta_y^2)+(4\beta_{40}\theta_x^3+3\beta_{31}\theta_x^2\theta_y+2\beta_{22}\theta_x\theta_y^2+\beta_{13}\theta_y^3)\\N_{\theta y}&=(\varepsilon_{21}\theta_x^2+2\varepsilon_{12}\theta_x\theta_y+3\varepsilon_{03}\theta_y^2)+(\beta_{31}\theta_x^3+2\beta_{22}\theta_x^2\theta_y+3\beta_{13}\theta_x\theta_y^2+4\beta_{04}\theta_y^3)\end{aligned}\right\}\qquad(1.9)$$

where the first terms in the right side represent the unsymmetrical nonlinear terms, and the second terms does the symmetrical ones. Equation (1.9) is represented by the stationary rectangular coordinates (θ_x, θ_y). In the rotating shaft system, however, if Eq. (1.9) is expressed with the polar coordinates (θ, φ) transformed by $\theta_x=\theta\cos\varphi$ and $\theta_y=\theta\sin\varphi$, the dynamical meanings of the spring characteristics become clear [38, 39]. Thus, adopting this polar coordinate expression, Eq. (1.8) is represented as follows:

$$\begin{aligned}V&=V_0+(\varepsilon_c^{(1)}\cos\varphi+\varepsilon_s^{(1)}\sin\varphi+\varepsilon_c^{(3)}\cos 3\varphi+\varepsilon_s^{(3)}\sin 3\varphi)\theta^3\\&\quad+(\beta^{(0)}+\beta_c^{(2)}\cos 2\varphi+\beta_s^{(2)}\sin 2\varphi+\beta_c^{(4)}\cos 4\varphi+\beta_s^{(4)}\sin 4\varphi)\theta^4\\&=V_0+\{\varepsilon^{(1)}\cos(\varphi-\varphi_1)+\varepsilon^{(3)}\cos 3(\varphi-\varphi_3)\}\theta^3\\&\quad+\{\beta^{(0)}+\beta^{(2)}\cos 2(\varphi-\varphi_2)+\beta^{(4)}\cos 4(\varphi-\varphi_4)\}\theta^4\end{aligned}\qquad(1.10)$$

where the notations in Eq. (1.10) are follows:

$$\left.\begin{aligned}&\varepsilon^{(1)}=\sqrt{\varepsilon_c^{(1)2}+\varepsilon_s^{(1)2}},\ \varepsilon^{(3)}=\sqrt{\varepsilon_c^{(3)2}+\varepsilon_s^{(3)2}},\ \beta^{(2)}=\sqrt{\beta_c^{(2)2}+\beta_s^{(2)2}},\\&\beta^{(4)}=\sqrt{\beta_c^{(4)2}+\beta_s^{(4)2}},\ \varphi_1=\tan^{-1}(\varepsilon_s^{(1)}/\varepsilon_c^{(1)}),\ \varphi_3=(1/3)\tan^{-1}(\varepsilon_s^{(3)}/\varepsilon_c^{(3)}),\\&\varphi_2=(1/2)\tan^{-1}(\beta_s^{(2)}/\beta_c^{(2)}),\ \varphi_4=(1/4)\tan^{-1}(\beta_s^{(4)}/\beta_c^{(4)})\end{aligned}\right\}\quad(1.11)$$

The magnitudes of the terms in Eq. (1.10) change periodically during one cycle of φ (from 0 to 2π). The numbers of times of these changes are represented by figures in the parentheses in the coefficients in Eq. (1.10). Hereafter, the nonlinear component which changes n times while φ changes from 0 to 2π is designated by the symbol $N(n)$. As for the nonlinear terms up to the third power terms of coordinates, $N(1)$ and $N(3)$ are the unsymmetrical nonlinear components, and $N(0)$, $N(2)$ and $N(4)$ the symmetrical nonlinear ones. Between the coefficients expressed by polar coordinates and those by rectangular coordinates, the following relationships hold[38, 39]:

$$\left.\begin{aligned}&\varepsilon_c^{(1)}=(3\varepsilon_{30}+\varepsilon_{12})/4,\ \varepsilon_s^{(1)}=(\varepsilon_{21}+3\varepsilon_{03})/4,\ \varepsilon_c^{(3)}=(\varepsilon_{30}-\varepsilon_{12})/4,\\&\varepsilon_s^{(3)}=(\varepsilon_{21}-\varepsilon_{03})/4,\ \beta^{(0)}=(3\beta_{40}+\beta_{22}+3\beta_{04})/8,\ \beta_c^{(2)}=(\beta_{40}-\beta_{04})/2,\\&\beta_s^{(2)}=(\beta_{31}+\beta_{13})/4,\ \beta_c^{(4)}=(\beta_{40}-\beta_{22}+\beta_{04})/8,\ \beta_s^{(4)}=(\beta_{31}-\beta_{13})/8\end{aligned}\right\}\quad(1.23)$$

Next, we obtain the dimensionless potential energy V in the four-degree-of-freedom system as follows[38]:

$$V=V_0+\sum_{\substack{i,j,k,l=0\\(i+j+k+l=3)}}^{3}\varepsilon_{ijkl}x^iy^j\theta_x^k\theta_y^l+\sum_{\substack{i,j,k,l=0\\(i+j+k+l=4)}}^{4}\beta_{ijkl}x^iy^j\theta_x^k\theta_y^l\qquad(1.13)$$

where V_0 is related to the linear spring characteristics, and ε_{ijkl} $(i+j+k+l=3)$ and β_{ijkl} $(i+j+k+l=4)$ are the coefficients of the unsymmetrical and the symmetrical nonlinear terms, respectively. The nonlinear terms N_x, N_y, $N_{\theta x}$ and $N_{\theta y}$ in Eqs. (1.2) and (1.6) are given by differentiating partially with respect to the coordinates designated by subscripts. Substituting the following transformation into Eq. (1.13):

$$x=r\cos\varphi_r,\ y=r\sin\varphi_r,\ \theta_x=\theta\cos\varphi_\theta,\ \theta_y=\theta\sin\varphi_\theta\qquad(1.14)$$

we get the equation represented by the polar coordinates as follows[38]:

$$\begin{aligned}V=V_0+\Big[&[(\varepsilon_{30c}^{(1)}\cos\varphi_r+\varepsilon_{30s}^{(1)}\sin\varphi_r)r^3+\{\varepsilon_{21c}^{(1)}\cos\varphi_\theta+\varepsilon_{21s}^{(1)}\sin\varphi_\theta\\&+\varepsilon_{21c}^{\prime(1)}\cos(2\varphi_r-\varphi_\theta)+\varepsilon_{21s}^{\prime(1)}\sin(2\varphi_r-\varphi_\theta)\}r^2\theta+\{\varepsilon_{12c}^{(1)}\cos\varphi_r\\&+\varepsilon_{12s}^{(1)}\sin\varphi_r+\varepsilon_{12c}^{\prime(1)}\cos(2\varphi_\theta-\varphi_r)+\varepsilon_{12s}^{\prime(1)}\sin(2\varphi_\theta-\varphi_r)\}r\theta^2\\&+(\varepsilon_{03c}^{(1)}\cos\varphi_\theta+\varepsilon_{03s}^{(1)}\sin\varphi_\theta)\theta^3]+[(\varepsilon_{30c}^{(3)}\cos3\varphi_r+\varepsilon_{30s}^{(3)}\sin3\varphi_r)r^3\\&+\{\varepsilon_{21c}^{(3)}\cos(2\varphi_r+\varphi_\theta)+\varepsilon_{21s}^{(3)}\sin(2\varphi_r+\varphi_\theta)\}r^2\theta\\&+\{\varepsilon_{12c}^{(3)}\cos(2\varphi_\theta+\varphi_r)+\varepsilon_{12s}^{(3)}\sin(2\varphi_\theta+\varphi_r)\}r\theta^2\end{aligned}$$

$$+(\varepsilon_{03c}^{(3)}\cos 3\varphi_\theta+\varepsilon_{03s}^{(3)}\sin 3\varphi_\theta)\theta^3]\Big]$$
$$+\Big[[\beta_{40}^{(0)}r^4+\{\beta_{31c}^{(0)}\cos(\varphi_r-\varphi_\theta)+\beta_{31s}^{(0)}\sin(\varphi_r-\varphi_\theta)\}r^3\theta$$
$$+\{\beta_{22}^{(0)}+\beta_{22c}^{(0)}\cos 2(\varphi_r-\varphi_\theta)+\beta_{22s}^{(0)}\sin 2(\varphi_r-\varphi_\theta)\}r^2\theta^2$$
$$+\{\beta_{13c}^{(0)}\cos(\varphi_\theta-\varphi_r)+\beta_{13s}^{(0)}\sin(\varphi_\theta-\varphi_r)\}r\theta^3+\beta_{04}^{(0)}\theta^4]$$
$$+[(\beta_{40c}^{(2)}\cos 2\varphi_r+\beta_{40s}^{(2)}\sin 2\varphi_r)r^4+\{\beta_{31c}^{(2)}\cos(\varphi_r+\varphi_\theta)$$
$$+\beta_{31s}^{(2)}\sin(\varphi_r+\varphi_\theta)+\beta_{31c}^{\prime(2)}\cos(3\varphi_r-\varphi_\theta)+\beta_{31s}^{\prime(2)}\sin(3\varphi_r-\varphi_\theta)\}r^3\theta$$
$$+\{\beta_{22c}^{(2)}\cos 2\varphi_r+\beta_{22s}^{(2)}\sin 2\varphi_r+\beta_{22c}^{\prime(2)}\cos 2\varphi_\theta+\beta_{22s}^{\prime(2)}\sin 2\varphi_\theta\}r^2\theta^2$$
$$+\{\beta_{13c}^{(2)}\cos(\varphi_\theta+\varphi_r)+\beta_{13s}^{(2)}\sin(\varphi_\theta+\varphi_r)+\beta_{13c}^{\prime(2)}\cos(3\varphi_\theta-\varphi_r)$$
$$+\beta_{13s}^{\prime(2)}\sin(3\varphi_\theta-\varphi_r)\}r\theta^3+(\beta_{04c}^{(2)}\cos 2\varphi_\theta+\beta_{04s}^{(2)}\sin 2\varphi_\theta)\theta^4]$$
$$+[(\beta_{40c}^{(4)}\cos 4\varphi_r+\beta_{40s}^{(4)}\sin 4\varphi_r)r^4$$
$$+\{\beta_{31c}^{(4)}\cos(3\varphi_r+\varphi_\theta)+\beta_{31s}^{(4)}\sin(3\varphi_r+\varphi_\theta)\}r^3\theta$$
$$+\{\beta_{22c}^{(4)}\cos 2(\varphi_r+\varphi_\theta)+\beta_{22s}^{(4)}\sin 2(\varphi_r+\varphi_\theta)\}r^2\theta^2+\{\beta_{13c}^{(4)}\cos(3\varphi_\theta+\varphi_r)$$
$$+\beta_{13s}^{(4)}\sin(3\varphi_\theta+\varphi_r)\}r\theta^3+(\beta_{04c}^{(4)}\cos 4\varphi_\theta+\beta_{04s}^{(4)}\sin 4\varphi_\theta)\theta^4]\Big] \qquad (1.15)$$

where the numbers in the parentheses of the coefficients represent n of $N(n)$. For example, the value of $\varphi_r-\varphi_\theta$ is constant while φ_r and φ_θ change from 0 to 2π. Therefore, the terms involving $\varphi_r-\varphi_\theta$ are the nonlinear components of $N(0)$. Similarly, the terms of $2\varphi_r-\varphi_\theta$, $3\varphi_r-\varphi_\theta$, $2\varphi_r+\varphi_\theta$ and $3\varphi_r+\varphi_\theta$ represent nonlinear components of $N(1)$, $N(2)$, $N(3)$ and $N(4)$, respectively. The following relations fold between the coefficients in Eqs. (1.13) and (1.15)[38]:

$$\varepsilon_{30c}^{(1)}=(3\varepsilon_{3000}+\varepsilon_{1200})/4, \qquad \varepsilon_{30s}^{(1)}=(3\varepsilon_{0300}+\varepsilon_{2100})/4,$$
$$\varepsilon_{21c}^{(1)}=(\varepsilon_{2010}+\varepsilon_{0210})/2, \qquad \varepsilon_{21s}^{(1)}=(\varepsilon_{0201}+\varepsilon_{2001})/2,$$
$$\varepsilon_{21c}^{\prime(1)}=(\varepsilon_{2010}+\varepsilon_{1101}-\varepsilon_{0210})/4, \qquad \varepsilon_{21s}^{\prime(1)}=(\varepsilon_{0201}+\varepsilon_{1110}-\varepsilon_{2001})/4,$$
$$\varepsilon_{12c}^{(1)}=(\varepsilon_{1020}+\varepsilon_{1002})/2, \qquad \varepsilon_{12s}^{(1)}=(\varepsilon_{0102}+\varepsilon_{0120})/2,$$
$$\varepsilon_{12c}^{\prime(1)}=(\varepsilon_{1020}+\varepsilon_{0111}-\varepsilon_{1002})/4, \qquad \varepsilon_{12s}^{\prime(1)}=(\varepsilon_{0102}+\varepsilon_{1011}-\varepsilon_{0120})/4,$$
$$\varepsilon_{03c}^{(1)}=(3\varepsilon_{0030}+\varepsilon_{0012})/4, \qquad \varepsilon_{03s}^{(1)}=(3\varepsilon_{0003}+\varepsilon_{0021})/4,$$
$$\varepsilon_{30c}^{(3)}=(\varepsilon_{3000}-\varepsilon_{1200})/4, \qquad \varepsilon_{30s}^{(3)}=(-\varepsilon_{0300}+\varepsilon_{2100})/4,$$
$$\varepsilon_{21c}^{(3)}=(\varepsilon_{2010}-\varepsilon_{1101}-\varepsilon_{0210})/4, \qquad \varepsilon_{21s}^{(3)}=(-\varepsilon_{0201}+\varepsilon_{1110}+\varepsilon_{2001})/4,$$
$$\varepsilon_{12c}^{(3)}=(\varepsilon_{1020}-\varepsilon_{0111}-\varepsilon_{1002})/4, \qquad \varepsilon_{12s}^{(3)}=(-\varepsilon_{0102}+\varepsilon_{1011}+\varepsilon_{0120})/4,$$
$$\varepsilon_{03c}^{(3)}=(\varepsilon_{0030}-\varepsilon_{0012})/4, \qquad \varepsilon_{03s}^{(3)}=(-\varepsilon_{0003}+\varepsilon_{0021})/4,$$

$$
\begin{aligned}
&\beta_{40}^{(0)}=\{3(\beta_{4000}+\beta_{0400})+\beta_{2200}\}/8, \qquad \beta_{04}^{(0)}=\{3(\beta_{0040}+\beta_{0004})+\beta_{0022}\}/8,\\
&\beta_{22}^{(0)}=(\beta_{2020}+\beta_{0202}+\beta_{2002}+\beta_{0220})/4,\\
&\beta_{31c}^{(0)}=\{3(\beta_{3010}+\beta_{0301})+(\beta_{2101}+\beta_{1210})\}/8,\\
&\beta_{31s}^{(0)}=\{-3(\beta_{3001}-\beta_{0310})+(\beta_{2110}-\beta_{1201})\}/8,\\
&\beta_{22c}^{(0)}=(\beta_{2020}+\beta_{0202}-\beta_{2002}-\beta_{0220}+\beta_{1111})/8,\\
&\beta_{22s}^{(0)}=(\beta_{0211}+\beta_{1120}-\beta_{2011}-\beta_{1102})/8,\\
&\beta_{13c}^{(0)}=\{3(\beta_{1030}+\beta_{0103})+(\beta_{0121}+\beta_{1012})\}/8,\\
&\beta_{13s}^{(0)}=\{3(\beta_{1003}-\beta_{0130})+(\beta_{1021}-\beta_{0112})\}/8,\\
&\beta_{40c}^{(2)}=(\beta_{4000}-\beta_{0400})/2, \qquad \beta_{40s}^{(2)}=(\beta_{3100}+\beta_{1300})/4,\\
&\beta_{31c}^{(2)}=\{3(\beta_{3010}-\beta_{0301})-(\beta_{2101}-\beta_{1210})\}/8,\\
&\beta_{31s}^{(2)}=\{3(\beta_{3001}+\beta_{0310})+(\beta_{2110}+\beta_{1201})\}/8,\\
&\beta_{31c}^{\prime(2)}=(\beta_{3010}-\beta_{0301}+\beta_{2101}-\beta_{1210})/8, \qquad \beta_{31s}^{\prime(2)}=(-\beta_{3001}-\beta_{0310}+\beta_{2110}+\beta_{1201})/8,\\
&\beta_{22c}^{(2)}=(\beta_{2020}-\beta_{0202}+\beta_{2002}-\beta_{0220})/4, \qquad \beta_{22s}^{(2)}=(\beta_{1120}+\beta_{1102})/4,\\
&\beta_{22c}^{\prime(2)}=(\beta_{2020}-\beta_{0202}-\beta_{2002}+\beta_{0220})/4, \qquad \beta_{22s}^{\prime(2)}=(\beta_{2011}+\beta_{0211})/4,\\
&\beta_{13c}^{(2)}=\{3(\beta_{1030}-\beta_{0103})-(\beta_{0121}-\beta_{1012})\}/8,\\
&\beta_{13s}^{(2)}=\{3(\beta_{0130}+\beta_{1003})+(\beta_{1021}+\beta_{0112})\}/8,\\
&\beta_{13c}^{\prime(2)}=(\beta_{1030}-\beta_{0103}+\beta_{0121}-\beta_{1012})/8, \qquad \beta_{13s}^{\prime(2)}=(-\beta_{0130}-\beta_{1003}+\beta_{1021}+\beta_{0112})/8,\\
&\beta_{04c}^{(2)}=(\beta_{0040}-\beta_{0004})/2, \qquad \beta_{04s}^{(2)}=(\beta_{0031}+\beta_{0013})/4,\\
&\beta_{40c}^{(4)}=(\beta_{4000}+\beta_{0400}-\beta_{2200})/8, \qquad \beta_{40s}^{(4)}=(\beta_{3100}-\beta_{1300})/8,\\
&\beta_{31c}^{(4)}=(\beta_{3010}+\beta_{0301}-\beta_{2101}-\beta_{1210})/8, \qquad \beta_{31s}^{(4)}=(\beta_{3001}-\beta_{0310}+\beta_{2110}-\beta_{1201})/8,\\
&\beta_{22c}^{(4)}=(\beta_{2020}+\beta_{0202}-\beta_{2002}-\beta_{0220}-\beta_{1111})/8,\\
&\beta_{22s}^{(4)}=(\beta_{2011}+\beta_{1120}-\beta_{1102}-\beta_{0211})/8,\\
&\beta_{13c}^{(4)}=(\beta_{1030}+\beta_{0103}-\beta_{0121}-\beta_{1012})/8, \qquad \beta_{13s}^{(4)}=(\beta_{0130}-\beta_{1003}+\beta_{1021}-\beta_{0112})/8,\\
&\beta_{04c}^{(4)}=(\beta_{0040}+\beta_{0004}-\beta_{0022})/8, \qquad \beta_{04s}^{(4)}=(\beta_{0031}-\beta_{0013})/8
\end{aligned}
\tag{1.16}
$$

We denote the natural frequency of the system by p, and put $2\omega-p=\bar{p}$. The frequency equations of Eqs. (1.4) and (1.7) of the two-degree-of-freedom systems are given as follows:

For the unsymmetrical rotor system;

$$G(p)G(\bar{p})-(\Delta_i p\bar{p})^2=(1+i_p\omega p-p^2)(1+i_p\omega\bar{p}-\bar{p}^2)-(\Delta_i p\bar{p})^2=0 \quad (1.17)$$

For the unsymmetrical shaft system;

$$G(p)G(\bar{p})-\Delta_s^2=(1+i_p\omega p-p^2)(1+i_p\omega\bar{p}-\bar{p}^2)-\Delta_s^2=0 \quad (1.18)$$

where

$$G(p)=1+i_p\omega p-p^2, \quad G(\bar{p})=(1+i_p\omega\bar{p}-\bar{p}^2) \quad (1.19)$$

Equations (1.17) and (1.18) are quadratic equations of p, and have four real roots at most against a certain value of ω. Among these roots, the natural frequencies corresponding to those of the symmetrical system where $\Delta_i=0$ and $\Delta_s=0$ (that is, the system where a disc is mounted on a round shaft) are denoted by p_f (>0) and p_b (<0). The other two roots which appear due to the unsymmetry of a rotor or a shaft are denoted by $\bar{p}_f$ ($=2\omega-p_f$) and $\bar{p}_b$ ($=2\omega-p_b$).

On the other hand, the frequency equations of Eqs. (1.2) and (1.6) of the four-degree-of-freedom system are given as follows[16]:
For the unsymmetrical rotor system;

$$\Phi_i(p)=\begin{vmatrix} 1-p^2 & 0 & \gamma & 0 \\ 0 & 1-\bar{p}^2 & 0 & \gamma \\ \gamma & 0 & G' & -\Delta_i p\bar{p} \\ 0 & \gamma & -\Delta_i p\bar{p} & \bar{G}' \end{vmatrix}=0 \quad (1.20)$$

For the unsymmetrical shaft system;

$$\Phi_s(p)=\begin{vmatrix} 1-p^2 & -\Delta_{11} & \gamma & -\Delta_{12} \\ -\Delta_{11} & 1-\bar{p}^2 & -\Delta_{12} & \gamma \\ \gamma & -\Delta_{12} & G' & -\Delta_{22} \\ -\Delta_{12} & \gamma & -\Delta_{22} & \bar{G}' \end{vmatrix}=0 \quad (1.21)$$

where

$$G'=\delta+i_p\omega p-p^2, \quad \bar{G}'=\delta+i_p\omega\bar{p}-\bar{p}^2 \quad (1.22)$$

Equations (1.20) and (1.21) are the 8th-degree polynomials of p, and have eight real roots at most. We donote the natural frequencies corresponding to those of a symmetrical system where $\Delta_i=0$ and $\Delta_{11}=\Delta_{12}=\Delta_{22}=0$ by p_i ($i=1\sim4$, $p_1>p_2>0>p_3>p_4$), and other four roots by $\bar{p}_i$ ($=2\omega-p_i$, $i=1\sim4$)

2. Nonlinear Forced Oscillations of a Rotating Shafs Carrying an Unsymmetrical Rotor at the Major Critical Speed[57]

2. 1. Introduction

There are many reports[4, 5, 12, 14~18, 63] concerning unstable vibrations in unstable regions at the major critical speeds of unsymmetrical rotor systems and unsymmetrical shaft systems with linear spring characteristics.

In this chapter, it is clarified both experimentally and theoretically that particular vibration phenomena appear in harmonic oscillations (that is, forced oscillations which have the same frequency as the angular velocity of the shaft) in the neighborhood of the major critical speed when the restoring force of a vertical shaft carrying an unsymmetrical rotor has nonlinear spring characteristics.

2. 2. Theoretical analysis of the harmonic oscillation at the major critical speed

Experiments were performed in a four-degree-of-freedom system where the deflection r and the inclination θ of the rotor are coupled with each other. If we suppose the case in which such coupling does not exist, the inclination oscillation and the deflection oscillation can be treated independently. Because, as explained later, this two-degree-of-freedom system for inclination oscillation has the same vibration characteristics as those of a four-degree-of-freedom system of the present experimental apparatus, we treat a two-degree-of-freedom system in theoretical analysis for simplicity.

Introducing the small parameter ε, we suppose that τ, c, Δ_i, N_{0x} and N_{0y} in Eq. (1.4) have the magnitudes of the same order as ε (we express this order by $O(\varepsilon)$). Therefore, we obtain the equations of motion with the accuracy of $O(\varepsilon)$ without involving the term $\Delta_i\tau = O(\varepsilon^2)$ in Eq. (1.4).

From the frequency equation (1.17), we get the $p-\omega$ diagram as shown in Fig. 2.1. This diagram has been calculated for $i_p=0.7$ and $\Delta_i=0.015$. In a rotating shaft system with linear spring characteristics, unstable vibrations with the frequency ω appear in the region between ω_{c1} $(=1/\sqrt{1-i_p+\Delta_i})$ and ω_{c2} $(=1/\sqrt{1-i_p-\Delta_i})$ which are derived by putting $p=\omega$ in Eq. (1.17).

In the following, we investigate the vibratory characteristics of a harmonic oscillation (that is, the oscillation with the frequency ω) in this speed range in the case where nonlinear spring characteristics exist. We put the solution

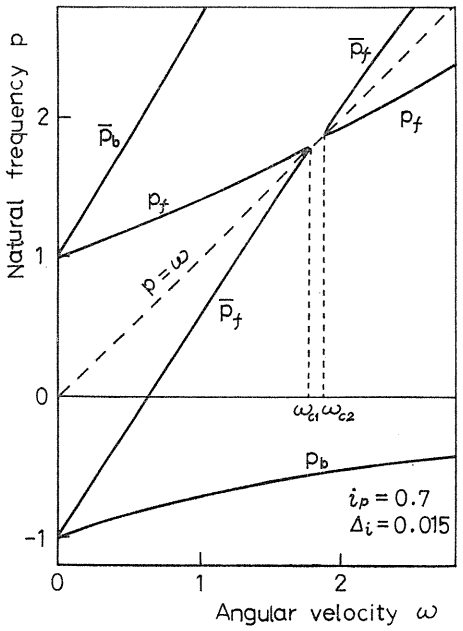

Fig. 2. 1. The p-ω diagram of the two-degree-of-freedom system.

with the frequency ω at the major critical speed in the following form.

$$\left.\begin{aligned}\theta_x&=P\cos(\omega t+\beta)+\varepsilon\{a_1\cos(\omega t+\beta)+b_1\sin(\omega t+\beta)\}\\ \theta_y&=P\sin(\omega t+\beta)+\varepsilon\{a_1'\sin(\omega t+\beta)+b_1'\cos(\omega t+\beta)\}\end{aligned}\right\}\qquad(2.1)$$

This solution is considered with the accuracy of $O(\varepsilon)$. The amplitudes P, a_1, a_1', b_1, b_1' and the phase angle β are quantities of $O(\varepsilon^0)$ which vary slowly with time. Because the nonlinear terms $N_{\theta x}$, $N_{\theta y}$ in the x- and y-directions in Eq. (1.4) are different as shown in Eq. (1.9), the whirling orbit of the shaft shifts slightly from a circle. The second terms in the right sides of Eq. (2.1) represent the degree of this discrepancy. Substituting Eq. (2.1) into the equations of motion and using the principle of harmonic balance concerning $\cos(\omega t+\beta)$ and $\sin(\omega t+\beta)$ with the accuracy of $O(\varepsilon)$, we obtain the following equations after some calculations Here, for convenience sake, the variables u and v ($u=P\cos\beta$, $v=P\sin\beta$) are used.

$$\left.\begin{aligned}(2-i_p)\omega\dot{u}&=-c\omega u-(G+4\beta^{(0)}P^2+\Delta_i\omega^2)v+F\sin\alpha_i\\ (2-i_p)\omega\dot{v}&=(G+4\beta^{(0)}P^2-\Delta_i\omega^2)u-c\omega v-F\cos\alpha_i\end{aligned}\right\}\qquad(2.2)$$

where

$$\left.\begin{aligned}&F=\tau\omega^2(1-i_p),\quad G=G(\omega)=1+i_p\omega^2-\omega^2,\\ &\beta^{(0)}=(3\beta_{40}+\beta_{22}+3\beta_{04})/8\end{aligned}\right\}\qquad(2.3)$$

As mentioned above, $\beta^{(0)}$ is the coefficient of an isotropic symmetrical nonlinear term[38]. Namely, it is known from Eq. (2.2) that only the nonlinear term which is uniform directionally has influence on this kind of oscillation. Expressing the stationary solutions of Eq. (2.2) by putting $u=u_0$, $v=v_0$, $P_0^2=u_0^2+v_0^2$, we get the following equations which give the stationary solution $P=P_0$ ($=\sqrt{u_0^2+v_0^2}$) and $\beta=\beta_0$ ($=\tan^{-1}(v_0/u_0)$):

$$\left.\begin{aligned}&\{k^2-(\Delta_i\omega^2)^2+(c\omega)^2\}^2P_0^2-\{k^2+(\Delta_i\omega^2)^2+(c\omega)^2\}F^2\\ &\qquad-2\Delta_i\omega^2F^2(k\cos 2\alpha_i+c\omega\sin 2\alpha_i)=0\\ &\tan\beta_0=\frac{(k-\Delta_i\omega^2)\sin\alpha_i-c\omega\cos\alpha_i}{(k+\Delta_i\omega^2)\cos\alpha_i+c\omega\sin\alpha_i}\end{aligned}\right\}\qquad(2.4)$$

where $k=G+4\beta^{(0)}P_0^2$. Considering small deviations from the stationary solutions and substituting $u=u_0+\xi$ and $v=v_0+\eta$ into Eq. (2.2), we obtain the differential equations for ξ and η. From the characteristic equation of this equation, we get the following condition for a stable stationary solution:

$$k^2-(\Delta_i\omega^2)^2+(c\omega)^2+8\beta^{(0)}P_0^2(k+\Delta_i\omega^2\cos 2\beta_0)>0\qquad(2.5)$$

Differentiating the first equation of Eq. (2.4) partially with respect to P_0 and putting $\partial\omega/\partial P_0=0$, we obtain

$$\begin{aligned}&P_0\{k^2-(\Delta_i\omega^2)^2+(c\omega)^2\}\{k^2-(\Delta_i\omega^2)^2+(c\omega)^2\\ &\qquad+8\beta^{(0)}P_0^2(k+\Delta_i\omega^2\cos 2\beta_0)\}=0\end{aligned}\qquad(2.6)$$

The relation $P_0\{k^2-(\Delta_i\omega^2)^2+(c\omega)^2\}\fallingdotseq 0$ holds in general, and we get

$$k^2-(\Delta_i\omega^2)^2+(c\omega)^2+8\beta^{(0)}P_0^2(k+\Delta_i\omega^2\cos 2\beta_0)=0 \qquad (2.7)$$

Therefore, from Eqs. (2.5) and (2.7), we know that the point where the tangent line becomes vertical is consistent with a boundary between a stable and an unstable resonance curves.

Examples of resonace curves calculated by Eq. (2.4) are shown in Figs. 2.2 (a) and 2.3 (a). These examples have been calculated for a positive value of $\beta^{(0)}$ and the resonance curves belong to a hard spring type. The ordinate represents the amplitude P_0, and the abscissa represents the angular velocity ω of the shaft.

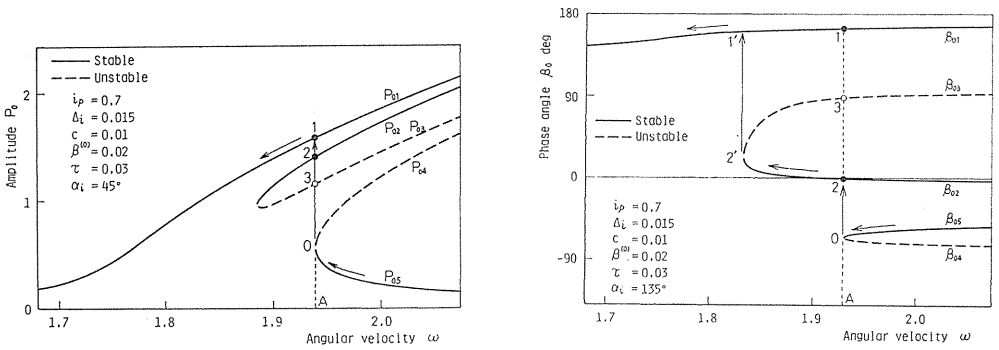

(a) Resonance curves. (b) A phase angle diagram.

Fig. 2.2. A case of jumping to (P_{02}, β_{02}).

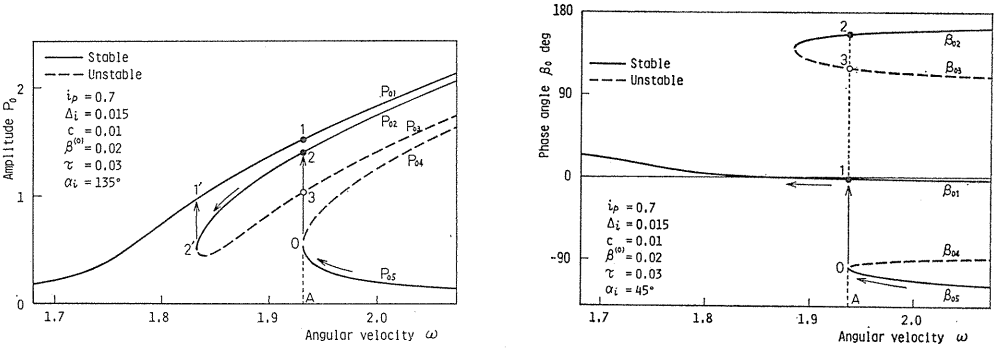

(a) Resonance curves. (b) A phase angle diagram.

Fig. 2.3. A case of jumping to (P_{01}, β_{01}).

The full and the broken lines represent the stable and the unstable solutions, respectively. The resonance curves have at most five values of amplitude for a given value of ω, and the stable solutions are named P_{01}, P_{02}, P_{05} while the unstable solutions are named P_{03}, P_{04} in order of magnitude. When the angular velocity ω decreases from the higher speed side, the amplitude changes along the stable curve P_{05} and jumps from the point 0 to the other point 1 or 2 on the

stable resonance curves P_{01} and P_{02} at the speed marked by A in the figure. By integrating Eq. (2.2) numerically and investigating the transient solution in jump phenomena, we find the point to which it jumps. Figures 2.2 (a) and 2.3 (a) are examples of the jump phenomena to the points 2 and 1, respectively, and the jumps are indicated by arrows. Figures 2.2 (b) and 2.3 (b) are phase angle diagrams corresponding to Figs. 2.2 (a) and 2.3 (a), respectively, and β_{01}, β_{02}, ... are phase angles corresponding to the amplitudes P_{01}, P_{02}, ... When the amplitude changes, the phase angle β_0 also jumps as indicated by arrows.

We shall investigate which type of jump phenomena between Figs. 2.2 and 2.3 occurs depending on the angular position α_i of dynamic unbalance τ. The result is shown in Fig. 2.4 where the magnitude and the angular position of dynamic unbalance are expressed by a polar coordinate system (τ, α_i). It jumps to the point 2 as in Fig. 2.2(a) in the shaded region and jumps to the point 3 as in Fig. 2.3(a) in the other region. The angles $\angle$AOA′ and $\angle$BOB′ in the figure are zero when $c=0$, and they increase as the damping coefficient c increases.

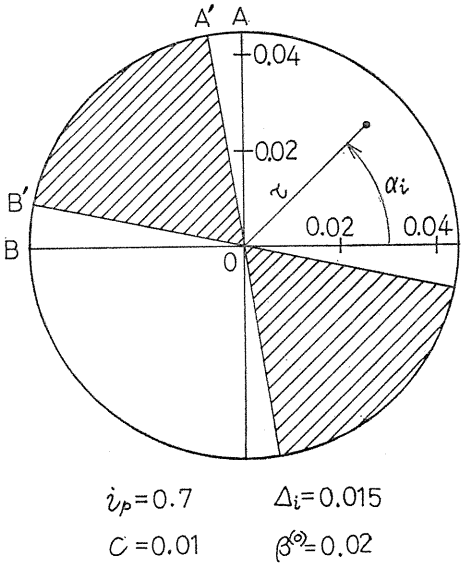

Fig. 2. 4. A relation between the type of jump and magnitude τ and phase angle α_i of the dynamic unbalance.

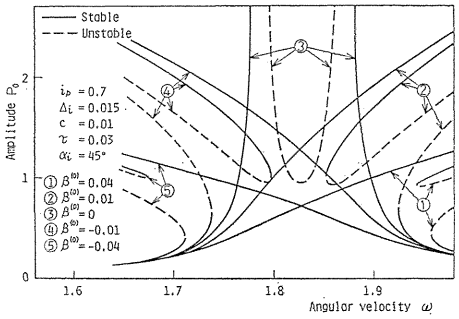

Fig. 2. 5. An effect of the coefficient of nonlinear terms $\beta^{(0)}$.

Figure 2.5 shows an effect of the coefficient $\beta^{(0)}$ of nonlinear term. The resonance curves become a hard spring type when $\beta^{(0)}$ is positive, they become a soft spring type when $\beta^{(0)}$ is negative; and they become a type of a linear system and an unstable region appears when $\beta^{(0)}=0$[16]. When $\beta^{(0)}\neq 0$, at least one stable solution exists and the unstable region disappears because the resonance curves bend toward higher speed side or lower speed side

2. 3. Theoretical analysis in a four-degree-of-freedom system

In this chapter, we shall analyze the same four-degree-of-freedom system where the deflection r and the inclination θ of the rotor are coupled like the experimental apparatus. From the results of this analysis, it follows that the constitution of equations in this system is the same as the corresponding equations in the two-degree-of-freedom system and consequently the vibratory characteristics are the same qualitatively in these two systems.

When Δ_i and τ have the magnitudes of $O(\varepsilon)$ in Eq. (1. 2), we get the dimensionless equations of motion omitting the product terms of Δ_i and τ with the accuracy of $O(\varepsilon)$. The solutions of these equations of motion in the neighborhood of the major critical speed can be expressed with the accuracy of $O(\varepsilon)$ as follows:

$$\left.\begin{aligned} x&=u_1\cos\omega t-v_1\sin\omega t+\varepsilon(d_1\cos\omega t+e_1\sin\omega t)\\ y&=u_1\sin\omega t+v_1\cos\omega t+\varepsilon(d_1'\sin\omega t+e_1'\cos\omega t)\\ \theta_x&=u_2\cos\omega t-v_2\sin\omega t+\varepsilon(d_2\cos\omega t+e_2\sin\omega t)\\ \theta_y&=u_2\sin\omega t+v_2\cos\omega t+\varepsilon(d_2'\sin\omega t+e_2'\cos\omega t)\end{aligned}\right\} \tag{2.8}$$

The amplitudes u_1, u_2, v_1, v_2, d_1, d_1', d_2, d_2', e_1, e_1', e_2, and e_2' are quantities of $O(\varepsilon^0)$ varying slowly with time. By substituting Eq. (2. 8) into the equations of motion, we get the equations corresponding to Eq. (2. 2). And from these equations, we obtain the following relations with the accuracy of $O(\varepsilon^0)$:

$$\frac{u_2}{u_1}=\frac{v_2}{v_1}=\frac{u_{20}}{u_{10}}=\frac{v_{20}}{v_{10}}=-\frac{1-\omega^2}{\gamma}=-\frac{\gamma}{\delta+i_p\omega^2-\omega^2}=\kappa \tag{2.9}$$

where u_{10} and v_{20} represent stationary solutions. With κ of Eq. (2. 9), the equations corresponding to Eq. (2. 2) are

$$\left.\begin{aligned} \omega\dot{u}_1&=-c'\omega u_1-(f+\beta^{(0)\prime}R^2+\Delta_i'\omega^2)v_1+F'\sin\alpha_i'\\ \omega\dot{v}_1&=(f+\beta^{(0)\prime}R^2-\Delta_i'\omega^2)u_1-c'\omega v_1-F'\cos\alpha_i'\end{aligned}\right\} \tag{2.10}$$

where

$$\left.\begin{aligned} &A=2G'-\gamma\kappa(2-i_p),\quad c'=\{G'(c_{11}+\kappa c_{12})-\gamma(c_{21}+\kappa c_{22})\}/A,\\ &F'=\omega^2\sqrt{(G'e)^2+\gamma^2\tau^2(i_p-1)^2-2G'\gamma(i_p-1)e\tau(\alpha_e-\alpha\tau)}\,/A,\\ &f=\{(1-\omega^2)G'-\gamma^2\}/A,\quad G'=\delta+i_p\omega^2-\omega^2,\quad R^2=u_1^2+v_1^2,\\ &\tan\alpha_i'=\{G'e\sin\alpha_e-\gamma\tau(i_p-1)\sin\alpha_\tau\}/\{G'e\cos\alpha_e-\gamma\tau(i_p-1)\cos\alpha_\tau\},\\ &\beta^{(0)\prime}=(G'\beta_1^{(0)}-\gamma\beta_2^{(0)})/A,\quad \beta_1^{(0)}=4\beta_{40}^{(0)}+3\kappa\beta_{31c}^{(0)}+2\kappa^2\beta_{22}^{(0)}+2\kappa^2\beta_{22c}^{(0)}+\kappa^3\beta_{13c}^{(0)},\\ &\beta_2^{(0)}=\beta_{31c}^{(0)}+2\kappa\beta_{22}^{(0)}+2\kappa\beta_{22c}^{(0)}+3\kappa^2\beta_{13c}^{(0)}+4\kappa^3\beta_{04}^{(0)},\quad \Delta_i'=\Delta_i(1-\omega^2)/A\end{aligned}\right\} \tag{2.11}$$

The coefficients $\beta_{40}^{(0)}$, $\beta_{31c}^{(0)}$, etc., and the coefficient $\beta^{(0)\prime}$ in Eqs. (2. 10) and (2. 11) are coefficients of isotropic symmetrical nonlinear terms[37]. They are the same kind of coefficients as $\beta^{(0)}$ in Eqs. (2. 2)$\sim$(2. 4).

By comparing Eq. (2.10) for a four-degree-of-freedom system with Eq. (2.2) for a two-degree-of-freedom system, we know that they are the same in construction and have the same dynamical characteristics of their coefficients. Therefore, it is clear that Eq. (2.10) gives qualitatively the same results as those of inclination oscillation in a two-degree-of-freedom system mentioned above.

2. 4. Experimental results

The experimental apparatus is shown in Fig. 1.1. An unsymmetrical rotor R_1 in Table 1.1 was mounted on a vertical elastic shaft with circular cross section S_1 in Table 1.2.

When the experimental apparatus was assembled carefully to attain good alignment of the center lines of the upper and the lower bearing pedestals and the bearing center line was situated at the middle of the angular clearance of the lower bearing, the restoring force of the shaft had strong symmetrical nonlinear spring characteristics[36]. After balancing the rotor sufficiently, we performed many experiments for various magnitudes and directions of the static unbalance by changing the small correction weight.

Typical examples of experimental results on resonance curves and phase angle curves are shown in Figs. 2.6 (a), 2.6 (b), 2.7 (a) and 2.7 (b). Due to the strong

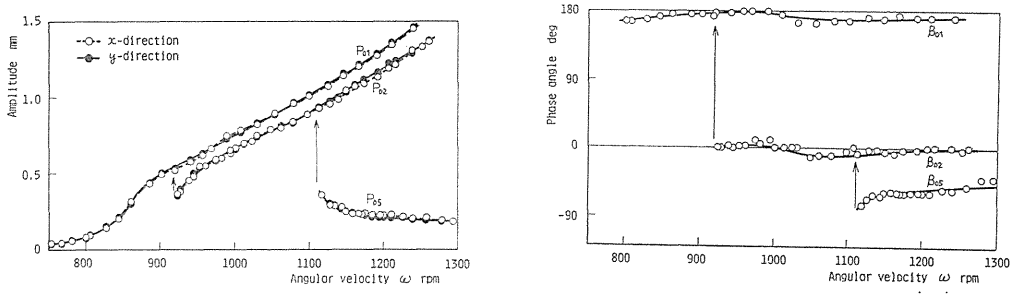

(a) Resonance curves. (b) Phase angle curves.

Fig. 2. 6. A case of jumping to (P_{02}, β_{02}).

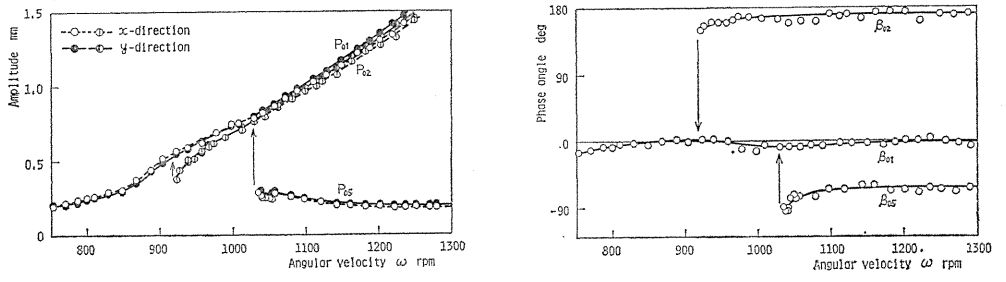

(a) Resonance curves. (b) Phase angle curves.

Fig. 2. 7. A case of jumping to (P_{01}, β_{01}).

symmetrical nonlinear spring characteristics, the resonance curves had hard spring types[36]. In Fig. 2.6(a), when the shaft was decelerated from the higher speed

side, the oscillation jumped to the curve P_{02} at $\omega=1111$ rpm, passed along the curve P_{02}, and jumped again to the curve P_{01} at $\omega=920$ rpm as shown by arrows. This figure has qualitatively the same characteristics as Fig. 2.2 (a). Figure 2.7 (a) shows the case where it jumped not to the curve P_{02} (shown by the symbols ① and ◑) but to the curve P_{01} at $\omega=1029$ rpm. Although the amplitudes P_{01} and P_{02} are almost the same in magnitude as shown in Fig. 2.7 (a), the values of phase angles β_{01} and β_{02} are distinctly different from each other as shown in Fig. 2.7(b). Therefore, we can make a clear distinction between the P_{01} curve and the P_{02} curve in recorded waves and can easily determine that the oscillation jumped to P_{01} in this case. The curve P_{02} in Fig. 2.7 (a) was obtained by forcing a jump to it with impulse. Figure 2.7(a) is qualitatively the same as Fig. 2.3 (a). The curves P_{01} in Figs. 2.6 (a) and 2.7 (a) were measured up to the amplitude about 1.5 mm for safty, and no jump phenomenon was observed in acceleration.

The relation between the type of jump and the magnitude and phase angle of unbalance of the rotor is shown in Fig. 2.8. As the discrepancy between the direction of the unbalance and the direction of the shaft deflection became large when

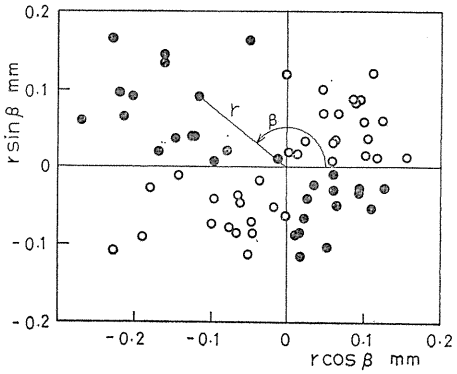

Fig. 2.8. The relation between the type of jump and the magnitude and phase angle of the unbalance (r and β are the amplitude and the phase angle of the static deflection at $\omega=800$ rpm. r and β correspond to τ and α_i in Fig. 2.4. The symbols ◉ and ○ mean the cases of jumping to (P_{02}, β_{02}) and (P_{01}, β_{01}), respectively.)

the shaft rotating speed approached the resonance point, we measured the amplitude r and the phase angle β at $\omega=800$ rpm where the rotating speed was at some distance from the resonance point and the discrepancy is almost negligible. The symbols ◉ and ○ in the figure correspond to the resonance curves of the types in Figs. 2.6 (a) and 2.7 (a), respectively. These experimental results agree with the theoretical results shown in Fig. 2.4. In the above-mentioned examples, (r, β) $=(0.176\text{mm}, 155.5°)$ in Fig. 2.6(a) and (r, β) $=(0.156\text{mm}, 19.5°)$ in Fig. 2.7(a).

We also experimented on the case of linear spring characteristics by changing the lower bearing to a self-aligning double-row ball bearing (#1204). The width of the unstable region was about 110 rpm.

2. 5. *Conclusions*

The theoretical and the experimental conclusions about the harmonic oscillations at the major critical speed in an unsymmetrical rotor system with symmetrical nonlinear spring characteristics are summarized as follows:

(1) The unstable region appearing in a linear system disappears in a nonlinear

system and stationary resonance curves of a hard or soft spring type are obtained.

(2) The resonance curves can be devided into three regions concernig speed, that is, the regions where one, three, and five stationary amplitudes exist, and jump phenomena occur at the rotating speeds of their boundaries.

(3) Among various kinds of nonlinear spring characteristics, only the isotropic nonlinear component has influence on this oscillation.

(4) The four-degree-of-freedom system where the deflection and the inclination of the shaft couple with each other and the two-degree-of-freedom system of inclination oscillation which does not couple with deflection oscillation have qualitatively the same vibratory characteristics.

(5) In the experiments with the above-mentioned unsymmetrical rotor, no jump phenomena appeared in acceleration processes.

(6) When the shaft was decelerated from the higher speed side, two types of resonance curves where one or two jumps appeared were obtained.

(7) It depends on the angular position of the rotor unbalance which type of these two kinds of vibration phenomena appears. The boundaries of these regions concerning angular position coincide approximately with the main axes of inertia of the rotor.

3. Summed-and-Differential Harmonic Oscillations of an Unsymmetrical Shaft[58]

3. 1. Introduction

Almost all the studies of nonlinear oscillations in rotating shaft systems have been concerned with elastic shafts with circular cross section (i. e., round shafts). When an elastic shaft with a disc is supported by single-row deep groove ball bearings, the restoring force of the shaft has a nonlinear spring characteristic owing to angular clearances[32] of the ball bearings. As for the nonlinear forced vibrations in such systems, we have reported on a series of experimental[32, 34, 36, 37] and theoretical studies[33, 35, 38]. We designate natural frequencies of this system by p_i, p_j, and p_k. In these papers, we concluded that there were similar characteristics between subharmonic oscillations of order 1/2 and summed-and-differential harmonic oscillations of the type $[p_i \pm p_j]$, and between subharmonic oscillations of order 1/3 and summed-and-differential harmonic oscillations of the types $[2p_i \pm p_j]$ or $[p_i \pm p_j \pm p_k]$.

Few researches have been reported on the nonlinear oscillation of an unsymmetrical shaft with directional nonuniformity of stiffness. Previously, we reported on a complex phenomenon of subharmonic oscillations of unsymmetrical shafts[56]. In that paper, we made it clear that a nonlinear component, which had no effects on the subharmonic oscillation of order 1/2 of the mode of forward precession in a round shaft system, had great influence on it through the unsymmetry of shaft stiffness.

In this chapter, summed-and-differential harmonic oscillations of an unsymmetrical shaft with nonlinear spring characteristics are treated theoretically and experimentally, and we shall clarify that they have similar characteristics to subharmonic oscillations previously reported[56]. Especially, in the case of the summed-and-differential harmonic oscillations of the type $[p_i - p_j]$ $(p_i > 0,\ p_j < 0)$, the

nonlinear component, which has no effects on the same types of oscillations in a round shaft system, has influence through the unsymmetry of shaft stiffness. Consequently, depending on the intensity of nonlinear characteristic and the degree of unbalance, the following types of resonance curves appear in experiments: a stable resonance curve of hard spring type, a stable one of soft spring type, an unstable region, and a case in which no summed-and-differential harmonic oscillations occur.

Experiments are performed in a four-degree-of-freedom system where the deflection and the inclination of a shaft couple with each other. In a theoretical analysis, a two-degree-of-freedom system is mainly treated for the sake of simplicity. As mentioned later, results of theoretical analysis in a four-degree-of-freedom system are qualitatively the same as those in the two-degree-of-freedom system.

3. 2. *Theoretical analysis of the summed-and-differential harmonic oscillation of the type* $[p_f-p_b]$

The experimental apparatus is a four-degree-of-freedom system where the deflection r and the inclination θ of a shaft at the position of a rotor couple with each other. After somewhat complex calculation of such a system, we can show that the amplitude ratio of an inclination oscillation to a deflection oscillation is constant with the accuracy of the zeroeth order of the small quantity ε (labelled $O(\varepsilon^0)$), and that the equations for resonance curves are qualitatively the same as those in the two-degree-of-freedom system as mentioned later.

Therefore, in this section, we analyze the inclination oscillation in a system where r and θ do not couple as a simple case of the whirling motion. Experimental results concerning the deflection oscillation of a four-degree-of-freedom system are explained by the analytical results of such a two-degree-of-freedom system.

In the theoretical analysis of the harmonic oscillation at the major critical speed in Chapter 2, we supposed the unsymmetry of moment of inertia of a rotor Δ_i to have the magnitude of $O(\varepsilon)$. In Chapters 4 and 5, however, we shall suppose Δ_i and the unsymmetry of the shaft stiffness Δ_s to have the magnitude of $O(\varepsilon^0)$ in the cases of nonlinear forced oscillations which occur at the speed far in excess of the major critical speed. Therefore, in the dimensionless equations of motion (1.7), the quantities Δ_s, θ_x, θ_y and τ are $O(\varepsilon^0)$, and c, $N_{\theta x}$ and $N_{\theta y}$ are $O(\varepsilon)$.

The summed-and-differential harmonic oscillation of the type $[p_f-p_b]$ means such an oscillation in which two vibrations with the frequencies ω_f (>0) and ω_b (<0) may occur in the neighborhood of the angular velocity where the relation $p_f-p_b=\omega$ holds, and in this case the relation

$$\omega_f-\omega_b=\omega, \quad \omega_f \fallingdotseq p_f, \quad \omega_b \fallingdotseq p_b \tag{3.1}$$

are satisfied. Since the unsymmetry Δ_s has the magnitude of $O(\varepsilon^0)$, the equations of motion (1.7) cannot be solved by adopting the transformation to normal coordinates[33]. Accordingly, we will obtain an approximate solution of Eq. (1.7) by using a refined harmonic balance method.

Because of the unsymmetry Δ_s and the difference of nonlinear characteristics in θ_x and θ_y directions, the approximate solution must be assumed in the following forms with the accuracy of $O(\varepsilon)$. We put $2\omega-\omega_f=\bar{\omega}_f$ and $2\omega-\omega_b=\bar{\omega}_b$ in the following equations:

$$\begin{aligned}\begin{matrix}\theta_x\\ \theta_y\end{matrix}=&R_f\begin{matrix}\cos\\ \sin\end{matrix}(\omega_f t+\delta_f)+R_b\begin{matrix}\cos\\ \sin\end{matrix}(\omega_b t+\delta_b)+\bar{R}_f\begin{matrix}\cos\\ \sin\end{matrix}(\bar{\omega}_f t-\delta_f)+\bar{R}_b\begin{matrix}\cos\\ \sin\end{matrix}(\bar{\omega}_b t-\delta_b)\\ &+P\begin{matrix}\cos\\ \sin\end{matrix}(\omega t+\beta)+\varepsilon\left[\begin{matrix}a_f\\ a'_f\end{matrix}\begin{matrix}\cos\\ \sin\end{matrix}(\omega_f t+\delta_f)+\begin{matrix}b_f\\ b'_f\end{matrix}\begin{matrix}\sin\\ \cos\end{matrix}(\omega_f t+\delta_f)+\begin{matrix}a_b\\ a'_b\end{matrix}\begin{matrix}\cos\\ \sin\end{matrix}(\omega_b t+\delta_b)\right.\\ &+\begin{matrix}b_b\\ b'_b\end{matrix}\begin{matrix}\sin\\ \cos\end{matrix}(\omega_b t+\delta_b)+\begin{matrix}\bar{a}_f\\ \bar{a}'_f\end{matrix}\begin{matrix}\cos\\ \sin\end{matrix}(\bar{\omega}_f t-\delta_f)+\begin{matrix}\bar{b}_f\\ \bar{b}'_f\end{matrix}\begin{matrix}\sin\\ \cos\end{matrix}(\bar{\omega}_f t-\delta_f)+\begin{matrix}\bar{a}_b\\ \bar{a}'_b\end{matrix}\begin{matrix}\cos\\ \sin\end{matrix}(\bar{\omega}_b t-\delta_b)\\ &+\begin{matrix}\bar{b}_b\\ \bar{b}'_b\end{matrix}\begin{matrix}\sin\\ \cos\end{matrix}(\bar{\omega}_b t-\delta_b)+\begin{matrix}d_f\\ d'_f\end{matrix}\begin{matrix}\cos\\ \sin\end{matrix}\{(2\omega+\omega_f)t+\delta_f\}+\begin{matrix}e_f\\ e'_f\end{matrix}\begin{matrix}\sin\\ \cos\end{matrix}\{(2\omega+\omega_f)t+\delta_f\}\\ &+\begin{matrix}d_b\\ d'_b\end{matrix}\begin{matrix}\cos\\ \sin\end{matrix}\{(2\omega+\omega_b)t+\delta_b\}+\begin{matrix}e_b\\ e'_b\end{matrix}\begin{matrix}\sin\\ \cos\end{matrix}\{(2\omega+\omega_b)t+\delta_b\}\\ &+\begin{matrix}f_f\\ f'_f\end{matrix}\begin{matrix}\cos\\ \sin\end{matrix}\{(2\omega+\bar{\omega}_f)t-\delta_f\}+\begin{matrix}h_f\\ h'_f\end{matrix}\begin{matrix}\sin\\ \cos\end{matrix}\{2\omega+\bar{\omega}_f)t-\delta_f\}\\ &\left.+\begin{matrix}f_b\\ f'_b\end{matrix}\begin{matrix}\cos\\ \sin\end{matrix}\{(2\omega+\bar{\omega}_b)t-\delta_b\}+\begin{matrix}h_b\\ h'_b\end{matrix}\begin{matrix}\sin\\ \cos\end{matrix}\{(2\omega+\bar{\omega}_b)t-\delta_b\}\right]\end{aligned}\tag{3.2}$$

In the above equation, however, we pick up only oscillation components required in a later calculation. It is assmed that amplitudes R_f, R_b, $\bar{R}_f$, $\bar{R}_b$, P, a_f, b_f, a'_f, b'_f, a_b, b_b, a'_b, b'_b, $\bar{a}_f$, $\bar{b}_f$, $\bar{a}'_f$, $\bar{b}'_f$, $\bar{a}_b$, $\bar{b}_b$, $\bar{a}'_b$, $\bar{b}'_b$, d_f, e_f, d'_f, e'_f, d_b, e_b, d'_b, e'_b, f_f, h_f, f'_f, h'_f, f_b, h_b, f'_b, h'_b and the phase angles δ_f, δ_b, and β are quantities of $O(\varepsilon^0)$, and are slowly varying functions of time t. Using the method of harmonic balance, we analyze these equations in the same way as in the previous report[56].

Substituting Eq. (3.2) into Eq. (1.7) and comparing the terms having the same frequencies with the accuracy of $O(\varepsilon^0)$, we obtain the amplitude ratios $\bar{R}_f/R_f$ and $\bar{R}_b/R_b$, and the solution of a harmonic oscillation as follows:

$$\frac{\bar{R}_f}{R_f}=\frac{G_f}{\Delta_s}=\frac{\Delta_s}{\bar{G}_f},\quad \frac{\bar{R}_b}{R_b}=\frac{G_b}{\Delta_s}=\frac{\Delta_s}{\bar{G}_b}\tag{3.3}$$

$$P_c\equiv P\cos\beta=\frac{(1-i_p)\tau\omega^2\cos\alpha_s}{G-\Delta_s},\quad P_s\equiv P\sin\beta=\frac{(1-i_p)\tau\omega^2\sin\alpha_s}{G+\Delta_s}\tag{3.4}$$

where we use the following symbols: $G_f=G(\omega_f)$, $G_b=G(\omega_b)$, $\bar{G}_f=G(\bar{\omega}_f)$, $\bar{G}_b=G(\bar{\omega}_b)$, and $G=G(\omega)$. Evidently, from Eq. (3.3) the relation

$$G_f\bar{G}_f=G_b\bar{G}_b=\Delta_s^2\tag{3.5}$$

holds with the accuracy of $O(\varepsilon^0)$.

Next, comparing the terms having the same frequencies with the accuracy of $O(\varepsilon)$, the amplitudes R_f, $\bar{R}_f$, R_b, and $\bar{R}_b$, and the phase angles δ_f and δ_b can be determined. Using Eqs. (3.3) and (3.5), we obtain the following equations[56]:

$$\left.\begin{aligned}A_fR_f\dot{\delta}_f=&-\sigma_fR_f-4\beta^{(0)}(g_fR_f^2+2\bar{g}_bR_b^2+2k_fP^2)R_f+6m_b(\beta_c^{(2)}\cos 2\phi\\ &-\beta_s^{(2)}\sin 2\phi)R_fR_b^2-2\varepsilon^{(1)}(a_c\cos\phi+a_s\sin\phi)PR_b\\ A_f\dot{R}_f=&c_fR_f+6m_b(\beta_s^{(2)}\cos 2\phi+\beta_c^{(2)}\sin 2\phi)R_fR_b^2+2\varepsilon^{(1)}(a_s\cos\phi\\ &-a_c\sin\phi)PR_b\end{aligned}\right|$$

$$\left.\begin{aligned} A_b R_b \dot{\delta}_b = &-\sigma_b R_b - 4\beta^{(0)}(g_b R_b^2 + 2\bar{g}_f R_f^2 + 2k_b P^2) R_b + 6m_f(\beta_c^{(2)}\cos 2\psi \\ &-\beta_s^{(2)}\sin 2\psi) R_f^2 R_b - 2\varepsilon^{(1)}(b_c\cos\psi + b_s \sin\psi) P R_f \\ A_b \dot{R}_b = &\, c_b R_b - 6m_f(\beta_s^{(2)}\cos 2\psi + \beta_c^{(2)}\sin 2\psi) R_f^2 R_b - 2\varepsilon^{(1)}(b_s\cos\psi \\ &-b_c \sin\psi) P R_f \end{aligned}\right\} \quad (3.6)$$

In the above equations, we introduce the notations as follows:

$$\left.\begin{aligned} &A_f = (i_p\omega - 2\omega_f)\bar{G}_f - (i_p\omega - 2\bar{\omega}_f) G_f, \\ &A_b = (i_p\omega - 2\omega_b)\bar{G}_b - (i_p\omega - 2\bar{\omega}_b) G_b, \\ &a_c = (\bar{G}_f + G_b + \Delta_s)\cos\beta, \qquad a_s = (\bar{G}_f + G_b - \Delta_s)\sin\beta, \\ &b_c = (G_f + \bar{G}_b + \Delta_s \bar{G}_b/\bar{G}_f)\cos\beta, \qquad b_s = (G_f + \bar{G}_b - \Delta_s \bar{G}_b/\bar{G}_f)\sin\beta, \\ &c_f = c(\omega_f \bar{G}_f - \bar{\omega}_f G_f), \qquad c_b = c(\omega_b \bar{G}_b - \bar{\omega}_b G_b), \\ &g_f = (G_f^2 + \bar{G}_f^2 + 4\Delta_s^2)/\bar{G}_f, \qquad g_b = (G_b^2 + \bar{G}_b^2 + 4\Delta_s^2)/\bar{G}_b, \\ &\bar{g}_f = \{(G_f + \bar{G}_f)(G_b + \bar{G}_b) + 2\Delta_s^2\}/\bar{G}_f, \\ &\bar{g}_b = \{(G_f + \bar{G}_f)(G_b + \bar{G}_b) + 2\Delta_s^2\}/\bar{G}_b, \\ &k_f = G_f + \bar{G}_f + \Delta_s\cos 2\beta, \qquad k_b = G_b + \bar{G}_b + \Delta_s\cos 2\beta, \\ &m_f = -\Delta_s(G_f + \bar{G}_b)/\bar{G}_f, \qquad m_b = -\Delta_s(G_f + \bar{G}_b)/\bar{G}_b, \\ &\beta_c^{(2)} = \beta^{(2)}\cos 2\varphi_2, \qquad \beta_c^{(2)} = \beta^{(2)}\sin 2\varphi_2, \\ &\beta^{(2)} = \sqrt{\beta_c^{(2)2} + \beta_s^{(2)2}}, \qquad 2\varphi_2 = \tan^{-1}(\beta_s^{(2)}/\beta_c^{(2)}), \\ &\psi = \delta_f - \delta_b, \qquad \sigma_f = G_f\bar{G}_f - \Delta_s^2, \qquad \sigma_b = G_b\bar{G}_b - \Delta_s^2 \end{aligned}\right\} \quad (3.7)$$

Among the coefficients of nonlinear terms, $\beta^{(0)}$, $\varepsilon^{(1)}$, and $\beta^{(2)}$ appear in Eq. (3.6). When $\Delta_s \to 0$ in this equation (simultaneously $G_f \to O(\varepsilon)$ and $G_b \to O(\varepsilon)$), we obtain the corresponding equation[38] for a round shaft system provided we ignore the quantities smaller than that of $O(\varepsilon)$. The presence of $\beta^{(2)}$, which has no effects on a round shaft system, causes complicated oscillation phenomena in the unsymmetrical shaft system This feature is similar to the case of the subharmonic oscillation[56] reported previously.

Putting $R_f = R_{f0}$, $R_b = R_{b0}$, $\delta_f = \delta_{f0}$, $\delta_b = \delta_{b0}$ and $\dot{R}_f = \dot{R}_b = \dot{\delta}_f = \dot{\delta}_b = 0$ in Eq. (3.6), we obtain four equations to evaluate the stationary solutions. With these four equations and the relation $\omega_f - \omega_b = \omega$, we can determine five quantities, that is, R_{f0}, R_{b0}, ψ_0 $(= \delta_{f0} - \delta_{b0})$, ω_f, and ω_b. Eliminating unknown quantities R_{b0}, ψ_0, ω_f, and ω_b by using those five equations, we have a double quartic equation about R_{f0}. We shall examine the stability of the stationary solutions which are not zero by the following procedure. We consider small deviations from the

stationary solutions and represent them by ξ_f, ξ_b, η_f, and η_b ($\eta=\eta_f-\eta_b$). We substitute $R_f=R_{f0}+\xi_f$, $R_b=R_{b0}+\xi_b$, $\delta_f=\delta_{f0}+\eta_f$, and $\delta_b=\delta_{b0}+\eta_b$ into Eq. (3.6), and ignore the terms smaller than the magnitude of $O(\varepsilon^2)$. By assuming the solutions in the following forms: $\xi_f=A_f^*e^{st}$, $\xi_b=A_b^*e^{st}$, and $\eta=A^*e^{st}$ (A_f^*, A_b^*, and A^*, however, are arbitrary constants), we can obtain a characteristic equation. Consequently, the stability can be determined by adopting the Routh-Hurwitz criteria to that equation. Also, the stability criteria of stationary solutions with zero amplitude must be performed by changing variables into u_f, v_f, u_b, and v_b with the transfomation $u_f=R_f\cos\delta_f$, $v_f=R_f\sin\delta_f$, $u_b=R_b\cos\delta_b$, and $v_b=R_b\sin\delta_b$. The equations which represent the resonance curves and the stability of these solutions are omitted because of their complexity. Only the results of computation are shown in Figs. 3.1~3.4.

Resonance curves change their shapes depending on the values of parameters. The influences of the coefficients of nonlinear terms $\beta^{(0)}$, $\varepsilon^{(1)}$, and $\beta^{(2)}$ and the dynamic unbalance τ are shown in Figs. 3.1~3.4, respectively. In these diagrams, the ordinates represent the stationary amplitude $R_{f0}+R_{b0}$, and the abscissas represent the rotating speed of the shaft ω. The solid line curves denote stable solutions, and the broken line curves unstable ones. In order to avoid confusion, we draw only the solutions $R_{f0}+R_{b0}\neq 0$, and eliminate the solutions $R_{f0}+R_{b0}=0$. The points at which resonance curves intersect with ω-axis give the boundaries between the stable parts and the unstable parts of zero amplitude solution. The solutions of $R_{f0}+R_{b0}=0$ are unstable between two such points and are stable outside them[56]. At those points resonance curves intersect ω-axis at righ angles. The effects of parameters are similar to the case of the subharmonic oscillation of 1/2 [$+2p_f$] reported previously[56].

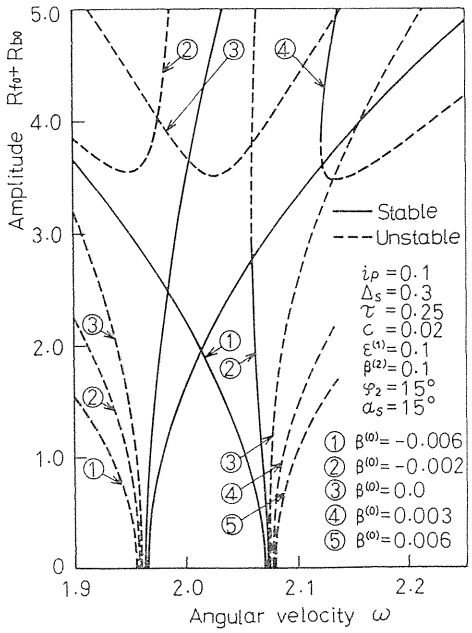

Fig. 3. 1. Effects of the of the nonlinear component $N(0)$ ($\beta^{(0)}$).

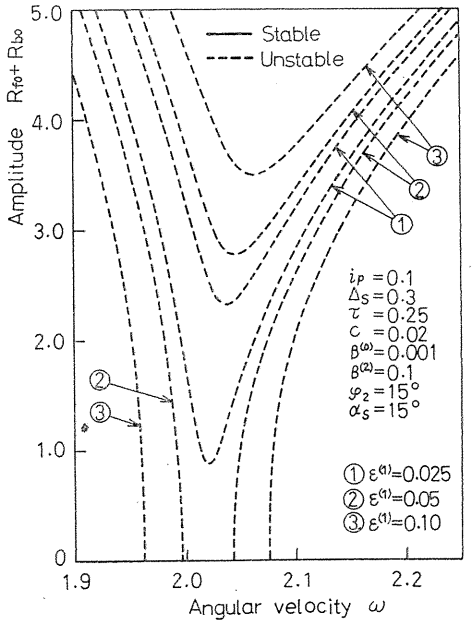

Fig. 3. 2. Effects of the nonlinear component $N(1)$ ($\varepsilon^{(1)}$).

The influence of the nonlinear component $\beta^{(0)}$ is shown by Fig. 3.1. The resonance curve has the shape of a hard spring type when $\beta^{(0)}$ takes a positive value, and that of a soft spring type when $\beta^{(0)}$ is negative. Especially, when the absolute value of $\beta^{(0)}$ is small, the resonance curve of $R_{f0}+R_{b0}\fallingdotseq 0$ is an unstable solution at any angular velocity ω. For example, when $\beta^{(0)}=0$, no stable solutions (including the solutions whose amplitudes are zero) exist between $1.96<\omega<2.07$; and an unstable region of ω appears. Also in this case, since the solution $R_{f0}+R_{b0}=0$ is stable at $\omega<1.96$ and $2.07<\omega$, no summed-and-differential harmonic oscillation occurs.

The effects of nonlinear component $\varepsilon^{(1)}$ are shown in Fig. 3.2. Because $\varepsilon^{(1)}$ is contained in Eq. (3.6) in the form of a product with the external force P, we may conclude that $\varepsilon^{(1)}$ has influence on resonance curves in the same way as P (or τ). When $\varepsilon^{(1)}=0.05$ or 0.10, the stable region appears. But when $\varepsilon^{(1)}$ has such a small value as 0.025, no resonance curves cross ω-axis, and the unstable region vanishes. In this case, the solution $R_{f0}+R_{b0}=0$ is stable at any ω. In the case of small $\varepsilon^{(1)}$, only the harmonic oscillations appear unless large disturbances exist.

The effects of the nonlinear component $\beta^{(2)}$ are shown in Fig. 3.3. The component $\beta^{(2)}$ has no influence on this kind of oscillation in a round shaft system, but it becomes a factor causing complicated phenomena in an unsymmetrical shaft system. The resonance curve for $\beta^{(2)}=0$ is the same as that of a round shaft system. In Fig. 3.3, the larger $\beta^{(2)}$ becomes, the wider the spread of the curves in the part of large amplitudes becomes. For example, the stable curve of a hard spring type for $\beta^{(2)}=0$ tends to bend toward the left side as $\beta^{(2)}$ increases. Finally it becomes an unstable curve which bends toward the left side, and an

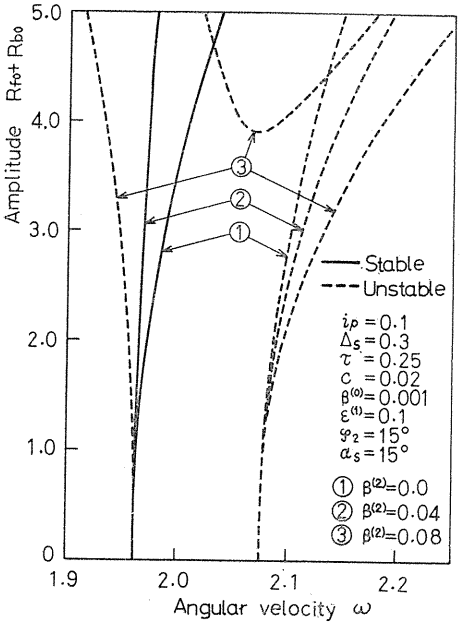

Fig. 3. 3. Effects of the nonlinear component $N(2)$ $(\beta^{(2)})$.

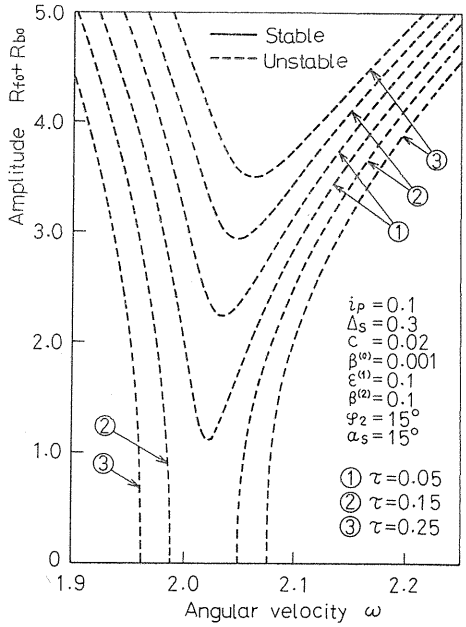

Fig. 3. 4. Effects of the unbalance τ.

unstable region appears.

The effects of the dynamic unbalance τ are shown in Fig. 3.4. Similar to the case of $\varepsilon^{(1)}$, the unstable region vanishes for a small τ.

There are qualitatively no big changes depending on the phase angle φ_2, or the angular position of the unbalance α_i.

3. 3. Other kinds of summed-and-differential harmonic oscillations

In a round shaft system, the summed-and-differential harmonic oscillations of the types $[p_f-2p_b]$ and $[2p_f-p_b]$ occur in addition to the type $[p_f-p_b]$[38]. We may expect the occurrence of these kinds of oscillations also in this unsymmetrical shaft system. Each resonance curve can be given by the same procedure as that in Section 3.2. From the results of such analyses, it becomes clear that the nonlinear components $\beta^{(0)}$ and $\beta^{(2)}$ have influence on resonance curves in the type $[p_f-2p_b]$, and only $\beta^{(0)}$ does in the type $[2p_f-p_b]$. Therefore, we find that these two oscillations are affected by the same nonlinear components as those in a round shaft system[38]; and that no other components have influence through the unsymmetry Δ_s. From the computation of these resonance curves, we see that those of the summed-and-differential harmonic oscillations of the types $[p_f-2p_b]$ and $[2p_f-p_b]$ are qualitatively the same as that in the case of a round shaft system.

3. 4. Theoretical analysis for the four-degree-of-freedom system

The experimental apparatus had four degrees of freedom, where the deflection vibrations and the inclination ones couple with each other. In Section 3.2, we have analyzed the problem for a two-degree-of-freedom system for simplicity. Now we shall obtain, qualitatively, the same results for a four-degree-of-freedom system by a similar procedure. The equations of motion are given by Eq. (1.6) in the dimensionless form.

For example, we will present the results of calculation for the summed-and-differential harmonic oscillation which occurs when the relation $p_i-p_j\fallingdotseq\omega$ holds among the frequencies p_i (>0), p_j (<0) and ω. We denote the amplitudes of $O(\varepsilon^0)$ of the deflection oscillation with the frequencies ω_i $(\fallingdotseq p_i)$ and ω_j $(\fallingdotseq p_j)$ by R_i and R_j, those of $O(\varepsilon^0)$ of the inclination oscillation by R_i' and R_j', and the respective phase angles by δ_i and δ_j. We put $\delta_i-\delta_j=\psi_{ij}$. In addition, we denote the amplitudes of $O(\varepsilon^0)$ with the frequencies $\bar{\omega}_i$ $(=2\omega-\omega_i)$ and $\bar{\omega}_j$ $(=2\omega-\omega_j)$ occuring due to the shaft unsymmetry by $\bar{R}_i$, $\bar{R}_i'$, and $\bar{R}_j$, $\bar{R}_j'$, respectively. We denote the amplitudes of $O(\varepsilon^0)$ of the deflection and the inclination of the harmonic oscillations with the frequency ω by P and Q, and their phase angles by β_1 and β_2. Using these quantities, we suppose the approximate solution with the accuracy of $O(\varepsilon)$ in the same manner as Eq. (3.2). Substituting this solution into Eq. (1.6) and using the principle of harmonic balance with the accuracy of $O(\varepsilon)$, we obtain the following equations for the amplitudes of the deflection oscillation R_i and R_j and the phase angle ψ_{ij}, corresponding to Eq. (3.6) in Section 3.2.

$$
\begin{aligned}
m_iR_i\dot{\delta}_i=&2\Phi_s(\omega_i)R_i+\{K_i^{(0)}R_i^2+L_i^{(0)}R_j^2+(\beta^{(0)}F^2)_i\}R_i\\
&+(B_c^{(2)}\cos 2\psi_{ij}-B_s^{(2)}\sin 2\psi_{ij})R_iR_j^2+\{(\varepsilon^{(1)}F)_i\cos\psi_{ij}\\
&+(\varepsilon^{(1)}F)_i'\sin\psi_{ij}\}R_j
\end{aligned}
\qquad\Big\backslash
$$

$$
\left.\begin{aligned}
m_i\dot{R}_i &= c_{i0}R_i + (B_s^{(2)}\cos 2\psi_{ij} + B_c^{(2)}\sin 2\psi_{ij})R_iR_j^2 - \{(\varepsilon^{(1)}F)'_i\cos\psi_{ij} \\
&\quad - (\varepsilon^{(1)}F)_i\sin\psi_{ij}\}R_j \\
m_jR_j\dot{\delta}_j &= 2\Phi_s(\omega_j)R_j + \{K_j^{(0)}R_j^2 + L_j^{(0)}R_i^2 + (\beta^{(0)}F^2)_j\}R_j \\
&\quad + (B_c^{(2)'}\cos 2\psi_{ij} - B_s^{(2)'}\sin 2\psi_{ij})R_i^2R_j + \{(\varepsilon^{(1)}F)_j\cos\psi_{ij} \\
&\quad + (\varepsilon^{(1)}F)'_j\sin\psi_{ij}\}R_i \\
m_j\dot{R}_j &= c_{j0}R_j - (B_s^{(2)'}\cos 2\psi_{ij} + B_c^{(2)'}\sin 2\psi_{ij})R_i^2R_j \\
&\quad + \{(\varepsilon^{(1)}F)'_j\cos\psi_{ij} - (\varepsilon^{(1)}F)_j\sin\psi_{ij}\}R_i
\end{aligned}\right\} \quad (3.8)
$$

where, with the accuracy of $O(\varepsilon)$, m_i, m_j are constants; c_{i0}, c_{j0} are the constants indicating the damping; $\Phi(\omega_i)$, $\Phi(\omega_j)$ are the quantities indicating the detuning; $K_i^{(0)}$, $K_j^{(0)}$, $L_i^{(0)}$, $L_j^{(0)}$ are the coefficients relating to $N(0)$; $B_c^{(2)}$, $B_s^{(2)}$, $B_c^{(2)'}$, $B_s^{(2)'}$ are the coefficients relating to $N(2)$; $(\beta^{(0)}F^2)_i$, $(\beta^{(0)}F^2)_j$ are the quadratic equations of the amplitude of a harmonic oscillation having the coefficients of the nonlinear component $N(0)$; and $(\varepsilon^{(1)}F)_i$, $(\varepsilon^{(1)}F)_j$, $(\varepsilon^{(1)}F)'_i$, $(\varepsilon^{(1)}F)'_j$, are the linear expressions of the amplitude of the harmonic oscillation having the coefficients of $N(1)$. We omit the complete forms of the expressions representing these notations. Equation (3.8) gives the amplitudes of the deflection oscillations in the four-degree-of-freedom system. Comparing with Eq. (3.6), we find that the shapes of resonance curves for Eqs. (3.6) and (3.8) are qualitatively the same because each equation has the same form. Therefore the results of calculation for the inclination oscillation in the two-degree-of-freedom system represented by Eq. (3.6) can be compared qualitatively with the experimental results for the deflection oscillation which will be mentioned in Section 3.5.

In the round shaft system having four degrees of freedom (the natural frequencies; $p_1>p_2>0>p_3>p_4$), the oscillations of the types $[p_1+p_2]$, $[-p_3-p_4]$, $[2p_i+p_j]$ $(i\neq j)$, $[-p_k-2p_l]$ $(k\neq l)$, $[p_1+p_2-p_k]$, and $[p_i-p_3-p_4]$ may occur, in addition to the oscillations of the types $[p_i-p_k]$, $[p_i-2p_k]$, $[2p_i-p_k]$ corresponding to those of the types $[p_f-p_b]$, $[p_f-2p_b]$, $[2p_f-p_b]$, respectively. The subscripts in these notations take the values of i, $j=1$, 2 and k, $l=3$, 4. The features of these kinds of the oscillations in an unsymmetrical shaft system can be examined by analyzing the equations for the four-degree-of-freedom system in the same way as previously mentioned. Except for the oscillations which are related to three natural frequencies, we can obtain qualitatively the same results as those for the four-degree-of-freedom system by analyzing the two-degree-of-freedom system if we cancel the restriction $\omega_f\fallingdotseq p_f>0$, and $\omega_b\fallingdotseq p_b<0$, and assume p_f and p_b can take both positive and negative values. For example, analyzing the oscillation of the type $[p_1+p_2]$ under the assumption of $\omega_f\to p_1>0$ and $\omega_b\to p_2>0$, we find that the nonlinear component $N(2)$ in addition to $N(0)$ and $N(1)$ is concerned with this oscillation in an unsymmetrical shaft system, and that this oscillation has the same features as those of the type $[2p_i]$ and $[p_i-p_k]$.

3. 5. Experimental results

The experimental apparatus is shown in Fig. 1.2. In experiments, we used two kinds of discs, i. e., R_3 (the larger disc) and R_4 (the smaller disc) in Table 1.1,

and the unsymmetrical shaft S_3 in Table 1.2. The summed-and-differential harmonic oscillations were observed under various assemblies. The values of the parameters of the system were varied by exchanging the disc and changing the assembly of the apparatus and the size and location of the existing unbalance.

The nonlinear spring characteristics of the shaft were determined by the position of the bearing center line to the angular clearance of the lower bearing. The typical resonance curves measured are shown in the following.

The $p-\omega$ diagram for the larger disc is shown in Fig. 3.5. This diagram was drawn on the basis of the experimental data in the assembly shown in Fig. 3.6.

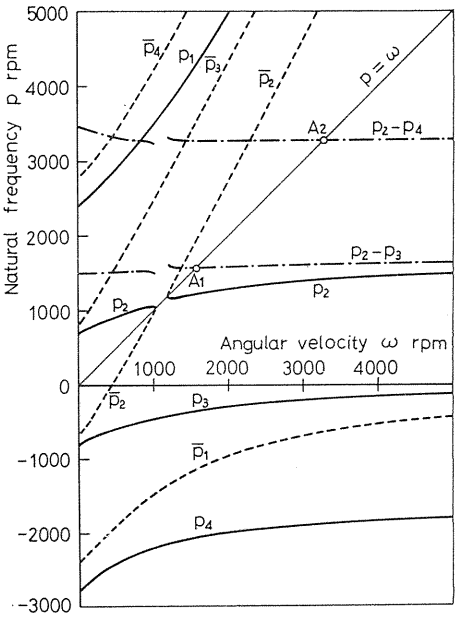

Fig. 3.5. The p-ω diagram (the larger disc was used in the four-degree-of-freedom system).

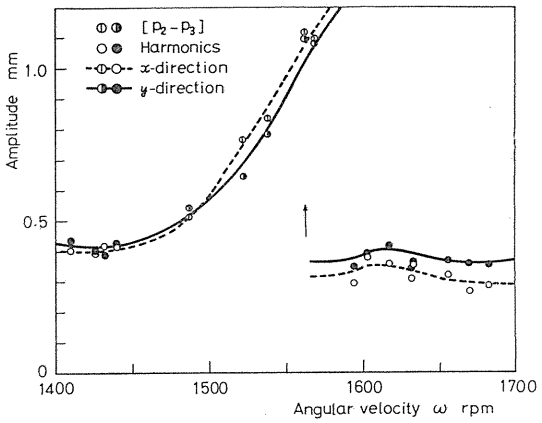

Fig. 3.6. Resonance curves of the summed-and-differential harmonic oscillation $[p_2-p_3]$ (hard spring type).

The parts of the curves which could not be obtained in the experiments were supplemented by the theoretically calculated values. The resonant angular velocities in Fig. 3.8 etc. are not coincident completely with those in Fig. 3.5. These discrepancies are due to the difference of assembly. We designate the natural frequency p_i $(i=1\sim4)$ by solid lines and $\bar{p}_i=2\omega-p_i$ by broken lines. The values of p_2-p_3 and p_2-p_4 are also drawn in chain lines in the diagram. The points A_1 and A_2 in this diagram give the resonance frequencies of the summed-and-differential harmonic oscillations of the types $[p_2-p_3]$ and $[p_2-p_4]$, respectively.

The resonance curves for the summed-and-differential harmonic oscillation of the type $[p_2-p_3]$ are shown in Figs. 3.6~3.9. Figure 3.6 (the larger disc was used) shows the resonance curve of a hard spring type. The arrow on this diagram means a jump phenomenon. This responce curve corresponds to the case in which $\beta^{(0)}$ takes a positive value in Fig. 3.2.

Figure 3.7 (the smaller disc was used) is an example of the resonance curve of a soft spring type. The resonance frequency is higher than that in Fig. 3.6.

Figure 3.8 (the larger disc was used) is the case in which an unstable vibration appeared. The discrepancy between the center lines of the upper and the

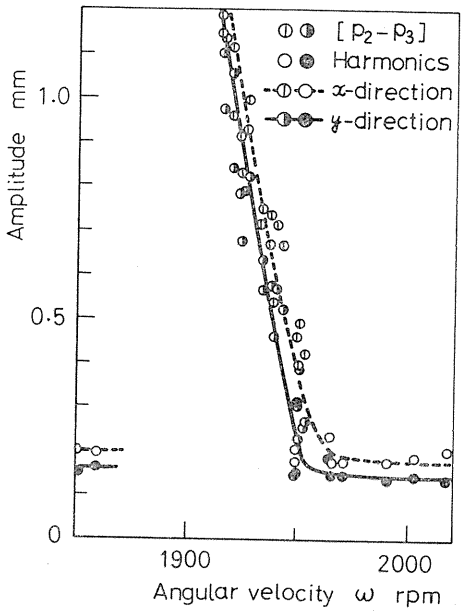

Fig. 3. 7. Resonance curves of the summed-and-differential harmonic oscillation[p_2-p_3] (soft spring type).

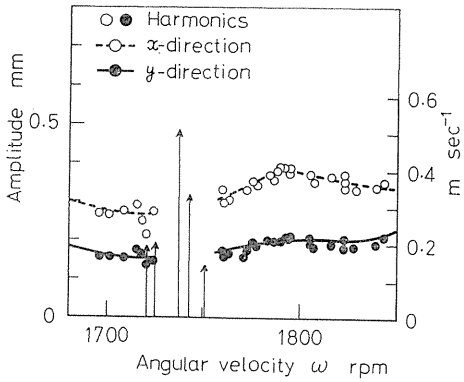

Fig. 3. 8. An unstable region of the summed-and-differential harmonic oscillation [p_2-p_3].

lower pedestals in Fig. 3.8 is larger than that in Fig. 3.6. Within the unstable region at the angular velocities from 1721 rpm to 1757 rpm, two oscillations, with the frequencies ω_2 ($\fallingdotseq p_2$) and ω_3 ($\fallingdotseq p_3$) satisfying the relation $\omega_2-\omega_3=\omega$, occurred simultaneously; and the amplitudes of these oscillations increased with time. The envelope of the recorded wave form is approximated by the expression A_0e^{mt} (A_0 : an arbitrary constant), and the length of the arrow in Fig. 3.8 represents the value of m sec^{-1}. The value m means the rate at which the amplitudes increase. Figure 3.8 corresponds to the theoretical curve whose $\beta^{(0)}$ is small and the unbalance τ is comparatively large in Fig 3.4.

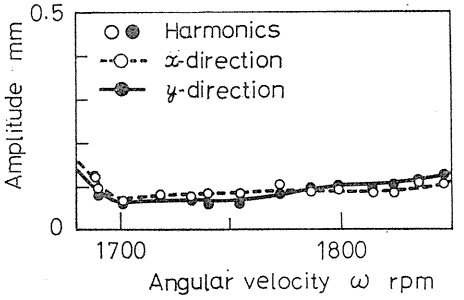

Fig. 3. 9. Resonance curves in the case that the summed-and-differential harmonic oscillation [p_2-p_3] did not appear (when we made the unbalance smaller on the same assembly condition as that of Fig. 3. 8.).

Figure 3.9 is a resonance curve in the case where we made the unbalance smaller in the same assembly as that of Fig. 3.8. In this case, only a harmonic oscillation appeared, but neither stable nor unstable summed-and-differential harmonic oscillations occurred. This diagram corresponds to the curve for $\tau=0.05$ in Fig. 3.4.

The summed-and-differential harmonic oscillations of the type $[p_2-p_4]$ appeared at the angular velocity indicated by the point A_2 in Fig. 3.5. We obtained three same kinds of resonance curves corresponding to those of the type $[p_2-p_3]$ in Figs. 3.6, 3.7 and 3.9, respectively.

3. 6. Conclusions

The conclusions about the summed-and-differential harmonic oscillations in an unsymmetrical shaft system may be summarized as follows:

(1) In an unsymmetrical shaft system, the characteristics of the summed-and-differential harmonic oscillation of the type $[p_f-p_b]$ are similar to those of the subharmonic oscillation of the type $[2p_f]$.

(2) For the summed-and-differential harmonic oscillation of the type $[p_f-p_b]$, the nonlinear component $N(2)$, which has no effects on a round shaft system, has great influence in addition to the components $N(0)$ and $N(1)$; and the oscillation phenomena which differ from those in a round shaft system appear.

(3) For the summed-and-differential harmonic oscillation $[p_f-p_b]$, changing the values of the parameters results in many types of resonance curves as follows: the stable solution of a hard spring type, that of a soft spring type, the unstable region, and the case in which no summed-and-differential harmonic oscillations occur.

(4) In the experiment with an unsymmetrical shaft supported by the single-row deep groove ball bearings, depending on the dimensions of the system, the assembly, and the size, location of the existing unbalance etc., we obtained four typical kinds of resonance curves for the summed-and-differential harmonic oscillation of the type $[p_2-p_3]$. They were the following: a stable resonance curve of a soft spring type, an unstable region where an unstable vibration occurred, and the case in which only a harmonic oscillation appeared and the summed-and-differential harmonic oscillation vanished. Thus, it is ascertained that the experimental results are qualitatively consistent with the theoretical ones.

(5) As for the summed-and-differential harmonic oscillation $[p_2-p_4]$, some kinds of resonance curves for the oscillation $[p_2-p_3]$ were obtained.

4. Subharmonic and Summed-and-Differential Harmonic Oscillations of an Unsymmetrical Rotor[59]

4. 1. Introduction

When a shaft is supported vertically by single-row deep groove ball bearings, the restoring force of the shaft has a nonlinear spring characteristic owing to angular clearances of the ball bearings. In this chapter, we shall investigate subharmonic oscillations and summed-and-differential harmonic oscillations in a nonlinear system where an unsymmetrical rotor is mounted on an elastic shaft with

circular cross section. In the case of the unsymmetrical shaft system carrying a disc, we have already reported on the subharmonic oscillations[56] and discussed the summed-and-differential harmonic oscillations in Chapter 3. We shall confirm that qualitatively the same phenomena as those in the unsymmetrical shaft system appear also in this unsymmetrical rotor system.

4. 2. Theoretical analyses of the subharmonic oscillation of order 1/2 and the summed-and-differential harmonic oscillation

The experimental apparatus is a four-degree-of-freedom system. The deflection r and the inclination θ of the shaft at the position where an unsymmetrical rotor is mounted couple with each other. But in the theoretical analysis, we consider only the inclination in the system where r and θ do not couple. The same procedure as that in the unsymmetrical shaft system shown in Chapter 3 can lead to the conclusion that the results for the four-degree-of-freedom system as in this experimental apparatus are qualitatively similar to those for the two-degree-of freedom system.

In this section, we shall find the approximate solutions of Eq. (1.4) for two kinds of oscillations by means of the same method as that used in the theoretical analyses for the unsymmetrical shaft system[56, 58]. We assume that θ_x, θ_y, and Δ_i are magnitudes of $O(\varepsilon^0)$, and c, $N_{\theta x}$, and $N_{\theta y}$ are maginitudes of $O(\varepsilon)$ in the equations of motion (1.4) in the two-degree-of-freedom system.

4. 2. 1. The subharmonic oscillation of order 1/2 of the type $[2p_f]$

When the frequency of the external force ω becomes nearly equal to the natural frequency of this system $2p_f$, this force performs a work on the system. Consequently, the oscillation with the frequency $\omega_f=1/2\cdot\omega(\fallingdotseq p_f)$ appears markedly, and we can observe a subharmonic oscillation having the mode of forward precession. We designate this kind of oscillation by the symbol $[2p_f]$. As the unsymmetry Δ_i is the quantity of $O(\varepsilon^0)$, this oscillation component of frequency $1/2\cdot\omega$ always yields a component of frequency $2\omega-1/2\cdot\omega=3/2\cdot\omega$ in the same magnitudes of amplitudes. Therefore, the approximate solution must be assumed in the following forms with the accuracy of $O(\varepsilon)$[56].

$$\begin{aligned}\begin{matrix}\theta_x\\ \theta_y\end{matrix}=&R\begin{matrix}\cos\\ \sin\end{matrix}\left(\frac{1}{2}\omega t+\delta_1\right)+\bar{R}\begin{matrix}\cos\\ \sin\end{matrix}\left(\frac{3}{2}\omega t-\delta_1\right)+P\begin{matrix}\cos\\ \sin\end{matrix}(\omega t+\beta)\\ &+\varepsilon\begin{matrix}f\left(\frac{1}{2}\omega,\ \omega,\ \frac{3}{2}\omega,\ \cdots\right)\\ f'\left(\frac{1}{2}\omega,\ \omega,\ \frac{3}{2}\omega,\ \cdots\right)\end{matrix}\end{aligned}\qquad(4.1)$$

where the amplitudes R and $\bar{R}$, and the phase angle δ_1, are the quantities of $O(\varepsilon^0)$ varying slowly with time. The functions $\varepsilon\cdot f$ and $\varepsilon\cdot f'$ are the components of $O(\varepsilon)$ which appear owing to the nonlinear terms in Eq. (1.9), and their concrete forms are the same as those of the unsymmetrical shaft system[56]. The amplitude P and the phase angle β of the harmonic oscillation can be determined with the accuracy of $O(\varepsilon^0)$ as follows:

$$P=\tau\omega^2\sqrt{\left(\frac{1-i_p+\Delta_i}{G-\Delta_i\omega^2}\cos\alpha_i\right)^2+\left(\frac{1-i_p-\Delta_i}{G+\Delta_i\omega^2}\sin\alpha_i\right)^2},$$

$$\left.\tan\beta=\frac{(G-\Delta_i\omega^2)(1-i_p-\Delta_i)}{(G+\Delta_i\omega^2)(1-i_p+\Delta_i)}\tan\alpha_i\right\} \tag{4.2}$$

where $G=G(\omega)=1+i_p\omega^2-\omega^2$.

As the next step, substituting Eq. (4.1) into Eq. (1.4) and setting the terms of the same frequencies to be zero separately with the accuracy of $O(\varepsilon)$, we obtain the simultaneous equations for amplitude R and the phase angle δ_1.

$$\left.\begin{aligned}A\omega R\dot{\delta}_1=&[\sigma+\beta^{(0)}(gR^2+kP^2)+4\Delta_i\Omega(\beta_s^{(2)}\sin 4\delta_1+\beta_c^{(2)}\cos 4\delta_1)R^2\\&+2\varepsilon^{(1)}P\{\overline{G}_1\cos(2\delta_1-\beta)+2\Delta_i\Omega\cos(2\delta_1+\beta)\}]\\A\omega\dot{R}=&[\bar{c}+4\Delta_i\Omega(\beta_c^{(2)}\sin 4\delta_1-\beta_s^{(2)}\cos 4\delta_1)R^2\\&+2\varepsilon^{(1)}P\{\overline{G}_1\sin(2\delta_1-\beta)+2\Delta_i\Omega\sin(2\delta_1+\beta)\}]R\end{aligned}\right\} \tag{4.3}$$

where we put $\varepsilon_c^{(1)}=\varepsilon^{(1)}$ (>0) and $\varepsilon_s^{(1)}=0$ by rotating the coordinate axes by some angles. The notations in Eq. (4.3) are as follows:

$$\left.\begin{aligned}&A=(1-i_p)\overline{G}_1+(i_p-3)G_1+2\Delta_i^2\Omega,\\&\bar{c}=c\omega(3G-\overline{G}_1)/2, && G(p)=1+i_p\omega p-p^2,\\&G_1=G\left(\frac{1}{2}\omega\right), && \overline{G}_1=G\left(\frac{3}{2}\omega\right),\\&g=4(G_1^2+4G_1\overline{G}_1+\overline{G}_1^2)/G_1, && k=8(G_1+\overline{G}_1+\Delta_i\Omega\cos 2\beta),\\&\beta^{(2)}=\sqrt{\beta_c^{(2)2}+\beta_s^{(2)2}}, && 2\varphi_2=\tan^{-1}(\beta_s^{(2)}/\beta_c^{(2)}),\\&\sigma=G_1\overline{G}_1-(\Delta_i\Omega)^2, && \Omega=\frac{3}{4}\omega^2\end{aligned}\right\} \tag{4.4}$$

By putting $\dot{\delta}_1=0$ and $\dot{R}=0$ in Eq. (4.3), the stationary solution $R=R_0$ can be classified into two kinds of solutions, i. e., $R_0\neq 0$ and $R_0=0$. Especially, it is noticeable that the nonlinear component $N(2)$, which has no effects on the subharmonic oscillation of order 1/2 in the symmetrical system, is contained in Eq. (4.3). This component $N(2)$ causes the theoretical resonance curves of the subharmonic oscillation $[2p_f]$ in the unsymmetrical rotor system to be complicated. We find that the right side of Eq. (4.3) coincides with the equation of the subharmonic oscillation $[2p_f]$ in the unsymmetrical shaft system if we replace Δ_s $(=\Delta\delta/\delta)$ with $\Delta_i\Omega$ $(=\Delta I/I\cdot(3/4\cdot\omega^2))$[56]. Therefore, this suggests that the shapes of the theoretical resonance curves in the unsymmetrical rotor system are qualitatively the same as those in the unsymmetrical shaft system. Introducing the small deviations from the stationary solutions, we can examine the stability of these solutions by the same procedure as that in the unsymmetrical shaft system[56].

Figures 4.1~4.5 show the typical theoretical resonance curves obtained by numerical computation. The stable and unstable solutions are drawn with solid and broken lines, respectively. In order to avoid confusion, we do not draw the solutions $R_0=0$. As for the stability of the solution $R_0=0$, the points at which the resonance curves for the solutions $R_0\neq 0$ intersect the ω-axis give the boun-

daries between the stable parts and the unstable ones, and the solutions are unstable between such two intersecting points, and stable outside them. If there are no intersecting points, the solutions of $R_0=0$ are stable at any value of ω.

Figure 4.1 shows the influence of the unsymmetry Δ_i. By making the value of Δ_i larger, the stable resonance curve tends to bend toward the lower angular velocity, and at last, all resonance curves of $R_0 \neq 0$ become unstable. In this case, all resonance curves containing the solution $R_0=0$ are unstable between two points at which the curves for $R_0 \neq 0$ intersect the ω-axis. Therefore, in this region (i. e., unstable region) no stable stationary oscillations are obtained, but an unstable vibration of frequency $+1/2\cdot\omega$ whose amplitude increases with time occurs. This is a marked phenomenon which is not observed in the symmetrical system.

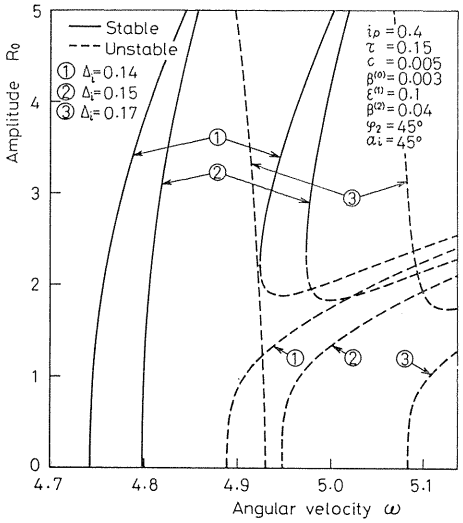

Fig. 4. 1. Theoretical resonance curves of the subharmonic oscillation $[2p_f]$ showing the influence of the unsymmetry Δ_i.

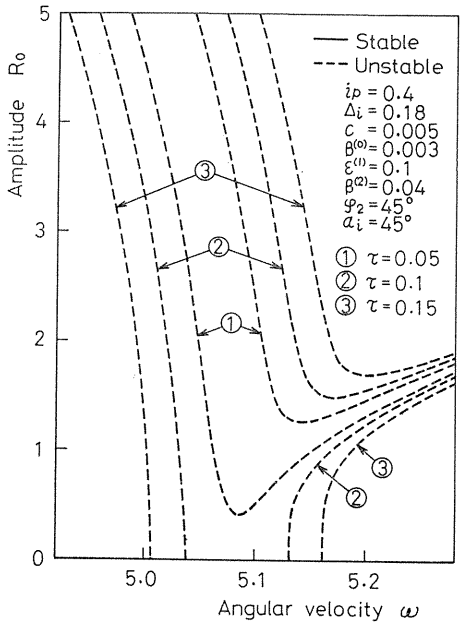

Fig. 4. 2. Theoretical resonance curves showing the influence of the dynamic unbalance τ.

The influence of the dynamic unbalance τ is shown in Fig. 4.2. This is such an example that all the solutions of $R_0 \neq 0$ are unstable. When the value of τ is larger, the curve for $R_0 \neq 0$ intersects the ω-axis, and then the unstable region appears. The value of τ has no direct effect on the stability of the resonance curve, but contributes to the difficulty of appearance of this vibration.

Figure 4.3 shows the influence of the nonlinear component $N(0)$ (i. e., $\beta^{(0)}$). The sign of the value of $\beta^{(0)}$ decides the type of the resonance curves; i. e., for the positive $\beta^{(0)}$ the curve is a hard spring type bending toward the higher angular velocity, and for the negative $\beta^{(0)}$ a soft spring type bending toward the lower angular velocity. Especially, when the absolute value of $\beta^{(0)}$ is comparatively small,

the unstable region appears.

Figure 4.4 shows the influence of the nonlinear component $N(2)$ (i. e., $\beta^{(2)}$). In this diagram where the curves for the comparatively large $\beta^{(0)}$ are shown, the value of $\beta^{(2)}$ gives a marked effect on the spread of the curve in the part of large amplitudes. Since Eq. (4.3) includes $\beta^{(2)}$ and Δ_i in the product form, Fig. 4.4 is

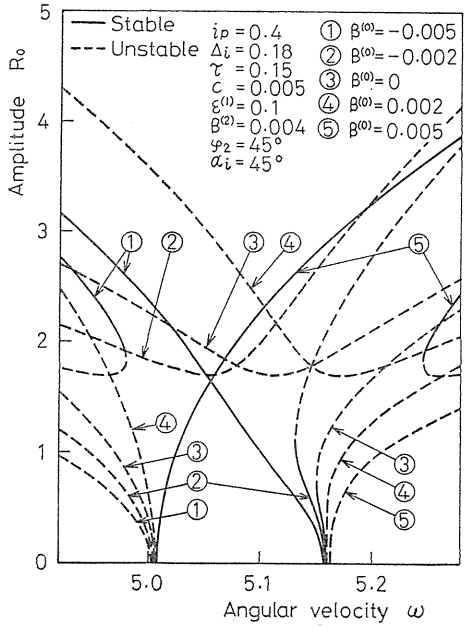

Fig. 4. 3. Theoretical resonance curves showing the influence of the nonlinear component $N(0)$ ($\beta^{(0)}$).

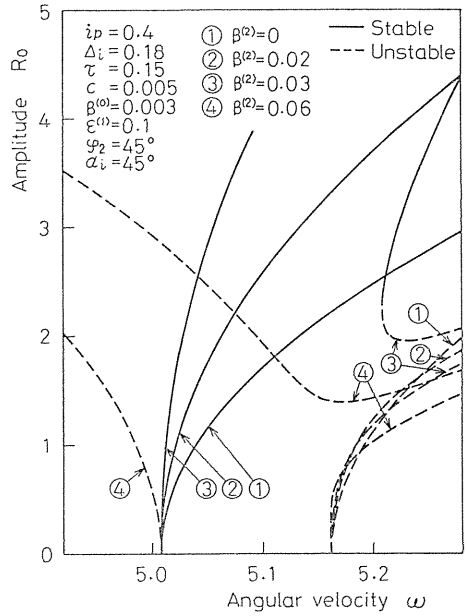

Fig. 4. 4. Theoretical resonance curves showing the influence of the nonlinear component $N(2)$ ($\beta^{(2)}$).

similar to Fig. 4.1 showing the influence of Δ_i. The fact that the unstable region appears in the unsymmetrical shaft or rotor system is due to the influence of the nonlinear component $N(2)$. This component has no effects on the symmetrical system, but has great influence through the unsymmetry of the shaft or the rotor.

Since Eq. (4.3) includes $\varepsilon^{(1)}$ and τ in the product form, the effect of $\varepsilon^{(1)}$ is qualitatively the same as that of τ shown in Fig. 4.2. There are qualitatively no big changes for various values of phase angle φ_2 of $\beta^{(2)}$ and the angular position α_i of τ.

4. 2. 2. The summed-and-differential harmonic oscillation of the type $[p_f-p_b]$

When the natural frequency p_f-p_b is nearly equal to the angular velocity ω in the nonlinear multi-degree-of-freedom shaft system, two oscillations with frequencies ω_f and ω_b, which are nearly equal to p_f and p_b, respectively, appear simultaneously. In this case, the equations

$$\omega_f \fallingdotseq p_f, \quad \omega_b \fallingdotseq p_b, \quad \omega_f-\omega_b=\omega \tag{4.5}$$

hold. We find that this kind of oscillation (which is designated by the symbol $[p_f-p_b]$) occurs also in the unsymmetrical rotor system, and that its vibratory characteristic is similar to that of the unsymmetrical shaft system[58]. We try to perform the theoretical analysis by the same procedure as that for the unsymmetrical shaft system. First, we suppose an approximate solution with the accuracy of $O(\varepsilon)$ in the form of Eq. (3.2). It is assumed that the amplitudes R_f, R_b, $\overline{R}_f$, $\overline{R}_b$ and the phase angles δ_f, δ_b are the quantities of $O(\varepsilon^0)$ varying slowly with time. Substituting this equation into Eq. (1.4), we set the *sine* and *cosine* terms of the respective frequencies ω_f, $\overline{\omega}_f$, ω_b and $\overline{\omega}_b$ to be zero separately with the accuracy of $O(\varepsilon)$. After arranging these simultaneous equations, we obtain the following equations:

$$\left.\begin{aligned}
A_fR_f\dot{\delta}_f&=-\sigma_fR_f-4\beta^{(0)}(g_fR_f^2+2\bar{g}_bR_b^2+2k_fP^2)R_f+6m_b(\beta_c^{(2)}\cos 2\psi\\
&\quad-\beta_s^{(2)}\sin 2\psi)R_fR_b^2-2\varepsilon^{(1)}(a_c\cos\psi+a_s\sin\psi)PR_b\\
A_f\dot{R}_f&=c_fR_f+6m_b(\beta_s^{(2)}\cos 2\psi+\beta_c^{(2)}\sin 2\psi)R_fR_b^2\\
&\quad+2\varepsilon^{(1)}(a_s\cos\psi-a_c\sin\psi)PR_b\\
A_bR_b\dot{\delta}_b&=-\sigma_bR_b-4\beta^{(0)}(2\bar{g}_fR_f^2+g_bR_b^2+2k_bP^2)R_b+6m_f(\beta_c^{(2)}\cos 2\psi\\
&\quad-\beta_s^{(2)}\sin 2\psi)R_f^2R_b-2\varepsilon^{(1)}(b_c\cos\psi+b_s\sin\psi)PR_f\\
A_b\dot{R}_b&=c_bR_b-6m_f(\beta_s^{(2)}\cos 2\psi+\beta_c^{(2)}\sin 2\psi)R_f^2R_b\\
&\quad-2\varepsilon^{(1)}(b_s\cos\psi-b_c\sin\psi)PR_f
\end{aligned}\right\}\quad(4.6)$$

where we put $\varepsilon_c^{(1)}=\varepsilon^{(1)}$ (>0) and $\varepsilon_s^{(1)}=0$. The notations

$$\left.\begin{aligned}
&A_f=(i_p\omega-2\omega_f)\overline{G}_f-(i_p\omega-2\overline{\omega}_f)G_f-4\Delta_i^2\Omega_f(\omega-\omega_f),\\
&A_b=(i_p\omega-2\omega_b)\overline{G}_b-(i_p\omega-2\overline{\omega}_b)G_b-4\Delta_i^2\Omega_b(\omega-\omega_b),\\
&a_c=\left(\overline{G}_f+\frac{\Omega_f}{\Omega_b}G_b+\Delta_i\Omega_f\right)\cos\beta,\quad a_s=\left(\overline{G}_f+\frac{\Omega_f}{\Omega_b}G_b-\Delta_i\Omega_f\right)\sin\beta,\\
&b_c=\left(\overline{G}_b+\frac{\Omega_b}{\Omega_f}G_f+\Delta_i\Omega_f\frac{\overline{G}_b}{\overline{G}_f}\right)\cos\beta,\quad b_s=\left(\overline{G}_b+\frac{\Omega_b}{\Omega_f}G_f-\Delta_i\Omega_f\frac{\overline{G}_b}{\overline{G}_f}\right)\sin\beta,\\
&c_f=c(\omega_f\overline{G}_f-\overline{\omega}_fG_f),\quad c_b=c(\omega_b\overline{G}_b-\overline{\omega}_bG_b),\quad G_f=G(\omega_f),\\
&G_b=G(\omega_b),\quad \overline{G}_f=G(\overline{\omega}_f),\quad \overline{G}_b=G(\overline{\omega}_b),\\
&g_f=(G_f^2+\overline{G}_f^2+4G_f\overline{G}_f)/\overline{G}_f,\quad g_b=(G_b^2+\overline{G}_b^2+4G_b\overline{G}_b)/\overline{G}_b,\\
&\bar{g}_f=\{(G_f+\overline{G}_f)(G_b+\overline{G}_b)+2\Delta_i^2\Omega_f\Omega_b\}/\overline{G}_f,\\
&\bar{g}_b=\{(G_f+\overline{G}_f)(G_b+\overline{G}_b)+2\Delta_i^2\Omega_f\Omega_b\}/\overline{G}_b,\\
&k_f=G_f+\overline{G}_f+\Delta_i\Omega_f\cos 2\beta,\quad k_b=G_b+\overline{G}_b+\Delta_i\Omega_b\cos 2\beta,\\
&m_f=-\Delta_i(\Omega_f\overline{G}_b+\Omega_bG_f)/\overline{G}_f,\quad m_b=-\Delta_i(\Omega_f\overline{G}_b+\Omega_bG_f)/\overline{G}_b,
\end{aligned}\right\}\quad(4.7)$$

$$\sigma_f=G_f\bar{G}_f-(\Delta_i\Omega_f)^2,\quad \sigma_b=G_b\bar{G}_b-(\Delta_i\Omega_b)^2,\quad \psi=\delta_f-\delta_b,$$
$$\Omega_f=\omega_f\bar{\omega}_f,\quad \Omega_b=\omega_b\bar{\omega}_b,$$

are used in Eq. (4.6). The solution of the harmonic oscillation is given by Eq. (4.2). From Eq. (4.6), we find that the nonlinear components $N(0)$, $N(1)$, and $N(2)$ have effects on the summed-and-differential harmonic oscillation of the type $[p_f-p_b]$. Similarly to the subharmonic oscillation of order 1/2 $[2p_f]$ in Section 4.2.1, the component $N(2)$, which has no influence on the symmetrical system, is related. In the same manner as that in the unsymmetrical shaft system[58], we can get the stationary solutions $R_f=R_{f0}$ and $R_b=R_{b0}$, and can examine the stabilities of them. The influences of various parameters on the resonance curves obtained by numerical computations are nearly the same as those in the subharmonic oscillation of order 1/2 $[2p_f]$. For example, the influence of the unsymmetry Δ_i is shown in Fig. 4.5. In this diagram, the ordinate represents the sum of the stationary amplitudes of the two oscillations with frequencies ω_f and ω_b. When Δ_i is large, an unstable vibration appears.

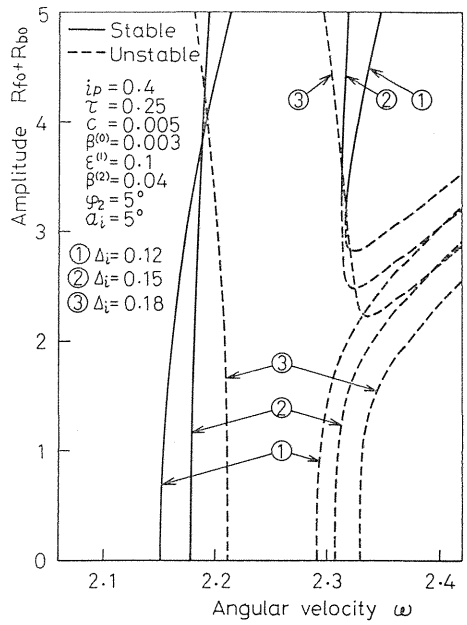

Fig. 4.5. Theoretical resonance curves of the summed-and-differential harmonic oscillation $[p_f-p_b]$ showing the influence of the unsymmetry Δ_i.

4.3. *Other kinds of subharmonic oscillation and summed-and-differential harmonic oscillations*

Up to the previous sections, we have shown that the vibratory characteristics of the subharmonic oscillation of order 1/2 $[2p_f]$ and the summed-and-differential harmonic oscillation $[p_f-p_b]$ in the unsymmetrical rotor system are quite different from those in the symmetrical system. In addition to these oscillations, the subharmonic oscillation of order 1/2 of the type $[-2p_b]$, the subharmonic oscillations of order 1/3 of the types $[3p_f]$ and $[-3p_b]$, and summed-and-differential harmonic oscillations of the types $[2p_f-p_b]$ and $[p_f-2p_b]$ may occur in the unsymmetrical rotor system with the nonlinear spring characteristics represented by Eq. (1.9). But, the theoretical calculations for these oscillations lead to the same results as those of the symmetrical system[38]. Their resonance curves are not influenced greatly by the unsymmetry Δ_i, and the nonlinear components related to each oscillation are the same as those in the symmetrical system, and the vibratory characteristics are qualitatively the same.

4.4. *Experimental results*

Experiments were performed in the system where the unsymmetrical rotor R_2

in Table 1.1 was mounted on the round shaft S_2 in Table 1.2 (see Fig. 1.1). The resonance curves were measured under various assemblies. The values of parameters were varied by changing the assembly of the apparatus and size and location of unbalance.

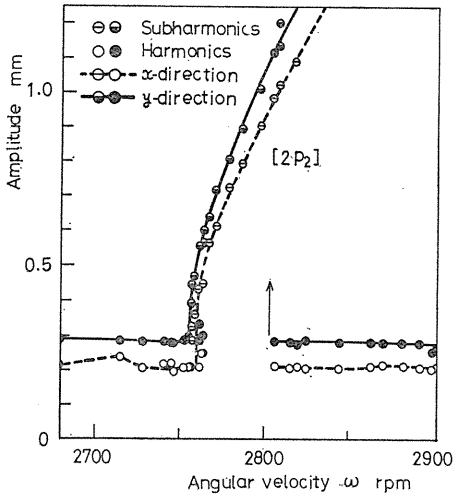

Fig. 4. 6. Experimental resonance curves of the subharmonic oscillation of order 1/2 $[2p_2]$ (a hard spring type).

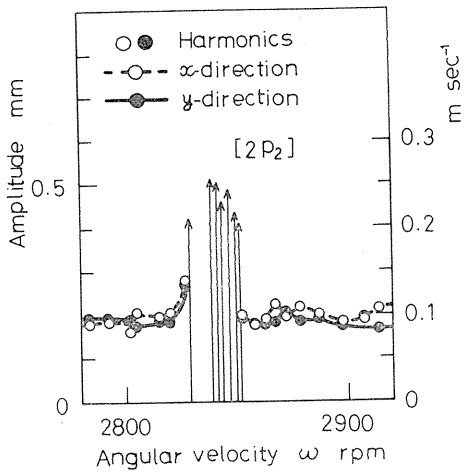

Fig. 4. 7. Experimental resonance curves of the subharmonic oscillation $[2p_2]$ where an unstable region existed.

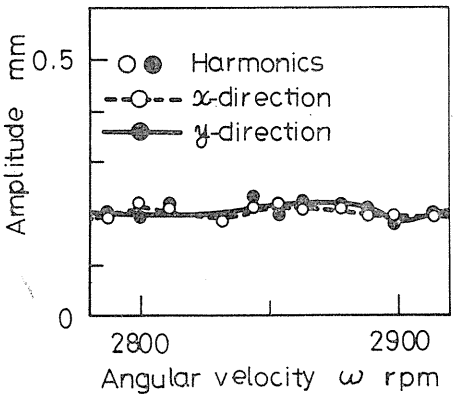

Fig. 4. 8. Experimental resonance curves where the subharmonic oscillation $[2p_2]$ disappeared and the harmonic oscillation remained.

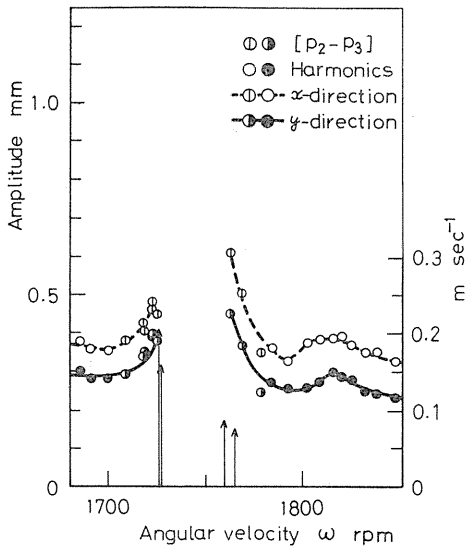

Fig. 4. 9. Experimental resonance curves of the summed-and-differential harmonic oscillation $[p_2-p_3]$ where an unstable region appeared.

A $p-\omega$ diagram of the experimental apparatus with four degrees of freedom is similar to that of an unsymmetrical rotor system[58]. Natural frequencies p_i ($i=1\sim4$) and $\bar{p}_i$ ($=2\omega-p_i$) coexist due to the unsymmetry of the rotor.

The experimental results for the subharmonic oscillations of order 1/2 $[2p_2]$ are shown in Figs. 4.6~4.8. Figure 4.6 is a hard spring type, and the arrow represents a jump phenomenon. Figure 4.7 is an example where an unstable vibration appeared under the different assembly from that in Fig. 4.6. Figure 4.8 has the same assembling condition as Fig. 4.7, and shows the case of a small unbalance. An unstable vibration does not appear and harmonic oscillations remain. This corresponds to that of the theoretical resonance curve for a small τ in Fig. 4.2.

In the experiments for the summed-and-differential harmonic oscillation $[p_2-p_3]$, we obtained the same four kinds of resonance curves as those of the oscillation $[p_2-p_3]$ in the unsymmetrical shaft system in Chapter 3 by changing the assembly condition of the apparatus. We show only one type of the resonance curve in Fig. 4.9 where the unstable vibration occurred.

As for the summed-and-differential harmonic oscillation of the type $[p_2-p_4]$, the resonance frequency was so high that we could not experiment on it sufficiently.

4. 5. Conclusions

(1) In an unsymmetrical rotor system with a nonlinear spring characteristic, the nonlinear components $N(0)$, $N(1)$, and $N(2)$ are concerned with the subharmonic oscillation of order 1/2 of the type $[2p_f]$ and the summed-and-differential harmonic oscillation of the type $[p_f-p_b]$. Especially, the component, which has no effct on a symmetrical system, plays an important part through the unsymmetry Δ_i in these oscillations. As the result, different phenomena from those in the symmetrical system appear.

(2) The theoretical resonance curves of these two kinds of oscillations are qualitatively the same. They can be classified into four typical groups as follows: the stable resonance curve of a hard spring type, that of a soft spring type, the resonance curve having an unstable region in which only the unstable solutions exist, and the case in which these oscillations do not occur unless a large disturbance gets into the system.

(3) In experiments on the unsymmetrical rotor system having a single-row deep groove ball bearing, we obtained the same resonance curves in form as those calculated in the theoretical analyses. The types of these resonance curves were changed depending on the degree of discrepancy between the center lines of the upper and the lower bearings and the size and location of the existing unbalance.

(4) In experiments, we obtained three kinds of resonance curves for the subharmonic oscillation of order 1/2 of the type $[2p_2]$, and four kinds of resonance curves for the summed-and-differential harmonic oscillation of the type $[p_2-p_3]$.

(5) The qualitative characteristics of the subharmonic oscillations and the summed-and-differential harmonic oscillations in the unsymmetrical rotor system are theoretically and experimentally the same as those in the unsymmetrical shaft system.

5. Super-Summed-and-Differential Harmonic Oscillations of an Unsymmetrical Shaft and an Unsymmetrical Rotor[60]

5. 1. Introduction

Nonlinear forced oscillations in a nonlinear multidegree-of-freedom vibratory system contain subharmoni coscillations, summed-and-differential harmonic oscillations, and super-summed-and-differential harmonic oscillations. When a periodic external force with frequency ω acts on a nonlinear reciprocating vibratory system with multiple degrees of freedom (whose natural frequencies are p_1, ..., and p_n), if the relation

$$N\omega \fallingdotseq \sum_{i=1}^{k} m_i p_i \quad (N=2,\ 3,\ \cdots,\ m_i=\pm 1,\ \pm 2,\ \cdots,\ 2 \leqq k \leqq n)$$

is satisfied, k harmonic components with frequencies ω_i satisfying

$$\omega_i \fallingdotseq p_i \quad (i=1,\ \cdots,\ k), \quad N\omega = \sum_{i=1}^{k} m_i \omega_i$$

can occur simultaneously. This kind of oscillation is called the super-summed-and-differential harmonic oscillation. Super-summed-and-differential harmonic oscillations in a rectilinear vibratory system have been discussed previously.[43, 44] But such oscillations in a rotating shaft system, which have different vibratory characteristics from those in a rectilinear vibratory system, have rarely been studied.

This chapter deals with super-summed-and-differential harmonic oscillations, in (A) nonlinear system where a disc is mounted on an unsymmetrical shaft (i. e., an unsymmetrical shaft system), and in (B) a nonlinear system carrying an unsymmetrical rotor on a rotating shaft with a circular cross section (i. e., an unsymmetrical rotor system). In this chapter we present theoretical and experimental analyses of these systems. Also, we compare this oscillation with one which occurs in a nonlinear system having a disc on a round shaft (i. e., a symmetrical system). As a result, we can conclude that the unsymmetry of a shaft or a rotor makes it easier for super-summed-and-differential harmonic oscillations to occur, and that the unsymmetry contributes to an unstable vibration which does not appear in a symmetrical system.

5. 2. Theoretical analyses of the super-summed-and-differential harmonic oscillation of the type $[(p_f-p_b)/2]$

Experiments were performed in a four-degree-of-freedom system where the deflection r and the inclination θ of the rotor coupled. In this chapter, for simplicity, we shall show only the theoretical analysis for the inclination oscillation in a two-degree-of-freedom system where r and θ do not couple. The same method as that in Chapters 2 and 3 can lead to the conclusion that the results of theoretical analyses for a four-degree-of-freedom system such as an experimental apparatus are qualitatively the same as those of this two-degree-of-freedom system.

The equations of motion for the inclination oscillation are given by Eq. (1. 7) in the unsymmetrical shaft system, and by Eq. (1. 4) in the unsymmetrical rotor

system. The equations of motion in the symmetrical system are obtained if we put $\Delta_s=0$ in Eq. (1. 7) or $\Delta_i=0$ in Eq. (1. 4). The vibratory characteristics of the systems represented by Eqs. (1. 4) and (1. 7) are similar. So in this chapter, we mainly analyze Eq. (1. 7) for the unsymmetrical shaft system. In those equations, we suppose the quantities θ_x, θ_y, Δ_s, Δ_i and τ to be $O(\varepsilon^0)$, and c, $N_{\theta x}$ and $N_{\theta y}$ to be $O(\varepsilon)$.

Figure 5. 1 shows a p-ω diagram for an unsymmetrical shaft system of two degrees of freedom when $i_p=0.7$ and $\Delta_s=0.2$. In the vicinity of the angular velocity of the shaft where the relation $p_f-p_b=2\omega$ is satisfied, two oscillations with frequencies ω_f ($\fallingdotseq p_f>0$) and ω_b ($\fallingdotseq p_b<0$) may appear simultaneously. This kind of nonlinear forced oscillation will be called the super-summed-and-differential harmonic oscillation, and it is represented by the symbol $[(p_f-p_b)/2]$ In this oscillation, the following relation holds:

$$\omega_f-\omega_b=2\omega \tag{5.1}$$

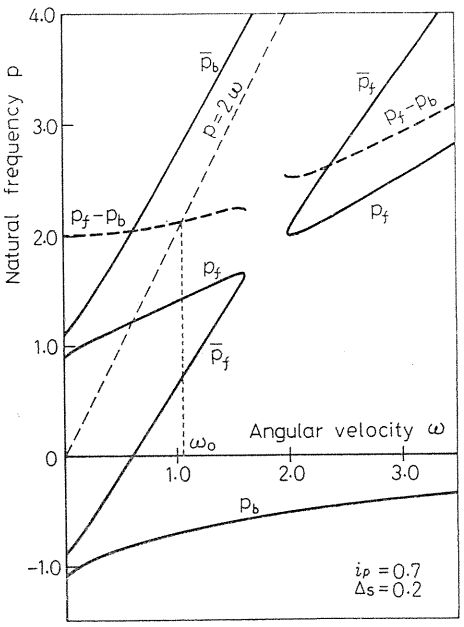

Fig. 5. 1. The p-ω diagram in the unsymmetrical shaft system (having two degrees of freedom).

Since the stiffness of the shaft is non-uniform, and since Δ_s is the quantity of $O(\varepsilon^0)$, in addition to the appearance of two oscillations of frequencies ω_f and ω_b, there appear the oscillations of frequencies $\bar{\omega}_f=2\omega-\omega_f$ and $\bar{\omega}_b=2\omega-\omega_b$ with the same order of magnitude of amplitude as the former oscillations. For example, substituting $\theta_x=A\cos\Omega t$ and $\theta_y=A\sin\Omega t$ into the terms of Δ_s in Eq. (1. 7) produces the terms $\Delta_s A\cos(2\omega-\Omega)t$ and $\Delta_s A\sin(2\omega-\Omega)t$. From Eq. (5. 1), the relations $\omega_b=-\bar{\omega}_f$ and $\omega_f=2\omega+\omega_b$ hold. The magnitudes of the nonlinear terms in the first and the second equations in Eq. (1. 7) are different. Because of this, we must assume that an approximate solution, with the accuracy of $O(\varepsilon)$, exists in the following form:

$$\begin{aligned}\begin{matrix}\theta_x\\ \theta_y\end{matrix}=&R_f\begin{matrix}\cos\\ \sin\end{matrix}(\omega_f t+\delta_f)+\begin{matrix}A\cos\\ A'\sin\end{matrix}(\omega_b t)+\begin{matrix}B\sin\\ B'\cos\end{matrix}(\omega_b t)+\bar{R}_b\begin{matrix}\cos\\ \sin\end{matrix}(\bar{\omega}_b-\delta_b)\\ &+P\begin{matrix}\cos\\ \sin\end{matrix}(\omega t+\beta)+\varepsilon\Bigg[\begin{matrix}a_f\cos\\ a'_f\sin\end{matrix}(\omega_f t+\delta)+\begin{matrix}b_f\sin\\ b'_f\cos\end{matrix}(\omega_f t+\delta_f)+\begin{matrix}\bar{a}_b\cos\\ \bar{a}'_b\sin\end{matrix}(\bar{\omega}_b t-\delta_b)\\ &+\begin{matrix}\bar{b}_b\sin\\ \bar{b}'_b\cos\end{matrix}(\bar{\omega}_b t-\delta_b)+\begin{matrix}d_f\cos\\ d'_f\sin\end{matrix}\{(2\omega+\omega_f)t+\delta_f\}+\begin{matrix}e_f\sin\\ e'_f\cos\end{matrix}\{(2\omega+\omega_f)t+\delta_f\}\\ &+\begin{matrix}f_b\cos\\ f'_b\sin\end{matrix}\{(2\omega+\bar{\omega}_b)t-\delta_b\}+\begin{matrix}h_b\sin\\ h'_b\cos\end{matrix}\{(2\omega+\bar{\omega}_b)t-\delta_b\}+\cdots\Bigg]\end{aligned} \tag{5.2}$$

where, as for the terms with the magnitudes of $O(\varepsilon)$, only vibratory components

required in the later calculation are written. We represented the amplitudes of terms $\bar{\omega}_f t-\delta_f$ and $\omega_b t+\delta_b$ as $\bar{R}_f$ and R_b, respectively in Chapter 3. The relations $A=R_b\cos\delta_b+\bar{R}_f\cos\delta_f$, $A'=R_b\cos\delta_b-\bar{R}_f\cos\delta_f$, $B=-R_b\sin\delta_b-\bar{R}_f\sin\delta_f$, and $B'=R_b\sin\delta_b-\bar{R}_f\sin\delta_f$ hold with the accuracy of $O(\varepsilon^0)$. Substituting Eq. (5. 2) into Eq. (1. 7) and setting the sine and the cosine terms of frequency ω to be zero with the accuracy of $O(\varepsilon^0)$, we get a solution of the harmonic oscillation which is given by Eq. (3. 4). We assume here that the amplitudes and the phase angles in Eq. (5. 2) (e. g., R_f, a_f, δ_f) are slowly varying functions of the time, and that the first and the second time derivatives of these quantities have the magnitudes of $O(\varepsilon)$ and $O(\varepsilon^2)$, respectively. Next, setting the sine and the cosine terms of frequencies ω_f and ω_b to be zero with the accuracy of $O(\varepsilon)$, respectivery, we obtain the following simultaneus equations:

$$\left.\begin{aligned}
A_fR_f\dot{\delta}_f=&-\sigma_fR_f-4\beta^{(0)}\bar{G}_f(g_1R_f^2+2g_2R_b^2+2k_1P^2)R_f\\
&-\bar{G}_fR_b[3\beta^{(2)}\{\Delta_s(3n_1R_f^2+n_2R_b^2+n_3P^2)\cos\psi\\
&+n_4P^2\cos(\psi-2\beta)\}+12n_5R_fR_b(\beta_c^{(4)}\cos2\psi-\beta_s^{(4)}\sin2\psi)]\\
A_f\dot{R}_f=&c_fR_f-\bar{G}_fR_b[3\beta^{(2)}\{\Delta_s(n_1R_f^2+n_2R_b^2+n_3P^2)\sin\psi\\
&+n_4P^2\sin(\psi-2\beta)\}+12n_5R_fR_b(\beta_c^{(4)}\sin2\psi+\beta_s^{(4)}\cos2\psi)]\\
A_bR_b\dot{\delta}_b=&-\sigma_bR_b-4\beta^{(0)}\bar{G}_b(2g_2R_f^2+g_3R_b^2+2k_2P^2)R_b\\
&-\bar{G}_bR_f[3\beta^{(2)}\{\Delta_s(n_1R_f^2+3n_2R_b^2+n_3P^2)\cos\psi\\
&+n_4P^2\cos(\psi-2\beta)\}+12n_5R_fR_b(\beta_c^{(4)}\cos2\psi-\beta_s^{(4)}\sin2\psi)]\\
A_b\dot{R}_b=&c_bR_b+\bar{G}_bR_f[3\beta^{(2)}\{\Delta_s(n_1R_f^2+n_2R_b^2+n_3P^2)\sin\psi\\
&+n_4P^2\sin(\psi-2\beta)\}+12n_5R_fR_b(\beta_c^{(4)}\sin2\psi+\beta_s^{(4)}\cos2\psi)]
\end{aligned}\right\}\quad(5.3)$$

where the notations are given as follows:

$$\left.\begin{aligned}
&A_f=(i_p\omega-2\omega_f)\bar{G}_f-(i_p\omega+2\omega_b)G_f,\quad A_b=(i_p\omega-2\omega_b)\bar{G}_b-(i_p\omega-2\bar{\omega}_b)G_b,\\
&c_f=c(\omega_f\bar{G}_f-\bar{\omega}_fG_f),\qquad c_b=c(\omega_b\bar{G}_b-\bar{\omega}_bG_b),\qquad G(p)=1+i_p\omega p-p^2,\\
&G_f=G(\omega_f),\qquad \bar{G}_f=G(\bar{\omega}_f),\qquad G_b=G(\omega_b),\qquad \bar{G}_b=G(\bar{\omega}_b),\\
&g_1=(G_f^2+\bar{G}_f^2+4\Delta_s^2)/\bar{G}_f^2,\qquad g_2=\{(G_f+\bar{G}_f)(G_b+\bar{G}_b)+2\Delta_s^2\}/(\bar{G}_f\bar{G}_b),\\
&g_3=(G_b^2+\bar{G}_b^2+4\Delta_s^2)/\bar{G}_b^2,\qquad k_1=(G_f+\bar{G}_f+\Delta_s\cos2\beta)/\bar{G}_f,\\
&k_2=(G_b+\bar{G}_b+\Delta_s\cos2\beta)/\bar{G}_b,\qquad n_1=(G_f+G_b+2\bar{G}_f)/\bar{G}_f^2,\\
&n_2=(\bar{G}_f+\bar{G}_b+2G_b)/(\bar{G}_f\bar{G}_b),\qquad n_3=2/\bar{G}_f,\qquad n_4=1+G_b/\bar{G}_f,\\
&n_5=G_f/\bar{G}_f,\qquad \sigma_f=G_f\bar{G}_f-\Delta_s^2,\qquad \sigma_b=G_b\bar{G}_b-\Delta_s^2,\qquad \psi=\delta_f-\delta_b
\end{aligned}\right\}$$

(5. 4)

Finally, the stationary solutions of R_f, R_b, ψ, ω_f and ω_b are decided from Eq. (5. 1) and the equations setting the right sides of Eq. (5. 3) as zero. In the same manner as in Chapter 3, we can simultaneously evaluate the stability of these stationary solutions. We put the stationary solutions $R_f=R_{f0}$ and $R_b=R_{b0}$. Setting the right sides of the second and the fourth equations in Eq. (5. 3) as zero, we get the following equations:

$$R_{b0}^2=\kappa R_{f0}^2, \quad \kappa=-c_f\overline{G}_b/(c_b\overline{G}_f)=\text{const.}\ (>0) \tag{5.5}$$

Since at the resonance point we have $\omega_f>0$, $\omega_b<0$, $\overline{\omega}_f>0$, $\overline{\omega}_b>0$, $G_f>0$, $G_b<0$, $\overline{G}_f>0$, $\overline{G}_b<0$ and $\omega_f>|\omega_b|$, we know that the value of κ in Eq. (5. 5) is positive. Therefore the amplitude R_{b0} is relative to R_{f0}. Typical examples of the resonance curves obtained by numerical computation are shown in Figs. 5. 2~5. 5. These curves are computed on the conditions that: first, the coefficients of the nonlinear terms $\beta_c^{(4)}$ and $\beta_s^{(4)}$ equal zero, since they are negligibly small in the practical rotating shaft system[38]; and secondly, that we put $\beta_s^{(2)}=0$ and $\beta_c^{(2)}=\beta^{(2)}$ by rotating the coordinate axes by some angle. In these diagrams, the ordinate represents the stationary amplitude $R_{f0}+R_{b0}$, and the abscissa does the angular velocity of the shaft ω. The stable and the unstable solutions are drawn in full and broken lines, respectively. It is seen from Eq. (5. 3) that the stationary solutions $R_{f0}=0$ and $R_{b0}=0$, that is, $R_{f0}+R_{b0}=0$ exists. In order to avoid confusion, however, these solutions of zero amplitudes are not shown in Figs. 5. 2~5. 5. As for the solution $R_{f0}+R_{b0}=0$, when the solution $R_{f0}+R_{b0}\neq 0$ intersects the ω-axis, an unstable region appears between the intersecting points. For example, in the case of $\Delta_s=0.2$ in Fig. 5. 2(a), the interval A~B is unstable. The intersecting points A and

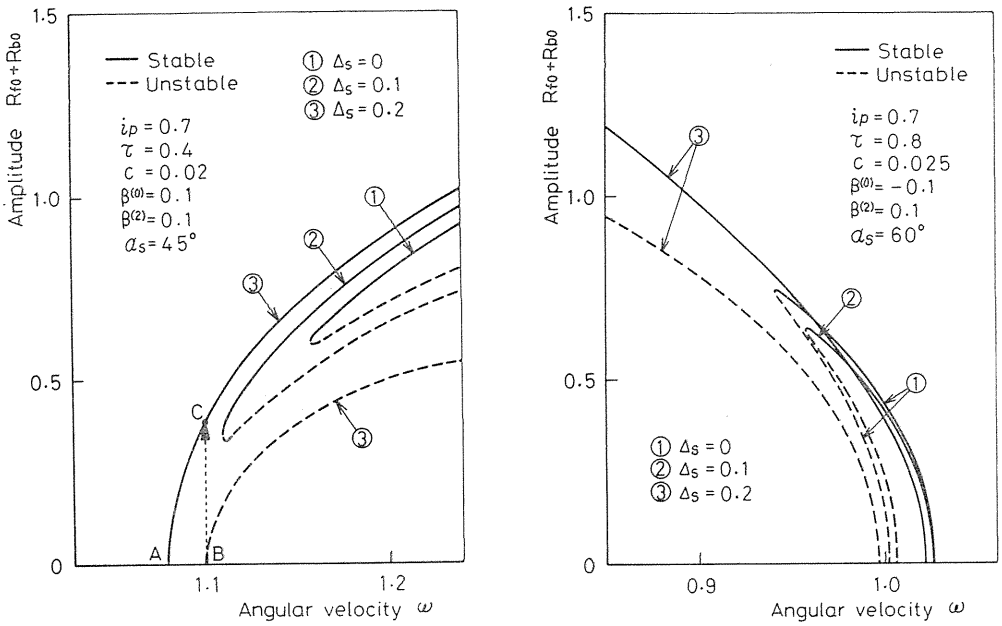

(a) In the case of a hard spring type.

(b) In the case of a soft spring type.

Fig. 5. 2. Theoretical resonance curves showing the influence of the unsymmetry Δ_s.

B are the boundaries between the stable and the unstable regions. The solution $R_{f0}+R_{b0}=0$ is stable outside the interval A~B. When the solution $R_{f0}+R_{b0}\neq 0$ does not intersect the ω-axis (e. g., in the case of $\Delta_s=0.1$ in Fig. 5. 2(a)), the solution $R_{f0}+R_{b0}=0$ is stable at any value of ω.

Figures 5. 2(a) and 5. 2(b) show resonance curves for various values of Δ_s. The former is in the case of a hard spring type ($\beta^{(0)}>0$), and the latter of a soft spring type ($\beta^{(0)}<0$). In the case where Δ_s equals 0 and 0.1, as in Fig. 5. 2(a), the resonance curves do not intersect the abscissa and they are away from the axis. Such cases mean that super-summed-and-differential harmonic oscillations will not occur unless disturbance forces act on the rotating shaft system. In the case of $\Delta_s=0.2$, however, the resonance curve intersects the ω-axis. As shown in Fig. 5. 2(a), when the value of ω reaches the point A from the lower side of ω, the oscillation of $R_{f0}+R_{b0}\neq 0$ begins to appear. This is because the solution $R_{f0}+R_{b0}=0$ is unstable in the interval A~B. On the other hand, when the value of ω reaches the point B from the higher range of ω, a jump phenomenon in amplitude occurs and an oscillation shown by the point C appears. Therefore we find that in the symmetrical system where $\Delta_s=0$, or in the case where Δ_s is small, this kind of oscillation appears less readily than that in the case where Δ_s is large.

Figure 5. 3 shows the effect of the dynamic unbalance τ. The larger the value of τ becomes, the more readily the oscillation appears.

The influence of the coefficient $\beta^{(0)}$ of the nonlinear component $N(0)$ is shown in Fig. 5. 4. The type of the resonance curve (that is, whether it is hard or soft) depends on the sign of $\beta^{(0)}$. When $\beta^{(0)}=0$, the solution $R_{f0}+R_{b0}=0$ is unstable between the intersecting points A and A′ of the resonance curve (i. e., $R_{f0}+R_{b0}\neq$

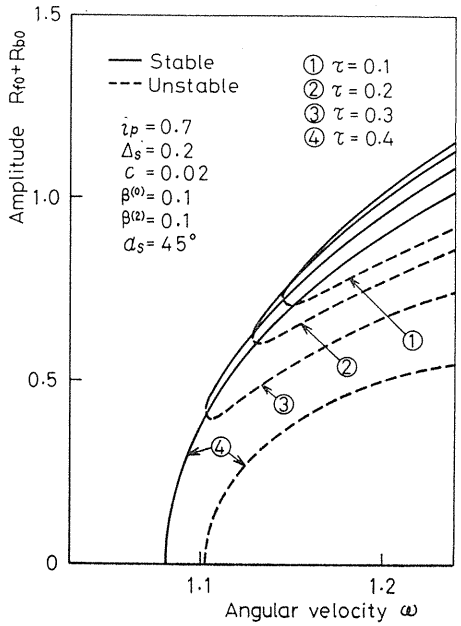

Fig. 5. 3. Theoretical resonance curves showing the influence of the dynamic unbalance τ.

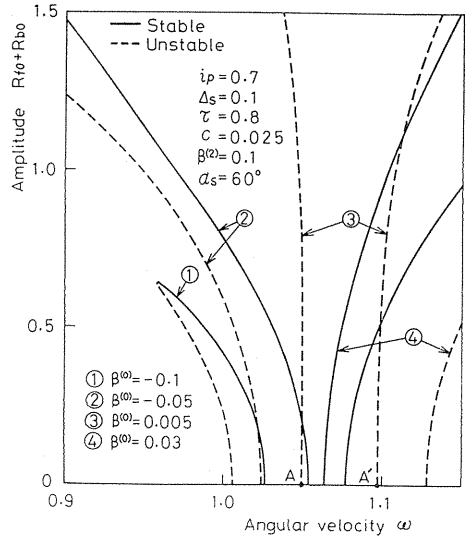

Fig. 5. 4. Theoretical resonance curves showing the influence of the nonlinear component $N(0)$ ($\beta^{(0)}$).

0) and the ω-axis, and furthermore no other stable solution exists in this region. Consequently, an unstable vibration appears in the region AA', after which the amplitude increases with time. It is common for such an unstable region to appear for small values of $\beta^{(0)}$

Figure 5. 5 shows the effects of the coefficient $\beta^{(2)}$ of the nonlinear component $N(2)$. For large values of $\beta^{(2)}$, the oscillation appears readily.

In the unsymmetrical rotor system, the resonance curves for the supper-summed-and-differential harmonic oscillation of the type $[(p_f-p_b)/2]$ can be obtained by the same method of analysis as that in the unsymmetrical shaft system. As an example, Fig. 5. 6 shows the influence of the unsymmetry of the rotor Δ_i. When Δ_i is large, the resonance curve intersects the ω-axis, and the oscillation appears more readily than that in the symmetrical system for $\Delta_i=0$. The effects of the other parameters are qualitatively the same as those in the unsymmetrical shaft system shown in Figs. 5. 2~5. 5.

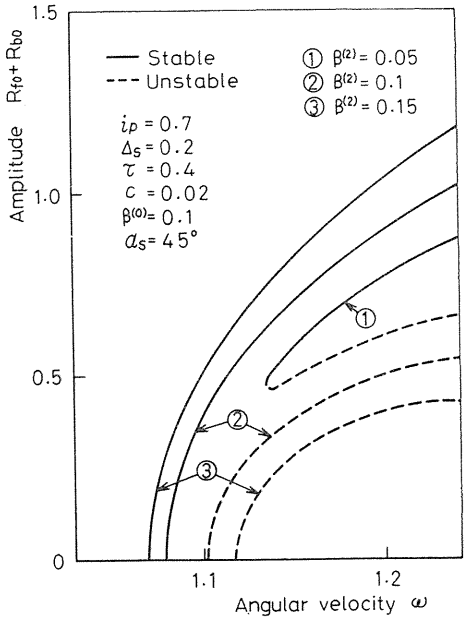

Fig. 5. 5. Theoretical resonance curves showing the influence of the nonlinear component $N(2)$ ($\beta^{(2)}$).

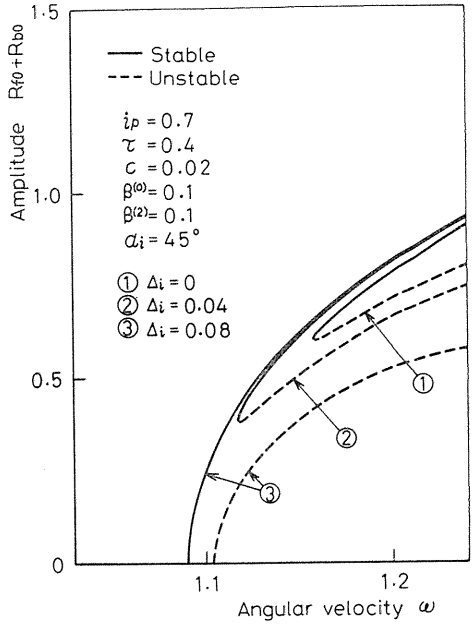

Fig. 5. 6. Theoretical resonance curves showing the influence of the unsymmetry of the rotor Δ_i.

5. 3. Experimental results

In experiments, we used rotors and shafts shown in Tables 1. 1 and 1. 2. In the unsymmetrical shaft system, the disc R_3 and the unsymmetrical shaft S_4 were used. In the unsymmetrical rotor system, the unsymmetrical rotor R_2 and the round shaft S_2 were used.

The nonlinear spring characteristics changed depending on the degree of the

discrepancy between the center lines of the upper and the lower bearings. Accordingly, the resonance curves of various types were obtained. The experimental apparatus is a four-degree-of-freedom system with the natural frequencies p_i and $\bar{p}_i$ ($\bar{p}_i=2\omega-p_i$, $i=1\sim4$, $p_4<p_3<0<p_2<p_1$). We obtained the p-ω diagram for the unsymmetrical shaft system which is the same type as Fig. 3. 5 in Chapter 3. At two resonance points given by abscissas of the points where the curves p_2-p_3 and p_2-p_4 intersect the straight line $p=2\omega$ in the $p-\omega$ diagram, super-summed-and-differential harmonic oscillations of the type $[(p_f-p_b)/2]$ as treated in Section 5. 2 occurred.

Figures 5. 7 and 5. 8 were obtained from the unsymmetrical shaft system.

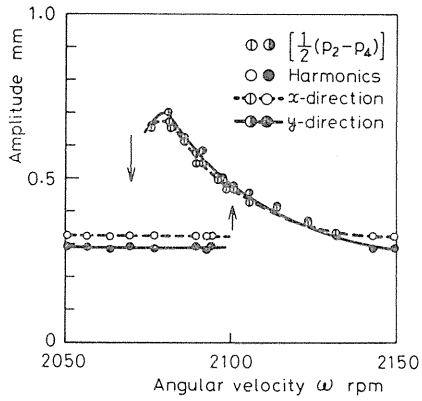

Fig. 5. 7. Experimental resonance curve of the super-summed-and-differential harmonic oscillation of the type $[(p_2-p_4)/2]$ (in the unsymmetrical shaft system).

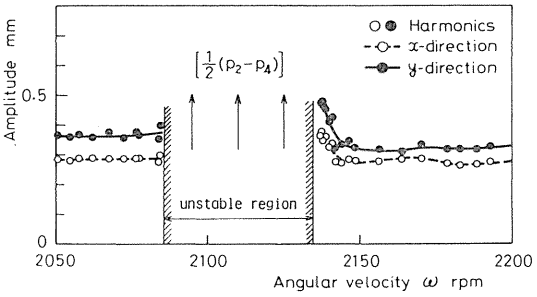

Fig. 5. 8. The unstable region of the oscillation $[(p_2-p_4)/2]$ (in the unsymmetrical shaft system).

Figure 5. 7 shows the resonance curve for the oscillation of the type $[(p_2-p_4)/2]$. This occurred in the vicinity of the rotating speed where the relation $p_2-p_4=2\omega$ held. The arrows in this figure represent the jump phenomena. Marks ○ and ● indicate the amplitudes of the harmonic oscillation with the same frequency as the rotating shaft speed, and marks ◐ and ◑ those of the super-summed-and-differential harmonic oscillation. The curve is of the soft spring type, which corresponds to the case of the negative $\beta^{(0)}$ in Fig. 5. 4. In Fig. 5. 8, an unstable vibration of this type appeared in the region $\omega=2086\sim2134.5$ rpm, as in-

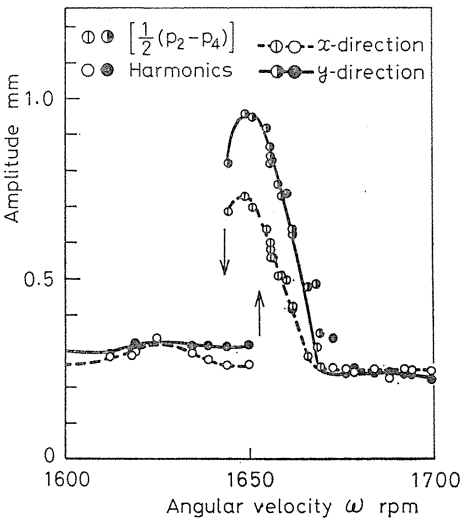

Fig. 5. 9. Experimental resonance curve of the super-summed-and-differential harmonic oscillation of the type $[(p_2-p_4)/2]$ (in the unsymmetrical rotor system).

dicated by the arrows. This figure corresponds to the resonance curve for $\beta^{(0)}=0.005$ in Fig. 5. 4.

In the oscillation of the type $[(p_2-p_3)/2]$, we obtained the same resonance curve in shape as that of Fig. 5. 7.

Figure 5. 9 shows an experimental resonance curve of the soft spring type of the oscillation $[(p_2-p_4)/2]$ obtained in the unsymmetrical rotor system. This curve is qualitatively the same as that in the unsymmetrical shaft system.

Throughout many experiments, no super-summed-and-differential harmonic oscillations were observed in the symmetrical system.

5. 4. Conclusions

(1) In the nonlinear rotating shaft systems (e. g., the unsymmetrical shaft system, the unsymmetrical rotor system, and the symmetrical system), it was verified theoretically and experimentally that super-summed-and-differential harmonic oscillations of the type $[(p_f-p_b)/2]$ may occur.

(2) The larger the unsymmetry of the shaft or the rotor, the more readily the oscillation will appear. In the symmetrical system, no super-summed-and-differential harmonic oscillations were observed throughout many experiments.

(3) If we consider nonlinear terms up to the third power of coordinates, the symmetrical nonlinear components $N(0)$, $N(2)$ and $N(4)$ have influence on this oscillation.

(4) The qualitative characteristics of this kind of oscillation are the same in both the unsymmetrical shaft system and the unsymmetrical rotor system.

(5) In the experiments on the unsymmetrical shaft system and the unsymmetrical rotor system, oscillations of the type $[(p_2-p_3)/2]$ and $[(p_2-p_4)/2]$ appeared.

(6) When the nonlinear component $N(0)$ (i. e., the absolute value of $\beta^{(0)}$) is small, the unsymmetry of the shaft or the rotor causes an unstable vibration of this type which does not appear in the symmetrical system.

6. Sub-Combination Tones of a Rotating Shaft due to Ball Bearings[61]

6. 1. Introduction

In the past, we have presented papers on various kinds of nonlinear forced oscillations.[32~38, 65] Most of them have dealt with the whirling motion of a rotating shaft, which had nonlinear spring characteristics due to the angular clearance of a single-row deep groove ball bearing. It has also been reported that combination tones and sub-combination tones appear when several periodic external forces act on a rectilinear nonlinear system.[45~50, 66] Besides these nonlinear forced oscillations, we reported that the difference in diameters of balls in a bearing caused the shaft whirling motion with the same frequency as the precessional speed of the balls (the angular velocity of the balls rotating around the center of the inner ring).[29]

This chapter deals with the sub-combination tones of a rotating shaft resulting from the difference in diameters of balls in a ball bearing. This oscillation can appear when the shaft has a proper nonlinear spring characteristic depending on

the assembly of the rotating shaft system. The whirling motion has a frequency of 3/2 times the precessional speed of the steel ball. We will describe the theoretical and experimental results relevant to the cause of appearance, the mechanism, and the vibratory characteristics of this type of oscillation.

6. 2. On the mechanism of occurrence of periodic external forces

Let the angular velocity of a rotating shaft be ω, and the angular velocity of the precessional motion of balls in a ball bearing be ω_1. Steel balls rotate around the center of the bearing in the same direction as the shaft rotation at the following angular velocity[29, 67]:

$$\omega_1=\frac{R}{2(R+r)}\omega=\alpha_1\omega \quad (\alpha_1: \text{constant}) \tag{6. 1}$$

This equation is derived from the assumption that the steel balls move in rolling contact with inner and outer rings, independent of the conditions of load, rotating speed and lubrication. In Eq (6. 1), R is the outer radius of inner ring and r is the radius of a steel ball. If a radial clearance exists even in the radius where the largest ball is located, the external forces of the frequencies ω_1 in Eq. (6. 1) and $2\omega_1$ occur by the following mechanism:

For the sake of simplicity, we treat the case in which there is a large steel ball of the radius $r+\varepsilon(\varepsilon\ll r)$. The construction of the bearing is schematically shown in Fig. 6. 1. The origin O of the xy coordinate system is taken in the center of the outer ring (bore diameter $2R_1$), and we denote the radial clearance of the bearing by $\mu(=R_1-2r-R)$. If $\mu>\varepsilon$, a clearance exists for the large ball. It usually happens in a vertical shaft system that a small discrepancy between the center lines of the upper and the lower bearings exists or the shaft is not strictly vertical. Therefore, the inner ring is not free in the bearing clearance but is slightly pressed in a certain direction in the non-rotating state, e. g., in the negative direction of the x-axis by the force F as shown in Fig. 6. 1. In Fig. 6. 1, let θ denote the angular position of the large ball, and θ_0 the angular position when the large ball starts to touch the inner ring (i. e., the direction of the radius OA). From the calculation,

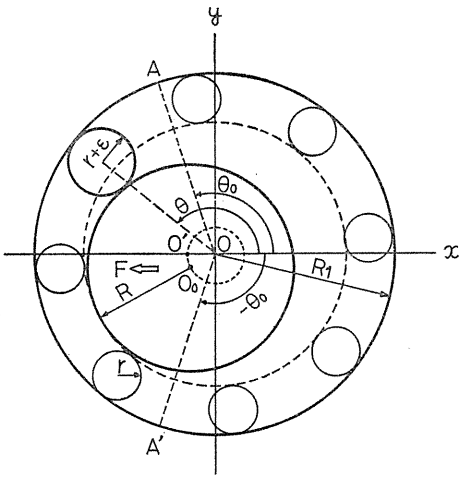

Fig. 6. 1. Construction of a single-row deep groove ball bearing.

$$\theta_0=\cos^{-1}(2\varepsilon/\mu-1) \tag{6. 2}$$

$$\left.\begin{aligned}&\pi/2>\theta_0>0 \text{ for } \mu>\varepsilon>\mu/2\\&\pi>\theta_0>\pi/2 \text{ for } \mu/2>\varepsilon>0\end{aligned}\right\} \tag{6. 3}$$

are obtained. The center of the inner ring is denoted by the point $O_0(x_0, y_0)$. When the large ball is located between the radial $OA'(-\theta_0<\theta<\theta_0)$, the inner ring is pressed in the negative direction of x-axis, and its center remains at the point $O'(-\mu, 0)$. If $\theta_0<\theta<2\pi-\theta_0$, the center of the inner ring moves away from the point O′ owing to the passage of the large ball. Neglecting the elastic deformation of the steel balls, we find that the center of the inner ring $O_0(x_0, y_0)$ fluctuates along full lines shown in Fig. 6. 2 while the large ball makes one revolution around the point O. During one rotation of the large ball, the center of the inner ring begins to move away from the position O′ $(-\mu, 0)$ when the large ball reaches the point A (i. e., $\theta=\theta_0$), and moves along full lines as shown in Fig. 6. 2, returning to the position O′ at the position A′ (i. e., $\theta=2\pi-\theta_0$). Because the angular position θ is expressed as $\theta=\omega_1 t+C_1$ (t: time, C_1: constant), the center of the inner ring moves periodically with the period $2\pi/\omega_1$. Hence, the coordinates x_0 and y_0 can be expanded into a Fourier series in the following form of the complex number:

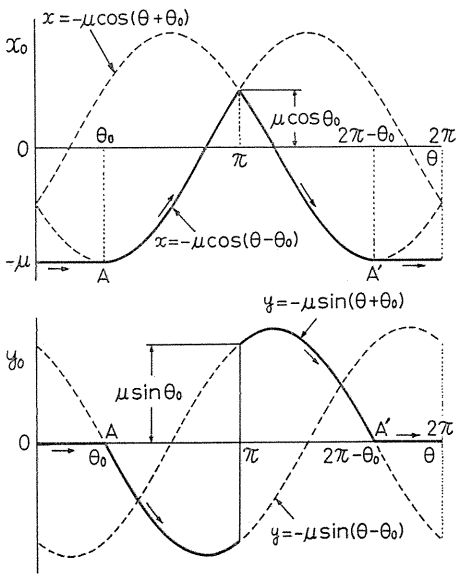

Fig. 6. 2. Displacement of a lower shaft end, i. e., the center of an inner ring (for $\theta_0=60°$ and $\varepsilon/\mu=0.75$).

$$x_0+iy_0=A_0e^{i\varphi_0}+A_1e^{i(+\omega_1t+\varphi_1)}+A_1'e^{i(-\omega_1t+\varphi_1')}$$
$$+A_2e^{i(+2\omega_1t+\varphi_2)}+A_2'e^{i(-2\omega_1t+\varphi_2')}+\cdots \qquad (6.4)$$

where A_0, A_1, ... are the amplitudes of various waves, and φ_0, φ_1, ... are their phase angles. The magnitudes of A_1, A_1', A_2, and A_2' for various values of ε and μ are presented in Table 6. 1. As shown in Table 6. 1, the amplitudes of ω_1 and $2\omega_1$ have the same order of magnitude. Owing to the periodic displacement of

Table 6. 1. Coefficients of Fourier series.

	$A_1(\omega_1)$	$A_1'(-\omega_1)$	$A_2(2\omega_1)$	$A_2'(-2\omega_1)$
$\varepsilon=\mu$	μ	0	0	0
$\varepsilon=(3/4)\mu$	0.61μ	0	0.41μ	0.14μ
$\varepsilon=(1/2)\mu$	0.32μ	0	0.32μ	0.11μ
$\varepsilon=(1/4)\mu$	0.11μ	0	0.14μ	0.05μ
$\varepsilon=0$	0	0	0	0

μ: radial clearance, $r+\varepsilon$: radius of a large ball ($\mu>\varepsilon$).

the center of the inner ring (namely, the shaft end) represented by Eq. (6. 4), the rotor undergoes the deflection e_1 (with components e_{1x}, e_{1y}) and the inclination τ_1 (with components τ_{1x}, τ_{1y}) as follows:

$$\left.\begin{aligned} e_{1x}&=a_0\cos\varphi_0+a_1\cos(\omega_1 t+\varphi_1)+a_2\cos(2\omega_1 t+\varphi_2)+\cdots\\ e_{1y}&=a_0\sin\varphi_0+a_1\sin(\omega_1 t+\varphi_1)+a_2\sin(2\omega_1 t+\varphi_2)+\cdots\\ \tau_{1x}&=b_0\cos\varphi_0+b_1\cos(\omega_1 t+\varphi_1)+b_2\cos(2\omega_1 t+\varphi_2)+\cdots\\ \tau_{1y}&=b_0\sin\varphi_0+b_1\sin(\omega_1 t+\varphi_1)+b_2\sin(2\omega_1 t+\varphi_2)+\cdots \end{aligned}\right\} \quad (6.5)$$

Accordingly, if follows that periodic external forces act on the rotating shaft system.[29]

6. 3. Equations of motion and occurrence of sub-combination tones

In this chapter, we consider the inclination oscillation in a system where the deflection and the inclination of the rotor do not couple. This two-degree-of-freedom system is the simplest case of the whirling motion. The experimental apparatus is a four-degree-of-freedom system in which the deflection and the inclination of the rotor couple with each other. Although we measure the amplitudes of the deflection oscillation in experiments, we can prove that the vibratory behavior of the inclination oscillation in this two-degree-of-freedom system is qualitatively the same as that of the deflection oscillation in the four-degree-of-freedom system.

The external forces due to the rotor unbalance are independent of sub-combination tones treated here. So we derive the equations of motion on the assumption that the rotor has no unbalance. Then the differential equations of motion:

$$\left.\begin{aligned} I\ddot{\theta}_x+I_p\omega\dot{\theta}_y+c\dot{\theta}_x+\delta(\theta_x-\tau_{1x})+N_{\theta x}&=0\\ I\ddot{\theta}_y-I_p\omega\dot{\theta}_x+c\dot{\theta}_y+\delta(\theta_y-\tau_{1y})+N_{\theta y}&=0 \end{aligned}\right\} \quad (6.6)$$

are obtained. In order to eliminate the constant terms which yield from the substitution of the terms $b_0\cos\varphi_0$ and $b_0\sin\varphi_0$ in Eq. (6. 5) into Eq. (6. 6), we move the coordinates θ_x and θ_y in parallel with themselves. Also, we can make $\varphi_1=0$ by sifting the origin of time. Let the mass of the rotor be m, and the spring constant for the deflection of the shaft be α. We introduce the quantity $e_0=mg/\alpha$ and use the following dimensionless quantities besides those in Eq. (1. 1):

$$\left.\begin{aligned} &\omega'_1=\omega_1/\sqrt{\alpha/m}, \qquad c'=c/(I\sqrt{\alpha/m}),\\ &\theta_{01}=b_1/(e_0\sqrt{m/I}), \qquad \theta_{02}=b_2/(e_0\sqrt{m/I}), \qquad \beta=\varphi_2-\varphi_1 \end{aligned}\right\} \quad (6.7)$$

Adopting these quantities, we obtain the dimensionless equations:

$$\left.\begin{aligned} \ddot{\theta}_x+i_p\omega\dot{\theta}_y+c\dot{\theta}_x+\delta\theta_x+N_{\theta x}&=\delta\theta_{01}\cos\omega_1 t+\delta\theta_{02}\cos(2\omega_1 t+\beta)\\ \ddot{\theta}_y-i_p\omega\dot{\theta}_x+c\dot{\theta}_y+\delta\theta_y+N_{\theta y}&=\delta\theta_{01}\sin\omega_1 t+\delta\theta_{02}\sin(2\omega_1 t+\beta) \end{aligned}\right\} \quad (6.8)$$

Here we omit the primes from the symbols. We neglect the component of $-2\omega_1$

in Eq. (6. 8) because it is small, as shown in Table 6. 1. The nonlinear terms $N_{\theta x}$ and $N_{\theta y}$ are given by Eq. (1. 9).

We may suppose the approximate solutions of Eq. (6. 8) are as follows:

$$\left.\begin{aligned}\theta_x &= R_f\cos(\omega_f t+\delta_f)+Q_1\cos\omega_1 t+Q_2\cos(2\omega_1 t+\beta)\\ &\quad+\varepsilon\{a_f\cos(\omega_f t+\delta_f)+b_f\sin(\omega_f t+\delta_f)\}\\ \theta_y &= R_f\sin(\omega_f t+\delta_f)+Q_1\sin\omega_1 t+Q_2\sin(2\omega_1 t+\beta)\\ &\quad+\varepsilon\{a'_f\sin(\omega_f t+\delta_f)+b'_f\cos(\omega_f t+\delta_f)\}\end{aligned}\right\} \tag{6.9}$$

where the following notation is used for simplicity:

$$\omega_f=(3/2)\omega_1=(3/2)\alpha_1\omega \tag{6.10}$$

In Eq. (6. 9), the parameter ε is small. Hereafter, it is assumed that the amplitude R_f and the phase angle δ_f of the sub-combination tone of frequency $(3/2)\omega_1$, and the amplitudes Q_1 and Q_2 of the harmonic oscillations due to the external forces of frequencies ω_1 and $2\omega_1$ are quantities of $O(\varepsilon^0)$. Substituting Eq. (6. 9) into Eq. (6. 8), setting the coefficients of $\cos(\omega_f t+\delta_f)$ and $\sin(\omega_f t+\delta_f)$ to be zero, and neglecting the terms smaller than that of $O(\varepsilon)$, we obtain the following equations which decide the stationary solutions:

$$\left.\begin{aligned}&\sigma-4\beta^{(0)}\{R_f^2+2(Q_1^2+Q_2^2)\}=8\beta^{(0)}Q_1Q_2\cos(\beta-2\delta_f)\\ &c\omega_f=8\beta^{(0)}Q_1Q_2\sin(\beta-2\delta_f)\end{aligned}\right\} \tag{6.11}$$

where σ means the detuning given by the following expression:

$$\sigma=-G'(\omega_f)=\omega_f^2-i_p\omega\omega_f-\delta=O(\varepsilon) \tag{6.12}$$

The coefficient $\beta^{(0)}$ in Eq. (6. 11) is given by Eq. (1. 16). From Eq. (6. 11), it follows that only the isotropic nonlinear component $N(0)$ has influence on this oscillation. Since the accuracy of $O(\varepsilon^0)$ is sufficient for Q_1 and Q_2 in Eq. (6. 11), they are given by the following equations:[68]

$$Q_1=\delta\theta_{01}/G'(\omega_1),\quad Q_2=\delta\theta_{02}/G'(2\omega_1) \tag{6.13}$$

The term $8\beta^{(0)}Q_1Q_2$ in the right side of Eq. (6. 11) has the same effects as the external force on this nonlinear forced oscillation. We call it "the apparent external force".[45]

It has been shown[49] that when two periodic external forces of the different frequencies Ω_1 and Ω_2 simultaneously act on a vibratory system having the third power nonlinear terms of coordinates, the sub-combination tone of frequency:

$$\omega_i=\frac{1}{2}(\Omega_1+\Omega_2) \tag{6.14}$$

can occur. The oscillation of frequency $(3/2)\omega_1$ treated in this chapter corresponds to a particular case of Eq. (6. 14), in which $\Omega_1=\omega_1$ and $\Omega_2=2\omega_1$, that is, $\Omega_1:\Omega_2=1:2$. Therefore, the frequency ratio $K\ (=\Omega_2/\Omega_1)$ equals 2, and $\omega_i=$

$(3/2)\omega_1$. We may say that this oscillation has a type of ultra-subharmonic oscillation when it is defined from the viewpoint of the resonance frequency. Tomas[48] treated the same kind of sub-combination tone in a nonlinear rectilinear vibratory system having a single degree of freedom.

In order to obtain the solutions to Eq. (6. 8), we substitute Eq. (6. 9) into Eq. (6. 8) and adopt the harmonic balance method for the frequencies ω_f, Ω_1 and Ω_2. Generally, in analyses of combination tones for various values of $K=\Omega_2/\Omega_1$, one ought to solve the simultaneous equations for R_f, Q_1, Q_2 and their phase angles, instead of Eq. (6. 11). In the present special case, however, where $\Omega_1=\omega_2$, $\Omega_2=2\omega_1$ and $\omega_f=(3/2)\omega_1$, the critical speed of the oscillation $(3/2)\omega_1$ locates approximately halfway between the two resonant points $\omega_1=p_f$ and $2\omega_1=p_f$ of the harmonic oscillations. It is far away from the critical speeds of the harmonics Ω_1 and Ω_2. Accordingly, we may use the simple equation (6. 13) for Q_1 and Q_2, and we may decide R_f and δ_f by Eq. (6. 11).[68]

From Eq. (6. 11), the resonance curve is given by the expression:

$$\{\sigma-4\beta^{(0)}(R_f^2+2Q_1^2+2Q_2^2)\}^2+(c\omega_f)^2=(8\beta^{(0)}Q_1Q_2)^2 \tag{6.15}$$

Solving Eq. (6. 15) for $R_f{}^2$, we have:

$$R_f=-2(Q_1^2+Q_2^2)+\{\sigma\pm\sqrt{(8\beta^{(0)}Q_1Q_2)^2-(c\omega_f)^2}\}/(4\beta^{(0)}) \tag{6.16}$$

The experimental apparatus is a four-degree-of-freedom system where the deflection and the inclination of a rotor couple with each other. Analyzing the sub-combination tones for the equations of motion in a four-degree-of-freedom system by means of the same procedure as that in a two-degree-of-freedom system, we obtain the equations for the deflection oscillation in a four-degree-of-freedom system corresponding to Eq. (6. 11)[61]. From these two equations, it follows that they are the same in construction and have the same dynamical meanings of their coefficients, and that the vibratory characteristics of the deflection oscillation of the sub-combination tone in the four-degree-of-freedom system are qualitatively the same as those of the inclination oscillation in the two-degree-of-freedom system.

6. 4. Characteristics of the oscillation

Equations (6. 11), (6. 15), and (6. 16) have nearly the same constitution as that for the subharmonic oscillation $+(1/2)\omega$ of the forward precessional motion type, due to the dynamic unbalance τ shown in the previous paper.[38] Comparing these two equations, we can see that these two kinds of oscillations have nearly the same vibratory characteristics (e. g., the form of resonance curves) except for the kinds of effective nonlinear components. The occurence of the oscillation $(3/2)\omega_1$ requires only a symmetrical nonlinear components $N(0)$, and the oscillation $+(1/2)\omega$ requires an unsymmetrical nonlinear component $N(1)$ besides $N(0)$.

We show the groups of the resonance curves for each value of the coefficient of the nonlinear term $\beta^{(0)}$, and the damping coefficient c in Figs. 6. 3 and 6. 4, respectively. In these figures, we put $\delta=1$ and $\alpha_1=3/8$. The chain line in Fig. 6. 4 represents the backbone curve. It can be seen that the resonance curves in each figure have the same characteristics as those for the subharmonic oscillation of order 1/2.[65] From investigation of the stability of solutions in the same manner as that in the previous report[65], it follows that the point on the resonance curve

which has a vertical tangent gives the boundary between a stable region and an unstable one. Stable and unstable stationary solutions are represented by full and broken lines, respectively.

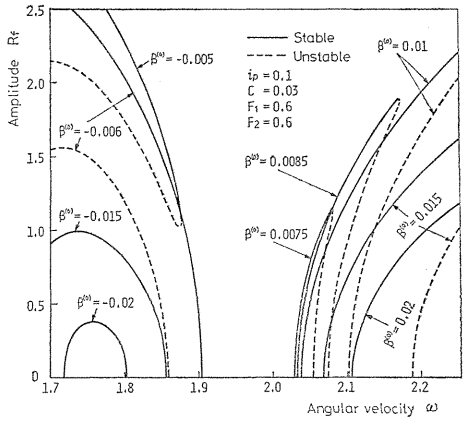

Fig. 6. 3. Theoretical resonance curves showing the influence of the nonlinear component $N(0)$ $(\beta^{(0)})$.

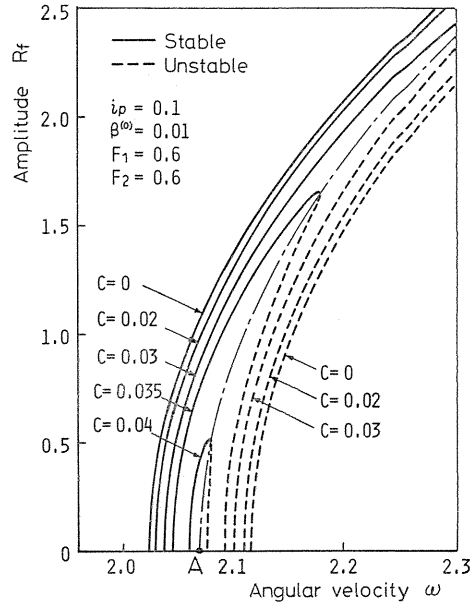

Fig. 6. 4. Theoretical resonance curves showing the influence of the damping coefficient c.

From Eq. (6. 16), the following condition for the amplitude to be real is obtained:

$$|8\beta^{(0)}Q_1Q_2| \geqq c\omega_f \quad (\doteqdot cp_f) \tag{6.17}$$

Therefore, in order that this sub-combination tone may occur against an inevitable damping, the value of the apparent external force $8\beta^{(0)}Q_1Q_2$ is required to satisfy Eq. (6. 17). As shown in Fig. 6. 4, the peak of the resonance curve becomes lower as the damping coefficient c increases. For c satisfying the equality of Eq. (6. 17), the curve is reduced to the point A. Such a critical damping coefficient c_c is given by the equation:

$$c_c = |8\beta^{(0)}Q_1Q_2|/p_f \tag{6.18}$$

For a damping larger than c_c, the oscillation does not appear.

6. 5. Experimental results and their discussions

Experiments were performed by using the same apparatus as shown in Fig. 1. 1. The disc R_3 and the shaft S_1 were used as shown in Tables 1. 1 and 1. 2, respectively.

If the apparatus is assembled under the condition that the discrepancy between the center lines of the upper and the lower bearings in the vertical shaft system is very small, the shaft center line is located in the middle of the angular clearance in the single-row deep groove ball bearing when the shaft is non-rotating. In this case, the symmetrical nonlinearity is more apparent in the restoring force of the shaft than the unsymmetrical nonlinearity.[36] As a result, the subharmonic oscillation of order 1/3 and the summed-and-differential harmonic oscillations of the types $[2p_i \pm p_j]$ and $[p_i \pm p_j \pm p_k]$ can occur, in addition to the subharmonic oscillation of order 1/2 and the summed-and-differential harmonic oscillations of the types $[p_i \pm p_j]$. We have already reported on these oscillations.[36] In the above assembly, we could also observe the occurrence of the sub-combination tone $(3/2)\omega_1$.

Figure 6. 5 shows the resonance curve for this kind of oscillation, as obtained in experiments. In this figure, the ordinate represents the amplitudes R of $(3/2)\omega_1$ which are obtained by taking away the small amplitudes of frequency ω from the wave forms. The resonant frequency of this oscillation, that is, the angular velocity of the shaft at which the relation $(3/2)\omega_1 = p_2 \quad (p_1 > p_2 > 0 > p_3 > p_4$ holds among natural frequencies) is satisfied is $\omega = 2120$ rpm (see Fig. 6 6). The resonance curve in Fig. 6. 5 is the same in shape as those in Fig. 6. 4. Since the disturbance forces resulting in the oscillation $(3/2)\omega_1$ are not large compared with the forces due to the static unbalance e and the dynamic one τ, we found that the amplitudes in Fig. 6. 5 are not so large as those of the subharmonic oscillation of order 1/3 owing to e and τ.

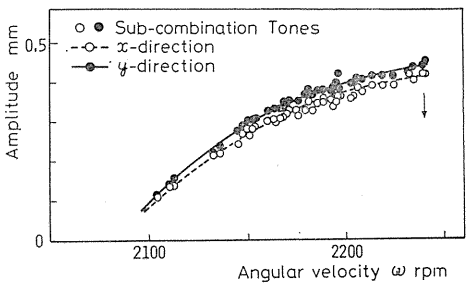

Fig. 6. 5. Experimental resonance curve of the sub-combination tone $[+(3/2)\omega_1]$.

The frequencies of the oscillation $(3/2)\omega_1$ are shown in Fig. 6. 6. By measuring the orbital angular velocity of a steel ball in a single-row deep groove ball bearing, we obtain the following values:

$$\omega_1 = \alpha_1 \omega = 0.387\omega, \quad \alpha_1 = 0.387 \tag{6.19}$$

The values of $(3/2)\alpha_1$ and $\omega_2 = (3/2)\alpha_1\omega$ obtained in Fig. 6. 5 are plotted in the upper and the lower diagrams of Fig. 6. 6, respectively. They are consistent with the values of Eq. (6. 19), within the accuracy of measurement.

An example of the wave form of Fig. 6. 5 is shown in Fig. 6. 7. In this picture, the white vertical lines represent the marks recorded at each revolution of the shaft. We find that a small oscillation of frequency ω is involved in this wave form. Nearly the same shape of wave repeats itself at the time interval AA. During the interval AA, the shaft makes 31 revolutions, and the number of peaks of the wave form is 18. Therefore, the relation:

$$\left.\begin{aligned} (3/2)\alpha_1 &= \{(3/2)\omega_1\}/\omega \fallingdotseq 18/31 \fallingdotseq 0.581 \\ \therefore \quad \alpha_1 &= 0.387 \end{aligned}\right\} \tag{6.20}$$

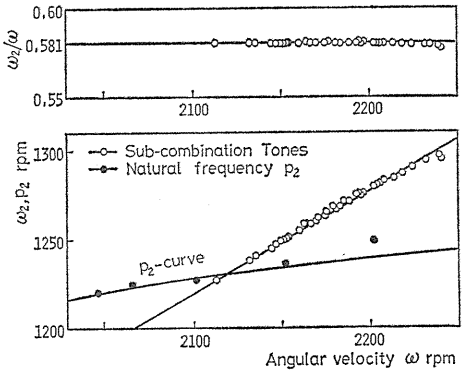

Fig. 6. 6. Experimental values of the frequency $\omega_2\left(=\frac{3}{2}\alpha_1\omega\right)$ and ω_2/ω.

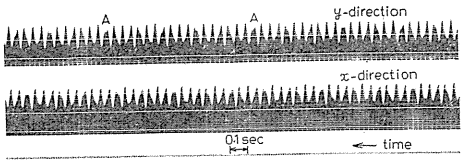

Fig. 6. 7. Wave form of the sub-combination tone $[+(3/2)\omega_1]$ ($\omega\fallingdotseq 2208.5$ rpm).

is obtained, and this value is consistent with Eq. (6. 19).

As mentioned in preceeding sections, the appearance of the sub-combination tone $(3/2)\omega_1$ requires external forces of frequencies ω_1 and $2\omega_1$. Figure 6. 8 proves experimentally that the diturbance force of frequency $2\omega_1$ exists in practice within this system. When the oscillation $(3/2)\omega_1$ occurred, a peak in the harmonic oscillation $2\omega_1$ appeared in the vicintiy of $\omega=1480$ rpm, where $2\omega_1\fallingdotseq p_2$ (p_2 : a natural frequency), as shown in Fig. 6. 8. On the other hand, we have already reported that a difference in diameters of balls in a bearing results in the appearance of a peak in the harmonic oscillation of frequency ω_1, and that the existence of the external force ω_1 was ascertained experimentally.[29]

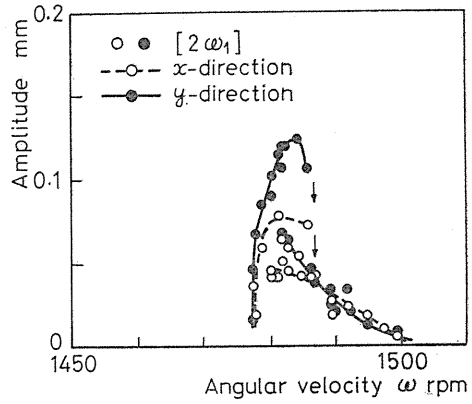

Fig. 6. 8. Experimental resonance curve of the harmonic oscillation $[+2\omega_1]$.

In the cases where the discrepancy between the center lines of the upper and the lower bearing pedestals is not small in a vertical shaft system, and where a static deflection of the shaft exists in a horizontal shaft system, the oscillation $(3/2)\omega_1$ does not occur experimentally. This is explained by the following two reasons: First, the restoring force of the shaft has strong unsymmetrical and weak symmetrical nonlinearity. This is verified by the fact that the subharmonic oscillation of order 1/2 and the summed-and-differential harmonic oscillations of the types $[p_i\pm p_j]$ appear, but the subharmonic oscillation of order 1/3 and the summed-and-differential harmonic one of the types $[2p_i\pm p_j]$ and $[p_i\pm p_j\pm p_k]$ do not appear.[32~34, 36, 37] Accordingly, the coefficient $\beta^{(0)}$, related to the symmetrical nonlinear component $N(0)$, takes a small value, and it follows that the magnitude of an apparent external force is not large enough to satisfy the condition of

appearance, that is, Eq. (6. 17). The case in the four-degree-of-freedom system is explained in the same way.

The above-mentioned result is also substantiated by the shape of resonance curve for the harmonic oscillation in the neighborhood of the major critical speed ω_c, and also by the shape of the subharmonic oscillation of order 1/2 of the type of a forward precessional whirling motion which was obtained in experiments. When the alignment of the center lines of both bearing pedestals is not good, the resonance curves at the frequencies ω_c and $\omega_{1/2}$ are minimally inclined toward the high frequency range because of a small component $N(0)$, (e. g., see Fig. 2 of the previous report[37]), and thus the oscillation $(3/2)\omega_1$ does not appear. On the other hand, Figs. 6 and 19 of the previous report[36] show the resonance curves in the vicinity of ω_c and those for the subharmonic oscillation of order 1/2, respectively, in the case where the oscillation $(3/2)\omega_1$ occurs. Their curves of hard spring type which are inclined considerably toward the right side show the existence of a large component $N(0)$ to be necessary for the occurrence of $(3/2)\omega_1$.

The second reason why bad alignment of the center lines of bearing pedestals results in no appearance of the oscillation $(3/2)\omega_1$ is that the value of Q_1 in Eq. (6. 17) representing an apparent external force is small. When the discrepancy between the center lines of both pedestals is comparatively large, not only the force F in Fig. 6. 1 but also the moment acts on the shaft even in a static state. In this case, the inner ring of the bearing inclines to the end of the angular clearance, and the steel balls are pressed by a large force against the inside wall of the outer ring in a thrust direction. Therefore the radial clearance in the ball bearing disappears, and in certain circumstances even an interference appears. Such circumstances are different from those described in Section 6. 2. In this case, the amplitudes a_2 and b_2 of the component $2\omega_1$, that is, the value of Q_2 becomes very small, and so the relation of Eq. (6. 17) does not hold.

The result mentioned above can also be ascertained from the following experimental results. When the oscillation $(3/2)\omega_1$ did not appear, due to the discrepancy between the center lines of both bearing pedestals, it was observed that the natural frequency of the non-rotating shaft took a somewhat large value in a certain direction. This was due to the facts that the radial clearance vanishes in this direction and the stiffness of the shaft becomes large.[30, 69] When there is such non-uniformity of stiffness of the shaft, synchronous backward precession occurs.[69, 70] This oscillation appears with greater amplitude when the oscillation $(3/2)\omega_1$ does not occur.[37, 69] When, however, the oscillation $(3/2)\omega_1$ does occur, this peak is very small, as shown in Fig. 6 of reference,[36] and thus the shaft hardly has the non-uniformity of stiffness.

If the spring characteristics of a shaft contain nonlinear terms of the third and fourth powers of coordinates, the ultra-subharmonic oscillation of frequency $(3/2)\omega_1$ can occur due to only one external force of ω_1.[42] But from the following fact, we can conclude that the oscillation treated here is not one of that sort: If the nonlinear term of the fourth power of coordinates is large enough to make this ultra-subharmonic oscillation occur against the damping, not only does the oscillation of $(3/2)\omega_1$ occur, but also the ultra-subharmonic oscillation of frequency $(3/2)\omega$ should occur with larger amplitudes than those of the former. This is because there exist disturbance forces of ω due to the unbalances of a rotor e and τ in this system which are considerably larger than the external force of ω_1 caused by the difference in diameters of steel balls in a ball bearing. But we did

not observe the oscillation of $(3/2)\omega$ through many experiments.

6. 6. Conclusions

The results of the theoretical analyses and experiments may be summarized as follows:

(1) In the system of the rotating shaft supported by a single-row deep groove ball bearing, when the alignment of center lines of both bearing pedestals is good, intensive symmetrical and weak unsymmetrical nonlinearities appear in the restoring force of the shaft. Also in this case, if there is a difference in diameters of steel balls in the ball bearing, two external forces of frequencies ω_1 and $2\omega_1$ appear. Owing to these forces in addition to the above-mentioned nonlinearities of stiffness, the sub-combination tone of frequency $(3/2)\omega_1$ of the type of a forward precessional motion occurs.

(2) Similar to the subharmonic oscillations of order 1/3 and summed-and-differential harmonic oscillations of the types $[2p_i \pm p_j]$ and $[p_i \pm p_j \pm p_k]$, the oscillation $(3/2)\omega_1$ appears only in the case where an intensive symmetrical nonlinearity of the shaft stiffness exists.

(3) Among the symmetrical nonlinear components, only the isotropic component $N(0)$ takes part in the oscillation $(3/2)\omega_1$.

(4) The equations for the amplitude and the phase angle of the oscillation are the same in constitution as those for the subharmonic oscillation of order 1/2 of a forward precessional type. Thus the vibratory characteristics of both oscillations are qualitatively the same.

(5) When the alignment of the center lines of both bearing pedestals is not good, the oscillation $(3/2)\omega_1$ does not appear. This is because strong unsymmetrical and weak symmetrical nonlinearities appear in the shaft stiffness, causing the component $N(0)$ to become small. Another reason is that the external force of $2\omega_1$ due to the difference in diameters of steel balls becomes small.

(6) The oscillation of $(3/2)\omega_1$ is different from ultra-subharmonic oscillations.

7. Unstable Vibrations of an Unsymmetrical Shaft at the Secondary Critical Speed due to Ball Bearings[62]

7. 1. Introduction

The dynamic phenomena of unsymmetrical rotating shafts with unequal bending stiffness have been studied mainly for unstable vibrations at the major critical speed ω_c and for vibrations at the secondary critical speed. The latter is due to the unsymmetry of the shaft and the gravity, and its mode is a stationary whirling motion with frequency $+2\omega$ (twice the frequency of the shaft rotating speed ω), where the positive sign $+$ represents a forward precessional whirling motion. This secondary critical speed has been studied by many researchers including Soderberg,[20] Smith,[4] and Taylor.[5] Kellenberger,[7] and Bishop & Parkinson[22] discussed these phenomena on an unsymmetrical shaft with distributed mass.

This chapter deals with an unstable vibration with frequency $+2\omega$ which occurs at the secondary critical speed owing to a single-row deep groove ball bearing in an unsymmetrical shaft system. Some researchers indicated the possibility of

unstable vibrations at the secondary critical speed in a system where an unsymmetrical shaft was supported by flexible bearing pedestals with unsymmetrical stiffness. For example, Foote et al.[6] and Tondl[71] have theoretically dealt with this sort of system. They concluded that unstable regions appear at speeds of 1/2, 1/3, 1/4, ... times the major critical speed but their widths are narrow and easily disappear due to a small damping. Moreover a few experiments have been made by Hull[12] and Messal & Bonthron[72], but it is not clear whether unstable regions exist or not.

In this chapter, both the theoretical and the experimental discussions are carried out about the unstable vibration which appears owing to coexistance of the unsymmetry of the shaft and the directional difference of the support condition[32] (that is, the unsymmetrical boundary condition for inclination at the shaft end). This directional difference is due to the angular clearance of a single-row deep groove ball bearing. In our experiments on an unsymmetrical shaft supported by single-row deep groove ball bearings, even when rigid bearing pedestals were used, we observed a wide unstable region in which the unstable vibration of the frequency $+2\omega$ occurred. In addition, it is concluded that this kind of unstable vibration does not appear in the unsymmetrical shaft supported by self-aligning double-row ball bearings, nor in the unsymmetrical rotor system which has similar vibratory characteristics to those of the unsymmetrical shaft system in general.

7. 2. Restoring forces of the shaft and equations of motion

First, we derive expressions for the restoring forces and equations of motion in the unsymmetrical rotating shaft system, when there exists a directional difference in the support condition at the lower end of the shaft.

As shown in Fig. 7. 1, a rotor is mounted on a vertical unsymmetrical shaft (its length is $l=a+b$) at the position of the ratio $a : b$. The boundary conditions are a simple support at the upper end for simplicity, and an elastic support having a directional difference at the lower end. The elastic support means that the inclination angle θ_0 of the shaft at the lower end is proportional to the bending moment M_0 at the end, namely the relation

$$M_0=K\theta_0 \tag{7.1}$$

holds. The proportional constant K is independent of the dimensions of a shaft and its configulation, and it is a sort of a spring constant (whose unit is N·m/rad) determined by only the condition of bearings. The case $K=0$ represents a simple support, and $K=\infty$ a fixed support. In this chapter, we regard all kinds of boundary conditions as an elastic support in a wide sense involving these particular cases, and assume that K can take values from 0 to ∞. The shaft shows a linear spring characteristic when it is supported elastically at both shaft ends. When the boundary condition is not expressed by Eq. (7. 1), a nonlinear spring characteristic appears in the shaft restoring force.

As shown in Fig. 7. 1, O-xyz is a stationary rectangular coordinate system whose origin O coincides with the equilibrium position of the point S (the center of the rotor), and whose z-axis is coincident with the bearing center line (that is, the line connecting the centers of the upper and the lower bearings). Now, we suppose that the strength of the elastic support has a directional differrence. If we suppose that the strength is the greatest in the yz-plane, it is the smallest in

the xz-plane. Putting the spring constants in Eq. (7. 1) in the xz- and yz-planes as K_x and K_y respectively, the relation

$$K_x<K_y \tag{7.2}$$

holds. We rewrite them as

$$K=(K_x+K_y)/2, \quad \Delta K=(K_y-K_x)/2 \tag{7.3}$$

where K represents the average spring constant, and ΔK the directional difference of them.

The system O-$x'y'z'$ is a rotating rectangular coordinate system where the x'- and y'-axes are taken in the directions of the principal axes of moment of inertia of area of the unsymmetrical shaft, and where the z'-axis coincides with the direction of the principal axis of polar moment of inertia of area of the shaft. We designate the moments of inertia of area of the unsymmetrical shaft about the x'- and y'-axes as I_x' and I_y' respectively (where $I_x'>I_y'$ is assumed), and Young's modulas as E. We put

$$EI_x'=B+\Delta B, \quad EI_y'=B-\Delta B \tag{7.4}$$

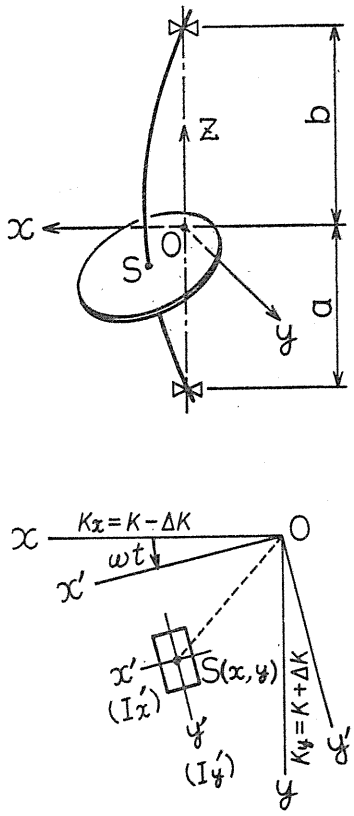

Fig. 7. 1. Coordinate systems.

In Eq. (7. 4), B represents the average bending stiffness of the unsymmetrical shaft, and ΔB the magnitude of the shaft unsymmetry.

Let a deflection of the rotor be r (having components x, y), an inclination angle be $\theta(\theta_x, \theta_y)$, and the restoring force and the moment which act from the shaft to the rotor be $-F(-F_x, -F_y)$ and $-M(-M_x, -M_y)$. We put

$$\left.\begin{aligned} &r=x+iy, \quad \bar{r}=x-iy, \quad \theta=\theta_x+i\theta_y, \\ &\bar{\theta}=\theta_x-i\theta_y, \quad F=F_x+iF_y, \quad M=M_x+iM_y \end{aligned}\right\} \tag{7.5}$$

where $i=\sqrt{-1}$.

Since the motion of the rotor is an infinitesimal vibrations, we assume the deflection r and the inclination θ to be small, and also the twist angle of the shaft during running to be small. Neglecting the higher order terms of these small quantities, the restoring forces in the case of the elastic support having the directional difference as above mentioned are represented in the following forms after some calculation:[73]

$$\left.\begin{aligned} F=&\alpha r+\gamma\theta+\sum_{n=0}^{\infty}(\Delta\alpha_{2n}\bar{r}+\Delta\gamma_{2n}\bar{\theta})e^{2in\omega t}+\sum_{n=1}^{\infty}\{(\Delta\alpha'_{2n}r+\Delta\gamma'_{2n}\theta)e^{-2in\omega t}\\ &+(\nabla\alpha_{2n}r+\nabla\gamma_{2n}\theta)e^{2in\omega t}+(\nabla\alpha'_{2n}\bar{r}+\nabla\gamma'_{2n}\bar{\theta})e^{-2in\omega t}\\ M=&\gamma r+\delta\theta+\sum_{n=0}^{\infty}(\Delta\gamma_{2n}\bar{r}+\Delta\delta_{2n}\bar{\theta})e^{2in\omega t}+\sum_{n=1}^{\infty}\{(\Delta\gamma'_{2n}r+\Delta\delta'_{2n}\theta)e^{-2in\omega t}\\ &+(\nabla\gamma_{2n}r+\nabla\delta_{2n}\theta)e^{2in\omega t}+(\nabla\gamma'_{2n}\bar{r}+\nabla\delta'_{2n}\bar{\theta})e^{-2in\omega t}\}\end{aligned}\right\}\quad(7.6)$$

where ω is the rotating speed of a shaft, and t denotes the time. The moment when the x'-axis becomes parallel to the xz-plane is taken as $t=0$. If the unsymmetry $\Delta B/B$ is a small quantity, the magnitudes of the coefficients such as $\Delta\alpha_{2n}$ and others in Eq. (7. 6) become smaller as $n(=1, 2, \ldots)$ increases.

Let the mass of a rotor be m, the polar moment of inertia be I_p, the diametral moment of inertia be I, and the damping coefficients be c_{11}, c_{12}, c_{21} $(=c_{12})$ and c_{22}. Using F and M in Eq. (7. 6), we then get the following equations of motion:

$$\left.\begin{aligned} &m\ddot{r}+c_{11}\dot{r}+c_{12}\dot{\theta}+F=0\\ &I\ddot{\theta}-iI_p\omega\dot{\theta}+c_{21}\dot{r}+c_{22}\dot{\theta}+M=0\end{aligned}\right\}\quad(7.7)$$

In the experimental apparatus mentioned later, there appear the nonlinear spring chracteristics[32] in the restoring force in addition to the directional difference of support condition at the shaft end due to the ball bearing. But, for simplicity, we consider the linear system represented by Eq. (7. 7), because the nonlinearity has no substantial influences in our discussion. Though forced oscillations $[+\omega]$ and $[+2\omega]$[64] also appear due to the unbalance of a rotor and the variation of the static deflection of a shaft, respectively, we neglect the external forces which cause these oscillations. This is because they have no direct influence on the unstable vibration treated here.

Using the symbol $[p]$, we express the forward and the backward precessional whirling motions of the frequency p corresponding to the sign of p. On account of the terms of the coefficients of $\Delta\alpha_{2n}$, $\Delta\alpha_{2n}'$, $\nabla\alpha_{2n}$, $\nabla\alpha_{2n}'$ and so on in Eq. (7. 6), the free vibration $[p]$ produces the whirling motions of $[2n\omega-p]$, $[-2n\omega+p]$, $[2n\omega+p]$, and $[-2n\omega-p]$ respectively.[16, 74]

7. 3. Unstable vibration at the secondary critical speed

We designate the natural frequency of the system by p. We shall obtain an approximate solution of Eq. (7. 7) near the rotating speed satisfying $p\fallingdotseq+2\omega$. The forms of the solution are put in the following:

$$r=Ae^{i(2\omega t+\varphi)},\quad \theta=A'e^{i(2\omega t+\varphi')}\quad(7.8)$$

Here, it is assumed that A (>0), A', φ, and φ' are slowly varying functions of time, and the first and the second time derivatives of them have the magnitudes of the small quantities $O(\varepsilon)$ and $O(\varepsilon^2)$ respectively. Also, the damping coefficients in Eq. (7. 7) and the third and the fourth terms in the right sides of Eq. (7. 6) are assumed to have the magnitude of $O(\varepsilon)$. Putting the coefficients of $e^{i(2\omega t+\varphi)}$ to zero after the substitution of Eq. (7. 8) into Eq. (7. 7), and neglecting the terms of $O(\varepsilon^2)$ and below, we obtain the following equations:

$$
\left.\begin{aligned}
&4m\omega A\dot{\varphi}=H(2\omega)A+\gamma A'\cos(\varphi-\varphi')+\{\Delta\alpha_4 A\cos 2\varphi\\
&\qquad+\Delta\gamma_4 A'\cos(\varphi+\varphi')\}-2\omega c_{12}A'\sin(\varphi-\varphi') \qquad \text{(i)}\\
&(4I-I_p)\omega A'\dot{\varphi}'\cos(\varphi-\varphi')=G(2\omega)A'\cos(\varphi-\varphi')+\gamma A\\
&\qquad+\{\Delta\gamma_4 A\cos 2\varphi+\Delta\delta_4 A'\cos(\varphi+\varphi')\}\\
&\qquad+(4I-I_p)\omega\dot{A}'\sin(\varphi-\varphi')+2\omega c_{22}A'\sin(\varphi-\varphi') \qquad \text{(ii)}\\
&4m\omega\dot{A}=\gamma A'\sin(\varphi-\varphi')+\{\Delta\alpha_4 A\sin 2\varphi+\Delta\gamma_4 A'\sin(\varphi+\varphi')\}\\
&\qquad-2\omega\{c_{11}A+c_{12}A'\cos(\varphi-\varphi')\} \qquad \text{(iii)}\\
&(4I-I_p)\omega\dot{A}'\cos(\varphi-\varphi')=G(2\omega)A'\sin(\varphi-\varphi')+\{\Delta\gamma_4 A\sin 2\varphi\\
&\qquad+\Delta\delta_4 A'\sin(\varphi+\varphi')\}+(4I-I_p)\omega A'\dot{\varphi}'\sin(\varphi-\varphi')\\
&\qquad-2\omega\{c_{12}A+c_{22}A'\cos(\varphi-\varphi')\} \qquad \text{(iv)}
\end{aligned}\right\} \quad (7.9)
$$

Here,

$$H(2\omega)=\alpha-m(2\omega)^2,\quad G(2\omega)=\delta+I_p\omega(2\omega)-I(2\omega)^2 \qquad (7.10)$$

Neglecting the small terms in Eq. (7. 9), we get the following relations satisfied with the accuracy of $O(\varepsilon^0)$:

$$
\left.\begin{aligned}
&\frac{A'}{A}=-\frac{H(2\omega)}{\gamma\cos(\varphi-\varphi')}=-\frac{\gamma}{G(2\omega)\cos(\varphi-\varphi')}\\
&\sin(\varphi-\varphi')=0 \qquad \therefore\quad \varphi'=\varphi,\ \text{or}\ \varphi'=\varphi+\pi
\end{aligned}\right\} \quad (7.11)
$$

Neglecting the small terms in Eq. (7. 7), we obtain the frequency equation as follows:

$$
\left.\begin{aligned}
&f(p)=(\alpha-mp^2)(\delta+I_p\omega p-Ip^2)-\gamma^2=H(p)G(p)-\gamma^2=0\\
&(H(p)=\alpha-mp^2,\qquad G(p)=\delta+I_p\omega p-Ip^2)
\end{aligned}\right\} \quad (7.12)
$$

After putting $2\omega=p$ in Eq. (7. 12), we designate the root of this equation by p_0. Using the symbols $H(p_0)=H_0$ and $G(p_0)=G_0$, we obtain the following relation near the rotating speed $p\fallingdotseq+2\omega$ with the accuracy of $O(\varepsilon^0)$:

$$H(2\omega)\doteqdot H(p)\doteqdot H_0,\quad G(2\omega)\doteqdot G(p)\doteqdot G_0 \qquad (7.13)$$

If the amplitude A' is assumed to take positive and negative values, we can adopt only the relation $\varphi'=\varphi$. Consequently, from Eq. (7. 11), it follows that

$$A'/A=-H_0/\gamma=-\gamma/G_0 \qquad (7.14)$$

Thus, it is known that the ratio of the amplitudes of inclination and deflection is constant with the accuracy of $O(\varepsilon^0)$. Referring to Eqs. (7. 13), (7. 14) and the relation $\varphi'=\varphi$, and after the calculations of (i)$\times G(2\omega)-$(ii)$\times\gamma$, and (iii)$\times G(2\omega)$

$-$(iv)$\times\gamma$ in Eq. (7. 9), we obtain the equations with the accuracy of $O(\varepsilon)$ as follows:

$$\left.\begin{aligned}\dot{\varphi}&=-\sigma-\Delta\cos 2\varphi=-\kappa\left(\omega-\frac{p_0}{2}\right)-\Delta\cos 2\varphi\\ \dot{A}&=-cA-\Delta\cdot A\sin 2\varphi\end{aligned}\right\}\qquad(7.15)$$

here

$$\left.\begin{aligned}&D=4mG_0+(4I-I_p)H_0,\quad \sigma=-2f(2\omega)/(p_0D)=\kappa\left(\omega-\frac{p_0}{2}\right),\\ &\kappa=4\{2mG_0+(2I-I_p)H_0\}/D\ \ (>0),\\ &\Delta=-2(G_0\Delta\alpha_4-2\gamma\Delta\gamma_4+H_0\Delta\delta_4)/(p_0D)\ \ (>0),\\ &c=2(G_0c_{11}-2\gamma c_{12}+H_0c_{22})/D\ \ (>0)\end{aligned}\right\}\qquad(7.16)$$

In Eq. (7. 15), σ is the so-called detuning term, Δ the coefficient due to the coexistence of the shaft unsymmetry and the directional difference of bearing support, and c the damping cofficient. Also it is easily verified that σ, Δ, and c are positive constants.

Equation (7. 15) is able to be solved in nearly the same manner as that of the previous paper,[75] and has the solutions as mentioned below.

The values of ω satisfying the relation $\Delta^2=\sigma^2$ are designated by ω_1' and ω_2' $(\omega_1'<\omega_2')$. From Eq. (7. 15), it follows that

$$\omega_1'=p_0/2-\Delta/\kappa,\quad \omega_2'=p_0/2+\Delta/\kappa\qquad(7.17)$$

(I) The case of $\Delta^2>\sigma^2$ (that is, $\omega_1'<\omega<\omega_2'$): When ω approaches the value of $p_0/2$ and the relation $\Delta^2>\sigma^2$ holds, the solution is given as follows:

$$r=e^{-ct}\{A_1e^{\mu t}e^{i(2\omega t+\varphi)}+A_2e^{-\mu t}e^{i(2\omega t-\varphi)}\}\qquad(7.18)$$

where A_1 and A_2 are arbitrary constants and

$$\mu=\sqrt{\Delta^2-\sigma^2}\ \ (>0)\qquad(7.19)$$

If μ is larger than the damping coefficient c, the first term in the right side of Eq. (7. 18) represents an unstable vibration of the frequency 2ω whose amplitude increases exponentially with time. The boundary frequencies ω_1 and ω_2 $(>\omega_1)$ of the unstable region in which the unstable vibration occurs are given by the equation $\mu-c=0$ as follows:

$$\omega_1=p_0/2-\sqrt{\Delta^2-c^2}/\kappa,\quad \omega_2=p_0/2+\sqrt{\Delta^2-c^2}/\kappa\qquad(7.20)$$

The unstable region is $\omega_1<\omega<\omega_2$. When $\sigma=0$, that is, $\omega=p_0/2$, μ takes the maximum value as follows:

$$\mu_{\max}=\Delta\qquad(7.21)$$

The phase angle φ is determined by the following equations.

$$\left.\begin{aligned}\cos 2\varphi &= -\sigma/\Delta = -\kappa(\omega - p_0/2)/\Delta \\ \sin 2\varphi &= -\mu/\Delta = -\sqrt{\Delta^2-\sigma^2}/\Delta\end{aligned}\right\} \tag{7.22}$$

From Eq. (7. 22), $\varphi=0$ for $\omega=\omega_1'$, $\varphi=-\pi/4$ for $\omega=p_0/2$, and $\varphi=-\pi/2$ for $\omega=\omega_2'$.

(II) The case of $\Delta^2<\sigma^2$ (that is, $\omega<\omega_1'$ and $\omega_2'<\omega$): When ω is slightly different from the value $p_0/2$, and $\Delta^2<\sigma^2$, the solution is given as follows:

$$\left.\begin{aligned}&\text{For } \omega<\omega_1', \\ &\qquad r=e^{-ct}\left[A_3 e^{i\{(2\omega+\nu)t+\beta\}}+\lambda A_3 e^{i\{(2\omega-\nu)t-\beta\}}\right] \\ &\text{For } \omega>\omega_2', \\ &\qquad r=e^{-ct}\left[A_4 e^{i\{(2\omega-\nu)t+\beta\}}+\lambda A_4 e^{i\{(2\omega+\nu)t-\beta\}}\right]\end{aligned}\right\} \tag{7.23}$$

Here, A and β are arbitrary constants, and ν and λ are as follows:

$$\left.\begin{aligned}\nu &= \sqrt{\sigma^2-\Delta^2}\quad(>0) \\ \lambda &= \frac{\sqrt{|\sigma|+\Delta}-\sqrt{|\sigma|-\Delta}}{\sqrt{|\sigma|+\Delta}+\sqrt{|\sigma|-\Delta}}<1\end{aligned}\right\} \tag{7.24}$$

Consequently, the amplitude of the whirling motion $[2\omega+\nu]$ becomes predominant in the lower side ($\omega<\omega_1'$) and that of $[2\omega-\nu]$ becomes predominant in the higher side ($\omega_2'<\omega$). But, it is seen from Eq. (7. 23) that they diminish with time.

Figure 7. 2 shows the frequencies of the vibration near $\omega=p_0/2$ and the unstable region. Broken lines represent the frequencies of decreasing vibrations with smaller amplitudes. When $\omega_1'<\omega<\omega_2'$ the vibration $[+2\omega]$ appears, and this vibration becomes unstable when $\omega_1<\omega<\omega_2$.

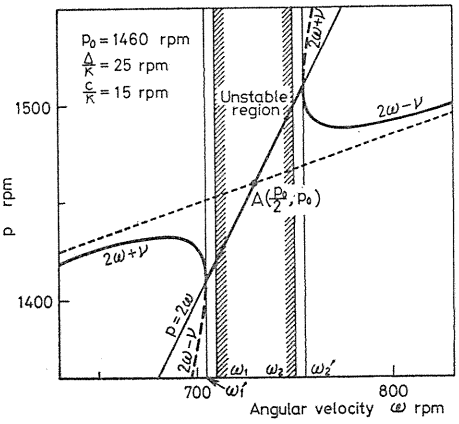

Fig. 7. 2. Frequencies near the secondary critical speed and the unstable region.

7. 4. On the value of the coefficient Δ

We appraise the value of the coefficient Δ, which is a main factor causing the unstable vibration $[+2\omega]$, when the upper shaft end is simply supported and the lower end is under an elastic support condition with a directional difference. The spring constants K_x and K_y ($K_x<K_y$) may take values from 0 to ∞. We introduce the small quantity ζ as a parameter available to appraise the magnitudes of the quantities. For example, $K_x=0$ represents a simple support, $K_x=\infty$ a fixed one, $K_x=O(\zeta)$ an elastic one close to the simple one, $K_x=O(\zeta^0)$ a medium-sized

elastic one (namely, K_x is neither large nor small), and $K_x=0(\zeta^{-1})$ an elastic one close to the fixed one. Though even in the above examples of bearing supports we can consider over twenty combinations depending on the magnitudes of K_x and K_y, the following relation always holds

$$\Delta\alpha_4 : \Delta\gamma_4 : \Delta\delta_4=\left(-\frac{3}{a}\right) : 1 : \left(-\frac{a}{3}\right) \tag{7.25}$$

where a is a distance from the lower shaft end to the rotor. Substituting Eq. (7. 25) into Eq. (7. 16), we get

$$\Delta=\left\{\frac{2}{p_0 D}\left(\frac{3G_0}{a}+2\gamma+\frac{H_0 a}{3}\right)\right\}\Delta\gamma_4 \tag{7.26}$$

Since the term in the braket { } in Eq. (7. 26) is a constant with the magnitude of $O(\zeta^0)$, we may appraise the value of $\Delta\gamma_4$ instead of the coefficient Δ. Among the above-mentioned combinations, we show the calculated values of $\Delta\gamma_4$ for several cases which are expected to be realized practically in experiments. The values of $\Delta\gamma_4$ are described only by the largest term with smaller terms neglected.

(a) In the case of the medium-sized elastic support in the y-direction and the simple support or the elastic one close to it in the x-direction (that is, $K_x=0$ or $O(\zeta)$, and $K_y=O(\zeta^0)$) :

$$\Delta\gamma_4=\frac{3aK_y^3(\Delta B)^2}{8B(4B+aK_y)^3} \tag{7.27 a}$$

(b) In the case of the medium-sized elastic supports both in the x- and y-directions, and the directional difference ΔK with the medium magnitude (that is, $K_x=O(\zeta^0)$, $K_y=O(\zeta^0)$, and $\Delta K=O(\zeta^0)$) :

$$\Delta\gamma_4=\frac{6a(K_y-K_x)\{2B(K_x+K_y)+aK_xK_y\}^2}{(4B+aK_x)^3(4B+aK_y)^3}(\Delta B)^2$$

$$=\frac{12a\Delta K\{4BK+aK^2-a(\Delta K)^2\}^2(\Delta B)^2}{(4B+aK+a\Delta K)^3(4B+aK-a\Delta K)^3} \tag{7.27 b}$$

(c) In the case of the medium-sized elastic supports both in the x- and y-directions, and the small ΔK (that is, $K_x=O(\zeta^0)$, $K_y=O(\zeta^0)$, and $\Delta K=O(\zeta)$) :

$$\Delta\gamma_4=\frac{12aK^2\Delta K(\Delta B)^2}{(4B+aK)^4} \tag{7.27 c}$$

If $\Delta B/B=O(\zeta)$, we know that $\Delta\gamma_4$ has the magnitude of $O(\zeta^2)$ in (a) and (b), and $O(\zeta^3)$ in (c). In the theoretical analysis in Section 7. 3, $\Delta\gamma_4$ is supposed as the magnitude of $O(\varepsilon)$ for any case (that is, $O(\zeta^2)=O(\varepsilon)$ for (a) and (b), and $O(\zeta^3)=O(\varepsilon)$ for (c)).

For comparison, we show the expressions for Δ and $\Delta\gamma_4$ in a system where an unsymmetrical shaft is supported by a flexible bearing pedestal having a directional difference (that is, a system having an unsymmetrical flexibility of the bearing support for deflection) at the lower shaft end. In this system, it is assumed that both of the shaft ends are simply supported. We denote the spring constants for

deflection in the x- and y-directions of the lower bearing pedestal by $k-\Delta k$ and $k+\Delta k$ respectively, and put $K_0=3B(a^2+ab+b^2)/(a^3bl)+k$ and $\Delta K_0=3\Delta B(a^2+ab+b^2)/(a^3bl)$. In the case of small $\Delta k/k$, we get the following equations:

$$\left.\begin{aligned}\Delta&=2\{(G_0/a+2\gamma+aH_0)/(p_0D)\}\Delta\gamma_4\\ \Delta\gamma_4&=\frac{9\Delta k}{a^5K_0^2}\left\{\frac{B^2(\Delta K_0)^2}{K_0^2}+\frac{B\Delta K_0\Delta B(l+b)}{lK_0}+\frac{b(\Delta B)^2}{l}\right\}\end{aligned}\right\}\quad(7.28)$$

When $\Delta k=O(\zeta)$, $\Delta\gamma_4$ in Eq. (7. 28) has the magnitude of $O(\zeta^3)$ and it is the same order as that of $\Delta\gamma_4$ in Eq. (7. 27c).

Incidentally, the coefficients $\Delta\alpha_2$, $\Delta\gamma_2$ and $\Delta\delta_2$, factors causing the unstable region at the major critical speed, have the magnitude of $O(\zeta)$ proportional to the unsymmetry of the shaft $\Delta B/B$ in all cases in the system treated here where there exists a directional difference of the bearing support at the shaft end.

7. 5. Experimental results

The experimental apparatus is a vertical shaft system where the disc R_3 in Table 1. 1 was mounted on the unsymmetrical shaft S_5 in Table 1. 2. When the bearing center line deviates slightly from the center of the angular clearance in the lower bearing, there appears the strongest elastic support in the direction of this deviation, and the weakest one in the normal direction to that. Consequently, the shaft end has a support condition having a directional difference for inclination.[32]

7. 5. 1. Natural frequencies in the non-rotating state

In the experimental apparatus, the deflections were measured in two mutually perpendicular directions. When the shaft was hammered in the state of $\omega=0$, two free vibrations occurred predominantly, and beat phenomena were observed. These vibrations correspond to the modes of vibrations with lowest frequencies in the directions of the maximum and the minimum flexibilities, respectively. We designate these two frequencies by p_{01} and p_{02} $(p_{01}>p_{02})$. Measuring the frequencies for various angular positions Θ of the rotor when $\omega=0$, we know that the values of p_{01} and p_{02} change twice periodically during one revolution of the rotor (from $\Theta=0$ to $\Theta=2\pi$). When the direction of the rotating directional difference (due to the shaft unsymmetry) coincides with that of the stationary directional difference (due to the difference of the boundary condition at the shaft end), namely when the x-direction coincides with the x'- or $-x'$-direction in Fig. 7. 1, $p_{01}-p_{02}$ takes a maximum value. When these directions are at right angles to each other (namely, when the x-direction coincides with the y'- or $-y'$-direction), $p_{01}-p_{02}$ takes a minimum value. The results of measurement can be expressed approximately by $p_{01}=\bar{p}_{01}+\Delta p_{01}\sin 2\Theta$, $p_{02}=\bar{p}_{02}+\Delta p_{02}\sin(2\Theta+\pi)$ where $\bar{p}_{01}=1361.5$ rpm, $\Delta p_{01}=36.5$ rpm, $\bar{p}_{02}=1104$ rpm, and $\Delta p_{02}=39$ rpm. Here, $\bar{p}_{01}-\bar{p}_{02}$ means the difference between the natural frequencies due to the unsymmetry of the shaft, and Δp_{01} (or Δp_{02}) does the magnitude of variation of the natural frequency due to the directional difference of the support condition at the shaft end. As the maximum values of p_{01} and p_{02} are not so different from the natural frequencies of the system where the unsymmetrical shaft having the bending stiffness of $B+\Delta B$ and $B-\Delta B$ was simply supported at both of the shaft ends, we can consider that the

direction of the weak elastic support (that is, the x-direction in Fig. 7. 1) is approximately under the simple support condition. Therefore, the state of our experimental apparatus corresponds to the case (a) in Section 7. 4.

7. 5. 2. Resonance phenomena near the resonance point $p_2=+2\omega$

In this experimental apparatus, in addition to the natural frequencies p_i ($i=1\sim 4$, $p_1>p_2>0>p_3>p_4$) corresponding to those in the symmetrical system (that is, the system carrying a disc mounted on a round shaft), the frequencies $\bar{p}_i$ ($=2\omega-p_i$), $-p_i$ and others are brought about by the unsymmetry of the shaft, the unsymmetrical support condition at the shaft end, or the coexistence of them.[16,74] We measured the resonance curve in the region of the rotating speeds less than $\omega=2700$ rpm in various assemblies of the experimental apparatus, and we observed unstable vibrations near the major critical speed satisfying $p_2=+\omega$ and near the secondary critical speed satisfying $p_2=+2\omega$. In addition, on account of use of a disc ($I_p/I\fallingdotseq 2$) as a rotor, no resonance points satisfying $p_1=+\omega$ and $p_1=+2\omega$ exist. Near the major critical speed satisfying $p_2=+\omega$, an unstable region exists in a broad range of $\omega=1530\sim 1790$ rpm. This corresponds to the unstable region which is generally observed in an unsymmetrical shaft system or in an unsymmetrical rotor system. Near the secondary critical speed satisfying $p_2=+2\omega$, we obtained the resonance curve shown in Fig. 7. 3. In Fig. 7. 3, the unstable region exists in the range of $\omega\fallingdotseq 705\sim 750$ rpm. It was already reported that the peak of the steady oscillation [$+2\omega$] appeared near the secondary critical speed owing to the gravity in a horizontal unsymmetrical shaft system. From Fig. 7. 3, however, it is found that the unstable region of the unstable vibration [$+2\omega$] occurs when there exists a directional difference of the support condition in the vertical unsymmetrical shaft system. The steady vibration [$+2\omega$] also appears in both sides of this unstable region. This vibration is caused by an external force of frequency 2ω which is due to the fluctuation of the static deflection of the shaft. The static deflection changes even in a vertical shaft system when the unsymmetrical shaft is supported elastically at the shaft end or when the shaft curvature and the angular clearance of a bearing coexist.[64]

We can verify the existence of this unstable region also by measuring the natural frequencies of this system. The experimental values of p_2 near the resonance point are shown in Fig. 7. 4. If there are no unstable regions, p_2 will take the values of the curve shown in a broken line in the figure. But the experimental p_2 curve is the same in shape as the full line in Fig. 7. 2 owing to the existence of the unstable region. We could not observe the vibrations with smaller amplitudes shown in broken lines in Fig. 7. 2.

This unstable region occurs owing to the coexistence of the shaft unsymmetry and the directional difference of the bearing support. Therefore, when the bearing

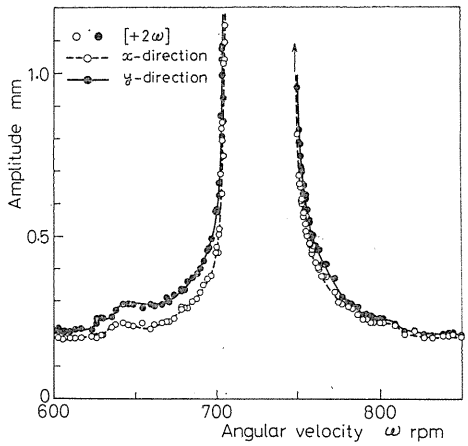

Fig. 7. 3. Experimental resonance curve near the secondary critical speed satisfying $p_2=+2\omega$ (in the case of presence of the unstable region).

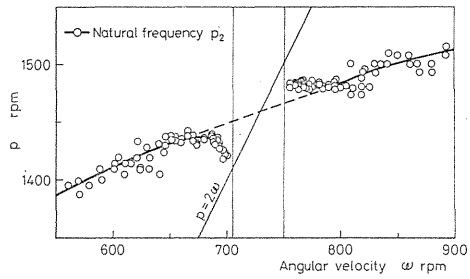

Fig. 7. 4. Natural frequencies near the secondary critical speed ($p_2=+2\omega$).

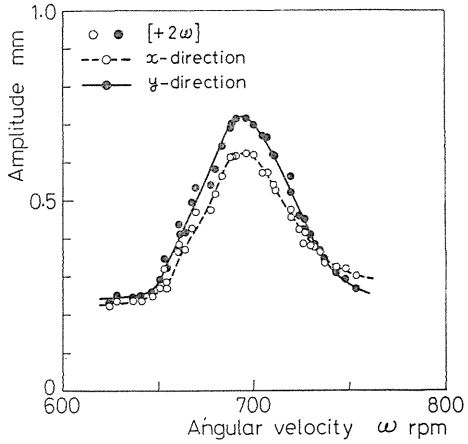

Fig. 7. 5. Experimental resonance curve near the secondary critical speed satisfying $p_2=+2\omega$ (in the case of absence of the unstable region).

center line shifts its position against the angular clearance of the bearing, the magnitude of the directional difference of the support condition at the shaft end varies, and thus the width of the unstable region changes. When the center lines of the upper and the lower bearings are in good alignment and there is little directional difference of the bearing support, $\Delta\gamma_4$ and others in Section 7. 4 become zero approximately. Then, as shown in Fig. 7. 5, the steady vibration $[+2\omega]$ appears with no unstable region. Furthermore, as the center lines of the upper and the lower bearings are in good alignment in Fig. 7. 5, the resonance point is lower than that in Fig. 7. 3 by about 35 rpm.

In the experiments where we used the same unsymmetrical shaft and the same bearing pedestals as those in the above experiments but exchanged only the lower bearing for a self-aligning double-row ball bearing, both the shaft ends were under the simple support condition, and no unstable vibration of $[+2\omega]$ occurred. Therefore, we conclude that the unsymmetry of the flexible bearing pedestals represented by Eq. (7. 28) in Section 7. 4 has no effect on the unstable vibration treated here.

7. 6. An unsymmetrical rotor system

An unsymmetrical rotor system often shows the same vibratory characteristics as those of an unsymmetrical shaft system, but no unstable vibration $[+2\omega]$ occurs in the former system. The experimental apparatus is a vertical shaft system where the unsymmetrical rotor R_2 in Table 1. 1 was mounted on the round shaft S_2 in Table 1. 2. Though experiments were performed for various assemblies, the resonance curves were all the same in shape as the curve of Fig. 7. 5, and no unstable region appeared. The steady vibration $[+2\omega]$ appeared as a result of resonance to the external force caused by variation of the static deflection as mentioned in the previous paper.[64]

In the unsymmetrical rotor system, the restoring force and moment working on the rotor are not expressed by Eq. (7. 6), but the following equations:

$$\left.\begin{aligned} F &= \alpha r + \gamma\theta + \Delta\alpha_{20}\bar{r} + \Delta\gamma_{20}\bar{\theta} \\ M &= \gamma r + \delta\theta + \Delta\gamma_{20}\bar{r} + \Delta\delta_{20}\bar{\theta} \end{aligned}\right\} \tag{7.29}$$

Therefore, Eq. (7. 29) does not involve any terms for the coefficients $\Delta\alpha_4$, $\Delta\gamma_4$, and $\Delta\delta_4$ in Eq. (7. 6) which are the factors causing an unstable vibration near $p_2 \fallingdotseq 2\omega$. Consequently, no unstable vibration $[+2\omega]$ can appear in the unsymmetrical rotor system.

7. 7. Conclusions

On the vibration near the secondary critical speed in a rotating shaft system where an unsymmetrical shaft is supported by a single-row deep groove ball bearing, the results of the theoretical and the experimental analyses are summarized as follows:

(1) Near the rotating speed satisfying $p_2 = +2\omega$, there exists an unstable region where the unstable vibration of the frequency 2ω appears.

(2) The cause of this unstable region is the coexistence of the rotating directional difference due to the shaft unsymmetry and the stationary directional difference due to the angular clearance of the bearing.

(3) Change of the assembly of the experimental apparatus gives rise to variations in the bearing support condition. Consequently, the width of the unstable region varies, and sometimes the unstable region vanishes.

(4) In the system where the elastic shaft with the circular cross section carrying an unsymmetrical rotor is supported by a single-row deep groove ball bearing, no unstable vibration $[+2\omega]$ occurs.

References

1) J. P. Den Hartog, *Mechanical Vibrations*, (1956), pp. 155-165, McGrow-Hill Book Company, Inc., New York.
2) *Handbook on Vibration Technology* (in Japanese), Yōkendō, (1976), Chapter 20.
3) Ref. (1), pp. 187-197.
4) D. M. Smith, "The Motion of a Rotor Carried by a Flexible Shaft in Flexible Bearing", *Proc. Roy. Soc. Lond.*, Ser. A, Vol. 142 (1933), pp. 92-118.
5) H. D. Taylor, "Critical-Speed Behavior of Unsymmetrical Shafts", *J. Appl. Mech.*, Vol. 7 (1940), pp. A71-A79.
6) W. R. Foote, H. Poritsky, and J. J. Slade, "Critical Speeds of Unequal Flexibility -I", *J. Appl. Mech.*, Vol. 10 (1943), pp. A77-A84.
7) W. Kellenberger, "Forced, Double-Frequency, Flexural Vibrations in a Rotating, Horizontal, Cylindrical Shaft", *Brown Boveri Rev.*, Vol. 42, No. 3 (1955), pp. 79-85.
8) T. Yamamoto and H. Ōta, "On the Dynamically Unstable Vibrations of the Shaft Carrying an Unsymmetrical Rotating Body", *Trans. Japan Soc. Mech. Engrs.* (in Japanese), Vol. 30, No. 209 (1964), pp. 149-160.
T. Yamamoto and H. Ōta, "On the Dynamically Unstable Vibrations of a Shaft Carrying an Unsymmetrical Rotating Body", *J. Appl. Mech., Trans. ASME*, Vol. 31, No. 3 (1964), pp. 515-522.
9) T. Yamamoto and H. Ōta, "The Damping Effect on Unstable Whirlings of a Shaft Carrying an Unsymmetrical Rotor", *Trans. Japan Soc. Engrs.* (in Japanese), Vol. 33, No. 247 (1967), pp. 365-376.

T. Yamamoto and H. Ōta, "The Damping Effect on Unstable Whirlings of a Shaft Carrying an Unsymmetrical Rotor", *Memoirs of the Faculty of Engineering*, Nagoya University, Vol. 19, No. 2 (1967), pp. 197-217.
10) Ref. (1), pp. 336-339.
11) W. Kellenberger, "Biegeschwingungen einer unrunden, rotiereden Welle in horizontaler Lage", *Ing. -Arch.*, 26 (1958), pp. 302-318.
12) E. H. Hull, "Shaft Whirling as Influenced by Stiffness Asymmetry", *Trans. ASME*, Ser. B, Vol. 83, No. 2 (1961), pp. 219-226.
13) F. M. Dimentberg, *Flexural Vibrations of Rotating Shafts*, (1961), pp. 155-222, Butterworths, London.
14) P. J. Brosens and S. H. Crandall, "Whirling of Unsymmetrical Rotors", *Trans. ASME*, Ser. E, Vol. 28 (1961), pp. 355-362.
15) S. H. Crandall and P. J. Brosens, "On the Stability of Rotation of a Rotor with Rotationally Unsymmetric Inertia and Stiffness Properties", *Trans. ASME*, Ser. E, Vol. 28 (1961), pp. 567-570.
16) T. Yamamoto and H. Ōta, "On the Vibrations of the Shaft Carrying an Unsymmetrical Rotating Body", *Bulletin of the JSME*, Vol. 6, No. 21 (1963), pp. 29-36.
17) T. Yamamoto and H. Ōta, "Unstable Vibrations of the Shaft Carrying an Unsymmetrical Rotating Body", *Bulletin of the JSME*, Vol. 6, No. 23 (1963), pp. 404-411.
18) S. T. Ariaratnam, "The Vibration of Unsymmetrical Rotating Shafts", *Trans. ASME*, Ser. E, Vol. 87, No. 1 (1965), pp. 157-162.
19) A. Tondl, *Some Problems of Rotor Dynamics*, (1965), pp. 70-113, Publishing House of the Czechoslovak Academy of Sciences.
20) C. R. Soderberg, "On the Subcritical Speeds of the Rotating Shaft", *Trans. ASME*, Vol. 54 (1932), pp. 45-52.
21) Ref. (19), pp. 76-78.
22) R. E. D. Bishop and A. G. Parkinson, "Second Order Vibration of Flexible Shafts", *Phil. Trans. Roy. Soc. Lond.*, Ser. A, Vol. 259, No. 1095 (1965), pp. 1-31.
23) Y. Matsukura, T. Inoue, and M. Tomizawa, "Double Frequency Vibration of Flexible Rotors with Asymmetric Flexural Rigidity", *Trans. Japan Soc. Mech. Engrs.* (in Japanese), Vol. 46, No. 406, C (1980), pp. 591-597.
24) A. H. Nayfeh and D. T. Mook, *Nonlinear Oscillations*, (1979), John Wiley & Sons, Inc..
25) B. L. Newkirk and H. D. Taylor, "Shaft Whipping due to Oil Action in Journal Bearings", *General Electric Rev.*, Vol. 28 (1925), pp. 559-568.
26) Y. Hori, "A Theory of Oil Whip", *Trans. ASME*, Ser. E, Vol. 26 (1959), pp. 189-198.
27) H. Nakane, R. Kokubo, S. Iida, and K. Takeshita, "1/2-Order Subharmonic Resonance of Rotating Shaft Supported by Sliding Journal Bearings", *Technical Review*, (1968-1), pp. 1-7, Mitsubishi Heavy Industries, LTD.
28) T. Yamaguchi and K. Shiraki, "Vibrations of Marine Engines (except for Internal Combustion Engines) and Their Vibration Preventions", *Journal of Marine Engineering Society in Japan* (in Japanese), Vol. 5, No. 4 (1960), pp. 235-260.
29) T. Yamamoto, "On the Critical Speed of a Shaft supported in Ball Bearing (Part 1)", *Trans. Japan Soc. Mech. Engrs.* (in Japanese), Vol. 20, No. 99 (1954), pp. 750-755.
T. Yamamoto, "On the Critical Speed of a Shaft", *Memoirs of the Faculty of Engineering*, Nagoya University, Vol. 6, No. 2 (1954), pp. 133-142.
30) T. Yamamoto, "On the Critical Speed of a Shaft supported in Ball Bearing (Part 2)", *Trans. Japan Soc. Mech. Engrs.* (in Japanese), Vol. 20, No. 99 (1954), pp. 755-760.
T. Yamamoto, "On the Critical Speeds of a Shaft", *Memoirs of the Faculty of Engineering*, Nagoya University, Vol. 6, No. 2 (1954), pp. 142-152.
31) T. Yamamoto, "On the Critical Speeds Induced by Ball Bearings in Lower Rotating Speeds", *Trans. Japan Soc. Mech. Engrs.* (in Japanese), Vol. 23, No. 135 (1957), pp. 838-841.
T. Yamamoto, "On the Vibrations of a Rotating Shaft", *Memoirs of the Faculty of Engineering*, Nagoya University, Vol. 9, No. 1 (1957), pp. 86-92.

32) T. Yamamoto, "On the Critical Speed of a Shaft of Sub-harmonic Oscillation", *Trans. Japan Soc. Mech. Engrs.* (in Japanese), Vol. 21, No. 111 (1955), pp. 853-858.
T. Yamamoto, "On the Vibrations of a Rotating Shaft", *Memoirs of the Faculty of Engineering*, Nagoya University, Vol. 9, No. 1 (1957), pp. 33-70.
33) T. Yamamoto, "On Sub-harmonic Oscillations and on Vibrations of Peculiar Modes in Non-linear Systems Having Multiple Degrees of Freedom", *Trans. Japan Soc. Mech. Engrs.* (in Japanese), Vol. 22, No. 123 (1965), pp. 868-875.
T. Yamamoto, "On the Vibrations of a Rotating Shaft", *Memoirs of the Faculty of Engineering*, Nagoya University, Vol. 9, No. 1 (1957), pp. 53-71.
34) T. Yamamoto, "Response Curves at the Critical Speeds of Sub-Harmonic and Summed-and-Differential Harmonic Oscillations", *Bulletin of the JSME*, Vol. 3, No. 12 (1960), pp. 397-403.
35) T. Yamamoto, "On Sub-Harmonic and Summed-and-Differential Harmonic Oscillations of Rotating Shaft", *Bulletin of the JSME*, Vol. 4, No. 13 (1961), pp. 51-58.
36) T. Yamamoto, Y. Ishida, and J. Kawasumi, "Oscillations of a Rotating Shaft with Symmetrical Nonlinear Spring Characteristics", *Bulletin of the JSME*, Vol. 18, No. 123 (1975), pp. 965-975.
37) T. Yamamoto, "On the Critical Speeds with Peculiar Modes of Vibration", *Trans. Japan Soc. Mech. Engrs.* (in Japanese), Vol. 22, No. 115 (1956), pp. 172-177.
T. Yamamoto, "On the Vibrations of a Rotating Shaft", *Memoirs of the Faculty of Engineering*, Nagoya University, Vol. 9, No. 1 (1957), pp. 43-53.
38) T. Yamamoto and Y. Ishida, "Theoretical Discussions on Vibrations of a Rotating Shaft with Nonlinear Spring Characteristics", *Trans. Japan Soc. Mech. Engrs.* (in Japanese), Vol. 41, No. 345 (1975), pp. 1374-1384.
T. Yamamoto and Y. Ishida, "Theoretical Discussions on Vibrations of a Rotating Shaft with Nonlinear Spring Characteristics", *Memirs of the Faculty of Engineering*, Nagoya University, Vol. 30, No. 1 (1978), pp. 90-108.
39) T. Yamamoto and Y. Ishida, "Theoretical Discussions on Vibrations of a Rotating Shaft with Nonlinear Spring Characteristics", *Ing. -Arch.*, 46 (1977), pp. 125-135.
40) C. P. Atkinson, "Superharmonic Oscillators as Solutions to Duffing's Equation as Solved by an Electronic Differential Analysis", *J. Appl. Mech.*, Vol. 24 (1957), pp. 520-525.
41) W. Szemplinska-Stupnika, "Higher Harmonic Oscillations in Heteronamas Non-Linear System with One Degree of Freedom", *Int. J. Non-Linear Mech.*, Vol. 3 (1968), pp. 17-30.
42) T. Yamamoto, K. Yasuda, and I. Nagasaka, "Ultra-Subharmonic Oscillations in a Nonlinear Vibratory System", *Bulletin of the JSME*, Vol. 19, No. 138 (1976), pp. 1442-1447.
43) T. Yamamoto, K. Yasuda, and T. Nagoh, "Super-Division Harmonic Oscillations in a Nonlinear Multidegree-of-Freedom System", *Bulletin of the JSME*, Vol. 18, No. 128 (1975), pp. 1082-1089.
44) T. Yamamoto, K. Yasuda, and T. Nagoh, "Super-Division Harmonic Oscillations Caused by Nonlinearity of the Fourth Order", *Bulletin of the JSME*, Vol. 20, No. 139 (1977), pp. 24-32.
45) T. Yamamoto and Y. Nakao, "Combination Tones of Summed Type in Nonlinear Vibratory Systems", *Bulletin of the JSME*, Vol 6, No. 24 (1963), pp. 682-689.
46) T. Yamamoto and S. Hayashi, "Combination Tones of Differential Type in Nonlinear Vibratory Systems", *Bulletin of the JSME*, Vol. 7, No. 28 (1964), pp. 690-698.
47) T. Yamamoto, K. Yasuda, and T. Nakamura, "Combination Oscillations in a Non-Linear Vibratory System", *Bulletin of the JSME*, Vol. 17, No. 107 (1974), pp. 560-568.
48) J. Tomas, "Ultrasubharmonic Resonance in a Duffing System", *Int. J. Non-Linear Mech.*, Vol. 6 (1971), pp. 625-631.
49) T. Yamamoto, K. Yasuda, and T. Nakamura, "Sub-Combination Tones in a Nonlinear Vibratory System (Caused by Symmetrical Nonlinearity", *Bulletin of the JSME*, Vol. 17, No. 113 (1974), pp. 1426-1437.

50) T. Yamamoto, K. Yasuda, and T. Nakamura, "Sub-Combination Tones in a Nonlinear Vibratory System", *ACTA TECHNICA ČSAV*, Vol. 19, No. 2 (1974), pp. 143-161.
51) Ref. (19), pp. 343-357.
52) P. R. Sethna, "Steady-State Undamped Vibrations of a Class of Nonlinear Discrete System", *Trans. ASME*, Ser. E, Vol. 81, No. 1 (1960), pp. 187-195.
53) T. Yamamoto and K. Yasuda, "On the Internal Resonance in a Nonlinear Two-Degree-of-Freedom System (Forced Vibrations near the Lower Resonance Point When the Natural Frequencies are in the Ratio 1 : 2)", *Bulletin of the JSME*, Vol. 20, No. 140 (1977), pp. 168-175.
54) T. Yamamoto, K. Yasuda, and I. Nagasaka, "On the Internal Resonance in a Nonlinear Two-Degree-of-Freedom System (Forced Vibrations near the Higher Resonance Point When the Natural Frequencies are in the Ratio 1 : 2)", *Bulletin of the JSME*, Vol. 20, No. 147 (1977), pp. 1093-1100.
55) T. Yamamoto, K. Yasuda, and I. Nagasaka, "On the Internal Resonance in a Nonlinear Two-Degree-of-Freedom System (When the Natural Frequencies are in Ratio 2 : 3)", *Bulletin of the JSME*, Vol. 22, No. 171 (1979), pp. 1274-1283.
56) T. Yamamoto, Y. Ishida, and K. Aizawa, "On the Subharmonic Oscillations of Unsymmetrical Shafts", *Bulletin of the JSME*, Vol. 22, No. 164 (1979), pp. 164-173.
57) T. Yamamoto, Y. Ishida, T. Ikeda, and M. Yamamoto, "Nonlinear Forced Oscillations of a Rotating Shaft Carrying an Unsymmetrical Rotor at the Major Critical Speed", *Bulletin of the JSME*, Vol. 25, No. 210 (1982), pp. 1969-1976.
58) T. Yamamoto, Y. Ishida, and T. Ikeda, "Summed-and-Differential Harmonic Oscillations of an Unsymmetrical Shaft", *Bulletin of the JSME*, Vol. 24, No· 187 (1981), pp. 183-191.
59) T. Yamamoto, Y. Ishida, T. Ikeda, and M. Yamada, "Subharmonic and Summed-and-Differential Harmonic Oscillations of an Unsymmetrical Rotor", *Bulletin of the JSME*, Vol. 24, No. 187 (1981), pp. 192-199.
60) T. Yamamoto, Y. Ishida, T. Ikeda, and H. Suzuki, "Super-Summed-and-Differential Harmonic Oscillations of an Unsymmetrical Shaft and an Unsymmetrical Rotor", *Bulletin of the JSME*, Vol. 25, No. 200 (1982), pp. 257-264.
61) T. Yamamoto, Y. Ishida, and T. Ikeda, "Sub-Combination Tones of a Rotating Shaft due to Ball Bearings", *Bulletin of the JSME*, Vol. 24, No. 196 (1981), pp. 1844-1852.
62) T. Yamamoto, Y. Ishida, and T. Ikeda, "Unstable Vibrations of an Unsymmetrical Shaft at the Secondary Critical Speed due to Ball Bearings", *Bulletin of the JSME*, Vol. 25, No. 210 (1982), pp. 2002-2009.
63) Ref. (1), pp. 336-343.
64) T. Yamamoto, "On the Critical Speed of a Shaft at Lower Rotating Speeds", *Trans. Japan Soc. Mech. Engrs.* (in Japanese), Vol. 22, No. 123 (1956), pp. 863-867.
T. Yamamoto, "On the Vibrations of a Rotating Shaft", *Memoirs of the Faculty of Engineering*, Nagoya University, Vol. 9, No. 1 (1957), pp. 79-86.
65) T. Yamamoto and S. Hayashi, "On the Response Curves and the Stability of Summed-and-Differential Harmonic Oscillations", *Bulletin of the JSME*, Vol. 6, No. 23 (1963), pp. 420-429.
66) R. Van Dooren, "Combination Tones of Summed Type in a Non-Linear Damped Vibratory System with Two Degrees of Freedom", *Int. J. Non-Linear Mech.*, Vol. 6, No. 2 (1971), pp. 237-254.
67) T. Sasaki, J. Nishikaze, M. Kitamura, and M. Horiguchi, "On the Planetary Motion of the Roller in the Roller Bearing", *Trans. Japan Soc. Mech. Engrs.* (in Japanese), Vol. 8, No. 31 (1942), pp. I64-I73.
68) C. Hayashi, *Nonlinear Oscillations in Physical Systems*, (1964), pp. 142-154, McGraw-Hill.
69) T. Yamamoto, "On the Critical Speeds of Synchronous Backward Precession", *Trans. Japan Soc. Mech. Engrs.* (in Japanese), Vol. 22, No. 115 (1956), pp. 167-171.
T. Yamamoto, "On the Vibrations of a Rotating Shaft", *Memoirs of the Faculty of*

Engineering, Nagoya University, Vol. 9, No. 1 (1957), pp. 71–78.

70) Y. Shimoyama and T. Yamamoto, "On the Critical Speeds of a Shaft due to the Deflections of Bearing Pedestals", *Trans. Japan Soc. Mech. Engrs.* (in Japanese), Vol. 20, No. 91 (1954), pp. 215–222.
T. Yamamoto, "On the Critical Speeds of a Shaft", *Memoirs of the Faculty of Engineering*, Nagoya University, Vol. 6, No. 2 (1954), pp. 109–133.

71) Ref. (19), Chapter 6.

72) E. E. Messal and R. J. Bonthron, "Subharmonic Rotor Instability due to Elastic Asymmetry", *Trans. ASME*, Ser, B, Vol. 94, No. 1 (1972), pp. 185–192.

73) A. E. H. Love, *A Treatise on the Mathematical Theory of Elasticity*, (1927), Chapter 18, Dover.

74) H. Ōta and K. Mizutani, 'Influence of Unequal Pedestal Stiffness on the Instability Regions of a Rotating Asymmetric Shaft", *Trans. ASME*, Ser. E, Vol. 45 (1978), pp. 400–407.

75) T. Yamamoto and A. Saito, "On the Oscillations of Summed-and-Differential Types under Parametric Excitation (Vibratory Systems width Damping)", *Bulletin of the JSME*, Vol. 11, No. 43 (1968), pp. 92–101.